Studies of Fundamental Theories and Retention Mechanism of Charge Transfer and Hypercrosslinked Phases in Normal Phase High Performance Liquid Chromatography

by

Di Wu

A thesis submitted in partial fulfillment of the requirements for the degree of

Doctor of Philosophy

Department of Chemistry
University of Alberta

Abstract

Polar compounds in petroleum, especially compounds containing nitrogen, cause numerous problems in the processing of oil, including deactivation of catalysts, corrosion, and storage instability. Chromatographic separation helps to identify and characterize these polar compounds at different stages in the refining of petroleum. Previous research in our group showed that the custom synthesized hypercrosslinked polystyrene stationary phase HC-Tol was capable of group-type separation of nitrogen compounds under normal phase liquid chromatography conditions. Group-type separation means that the pyrroles, pyridines and polycyclic aromatic hydrocarbons (PAHs) were separated into three distinct groups. The commercial dinitroanilinopropyl (DNAP) column also separated nitrogen compounds from PAHs. Despite the potential of the HC-Tol and DNAP columns for petroleum separations, their retention mechanisms were not fully understood.

In this thesis, the Snyder–Soczewiñski model and linear solvation energy relationships (LSERs) were used to gain a better understanding of the HC-Tol and DNAP columns. This thesis focuses on the fundamental theories of normal phase high performance liquid chromatography (HPLC), especially on the retention mechanisms of the HC-Tol and DNAP columns. The normal phase retention on the HC-Tol column was investigated using the Snyder–Soczewiñski model. The solvent strength of binary hexane-solvent mixtures can be predicted using the solvent strength of the pure strong solvents. The HC-Tol column was shown to be a localizing adsorptive phase with

adsorption sites extending above the surface. HC-Tol was also characterized by linear solvation energy relationships (LSERs) and compared to the classical amino phase and another hypercrosslinked phase (5-HGN). On both the HC-Tol and amino columns, the solute hydrogen bond acidity (*A*), hydrogen bond basicity (*B*) and polarity (*S*) all contribute significantly to retention, while solute excess polarizability *E* has a small but negative effect on retention. Solute volume *V* has no impact on retention on the amino column, while *V* has a slightly negative influence on retention for the HC-Tol column. The differences in coefficient *v* between the amino and the HC-Tol columns might explain why the HC-Tol is capable of group-type separations. 5-HGN phase has smaller *a* and *b* values, which means that 5-HGN is not as basic or acidic in terms of hydrogen bonds as is HC-Tol. This suggests that the hydrogen bonding character of the HC-Tol phase arises from its silica substrate.

The slope of the linear relationship between retention and the mobile phase composition (Snyder-Soczewiñski model) in normal phase liquid chromatography (NPLC) was studied for both bonded and charge-transfer phases. Knowing the slope is important for retention prediction, mobile phase adjustment, and even column selection. The Snyder model and the Soczewiñski model were compared on classic NPLC bonded phases using literature data, and on the DNAP column using experimentally collected data. Overall, the Snyder model slightly better predicted the *n*-slope than the Soczewiñski model. However, both models had comparable uncertainty in predicting the *n*-slope for a given compound. The number of aromatic double bonds was the most suitable descriptor for

estimating the relative *n*-slope of PAHs. On the DNAP phase, a modified Soczewiñski model was suggested to allow for the significant contribution of the aromatic rings to the *n*-slope. Coupling the modified Soczewiñski model and one gradient run, a gradient method was developed to build a LSER for normal phase chromatography. LSER model built based on gradient separation was as good as those based on isocratic separation but required less trial and error experiments.

Preface

Chapter 2 has been published as D. Wu, G.K. Nedev, C.A. Lucy, "Retention mechanism of hypercrosslinked polystyrene silica hybrid phase in normal phase chromatography", J. Chromatogr. A 1370 (2014) 50-55. I was responsible for the experiments and data analysis, as well as preparation of the manuscript. George K. Nedev was responsible for column synthesis and packing.

A version of **Chapters 3 and 4** has been accepted by Journal of Chromatography A as D. Wu and C. A. Lucy, "Study of the slope of the linear relationship between retention and mobile phase composition (Snyder-Soczewiñski model) in normal phase liquid chromatography with bonded and charge-transfer phases". I conducted all experiments and wrote the manuscript.

The supervisory author, Charles A. Lucy, was involved throughout the projects in concept formation and manuscript composition.

Acknowledgements

I would like to thank my supervisor, Dr. Charles A. Lucy, for his guidance, support and encouragement throughout my degree. Being a very thoughtful, understanding and patient professor, he not only supervises my research but also helps me to sharpen my transferable skills. He provides lots of conference and industrial tour opportunities to students in our lab including me to broaden my perspective.

I would like to express my gratitude and appreciation to my committee: Dr. Susan Olesik, Dr. Robert Campbell, Dr. Mike Serpe, and Dr. Sarah Styler for their time and input on this thesis. I also need to thank other members of my supervisory committee: Dr. James Harynuk and Dr. Yunjie Xu for their invaluable comments and advice on my research.

I would like to thank all Lucy group members for the enjoyable time that I spent with them. Many of them became my lifetime friends. Thanks to Lei for always listening to me and being supportive. Thanks to Ya for being on my side regardless of the circumstances. Thanks to Ping and Chad for their collaborative work. Thanks to George for synthesizing the column and the research discussion. Thanks to Nicole for her professional trainings.

I would like to express my appreciation to all the support staff in the Department of Chemistry.

Last but not least, I would like to express my deepest thanks to my parents and my husband, Ling for constantly motivating and supporting me.

This thesis was supported by the University of Alberta and the Natural Sciences and Engineering Council of Canada (NSERC).

Table of Contents

List of Tables

List of Figures

List of Symbols and Abbreviations

2D	Two dimensional
5-HGN	5 μm hypercrosslinked, gel type and nonactivated beaded polystyrene phase
A	Solute hydrogen bond donating ability
A	Weak solvent in the mobile phase
a	Differences in hydrogen bond accepting ability between two phases
A'	Constant in Scott-Kucera equation
A_B	Relative area of interaction between the solvent B and the adsorbent surface
Abs. Dev.	Absolute deviation
ANOVA	Analysis of variance
A_S	Relative area of interaction between the solute and the adsorbent surface
B	Solute hydrogen bond accepting ability
B	Strong solvent in the mobile phase
b	Differences in hydrogen bond donating ability between two phases
B'	Constant in Scott-Kucera equation
c	Intercept of the LSERs equation
c_m	Concentration of solute in the mobile phase
CN	Cyano stationary phase
c_s	Concentration of solute in the stationary phase
DCM	Dichloromethane
DNAP	Dinitroanilinopropyl stationary phase
DVB	Divinylbenzene
E	Solute excess polarizability
e	Differences in excess polarizability between two phases
EA	Ethyl acetate
E_{Xm}	Free energies of solute X in the mobile phase

E_{Xs}	Free energies of solute *X* in the stationary phase
E_{Ym}	Free energies of solvent *Y* in the mobile phase
E_{Ys}	Free energies of solvent *Y* in the stationary phase
F	Significance of all the independent variables
G1	Gradient 1
G2	Gradient 2
G3	Gradient 3
G4	Gradient 4
H	Plate height
h	Height of peak
HC	Hypercrosslinked
HC-C_8	Hypercrosslinked polystyrene with octyl group stationary phase
HC-COOH	Hypercrosslinked polystyrene with carboxyl group stationary phase
HC-Tol	Hypercrosslinked polystyrene with toluene group stationary phase
HPLC	High performance liquid chromatography
IPA	Isopropyl alcohol
K	Distribution constant
k	Retention factor
k_0	Retention factor in pure nonpolar mobile phase
$k_{0.1}$	Retention factor with 10% strong solvent as mobile phase
k_1	Retention factor in pure strong solvent
k_{AB}	Retention factor in a mobile phase consisting of mixture of a weak solvent A and a strong solvent B
k_i	Retention factor in mobile phase i
k_j	Retention factor in mobile phase j
k_m	Retention factor of the later eluting solute
k_n	Retention factor of the earlier eluting solute

L	Length of column
LC	Liquid chromatography
LSER	Linear solvation energy relationship
m	Mobile phase
MEK	Methyl ethyl ketone
MLR	Multiple linear regression
MS	Mass spectrometry
N	Plate number
n	Number of molecules of solvent displaced by solute
n	Slope of the Snyder–Soczewiñski equation
N_B	Mole fraction of strong solvent B
N_{double}	Number of double bonds in the solute molecule
NPLC	Normal phase liquid chromatography
N_{Polar}	Number of polar substituent groups in the solute molecule
n-slope	Slope of the Snyder–Soczewiñski equation
n_{Snyder}	n-slope in Snyder model
$n_{Soczewiñski}$	n-slope in Soczewiñski model
PAC	Polycyclic aromatic compound
PAH	Polycyclic aromatic hydrocarbon
PBB	Pentabromobenzyl
PLS	Partial least squares
PSA	Polar surface area
R	Correlation coefficient
R	The gas constant
R^2	Coefficient of determination
Ref.	Reference
RMSECV	root mean square error of cross-validation

R_s	Resolution
S	Solute dipolarity and polarizability
s	Stationary phase
s	Differences in dipolarity/polarizability between two phases
SE	Standard error
SP	Free energy term
S-S	Snyder–Soczewiñski
t	Time
T	Temperature
t_0	Dead time
t_G	Gradient time
THF	Tetrahydrofuran
TPSA	Topological polar surface area
t_R	Retention time
UV	Ultraviolet absorption
V	Solute McGowan volume
v	Differences in cavity formation ability between two phases
v_m	Volume of the mobile phase, dead volume
V_R	Retention volume
v_s	Volume of the stationary phase
W	Baseline peak width
$W_{1/2}$	Half height peak width
W_{av}	Average of baseline peak widths
X	Solute
X	Independent variable
X_m	Solute X in the mobile phase
X_s	Solute X on the stationary phase

Y	Solvent
Y	Dependent variable
Y_m	Solvent Y on the stationary phase
Y_s	Solvent Y on the stationary phase
α	Selectivity factor
α	Activity factor
β	Phase ratio
ΔE	Net free energy
Δ_{eas}	Secondary term to correct for all secondary solvent effects not considered in the simplest S-S equation
Δ_{easAB}	Δ_{eas} in a mobile phase consisting of mixture of a weak solvent A and a strong solvent B
Δ_{easB}	Δ_{eas} in the pure strong solvent B
ΔG_1	Free energy of solute transfer from pure strong solvent to the stationary phase
ΔG_m	Free energy required for the solute to transfer from 10% strong solvent to pure strong solvent
Δt_R	Difference between the retention times of two peaks
$\Delta\phi$	Change of volume fraction of strong solvent during the gradient run
ε	Solvent strength
ε_A	Solvent strength of the weak solvent A
ε_{AB}	Solvent strength of a mixture of weak solvent A and strong solvent B
$\varepsilon_{benzene}$	Solvent strength of benzene
ε_B	Solvent strength of the strong solvent B
ε_i	Solvent strength of solvent i
ε_i	Solvent strength of solvent j
ε_{THF}	Solvent strength of tetrahydrofuran

σ	Standard deviation
ϕ	Volume fraction of strong solvent
ϕ_0	Initial volume fraction of strong solvent during a gradient run
ϕ_G	Final volume fraction of strong solvent during a gradient run

Chapter One. Introduction

1.1 Motivation and thesis overview

Petroleum is a mixture of hundreds of thousands of different hydrocarbons. It is everywhere in our life. Compositional knowledge would facilitate more effective production and refining of petroleum, determination of sources of pollution, and reduce fouling. Polar compounds in petroleum especially those containing nitrogen cause numerous problems such as deactivation, corrosion and storage instability [1]. Because of the complexity of petroleum, separation by group type (e.g., pyrroles and pyridines for nitrogen) is desired rather than individual compound separations [2, 3]. Previous research in our group showed that a toluene derived hypercrosslinked polystyrene phase (HC-Tol) was capable of group-type separation of nitrogen compounds under normal phase liquid chromatography conditions [4]. Nitrogen group-type separation means pyrroles, pyridines and polycyclic aromatic hydrocarbons (PAHs) are separated into three distinct groups. Our group also explored commercialized columns, and the dinitroanilinopropyl (DNAP) column was found to be able to separate nitrogen-containing compounds from PAHs [5].

Despite the usage of HC-Tol and DNAP in petroleum separation, their retention mechanisms were not fully understood. The first step to understand a retention mechanism is to explore the dependence of retention on the mobile phase composition and solvent strength. This dependence in normal phase can be best described by the Snyder–Soczewiñski (S-S) model [6-10]. The displacement model has provided understanding of retention on many types of phases under normal phase conditions, including silica [11], alumina [12, 13] and bonded phases [10]. In the S-S model, the linear relationship between retention and mobile phase composition governs changes in retention and selectivity with mobile phase composition. However, the slope of this dependence is not fully understood. The second step to understand the retention mechanism is to explore the characteristics of the HC-Tol and DNAP phases. What

makes HC-Tol and DNAP phases so special? Linear solvation energy relationships (LSERs) [14-20] are widely used to characterize stationary phases. LSERs relate the fundamental molecular interactions between the solutes and the solvents and stationary phase with the observed retention. Isocratic separations are typically used to build the LSER models [15, 21, 22]. However, gradient elution is a more powerful means of collecting retention data for multicomponent samples which have a wide range of polarities. Previously, gradient elution has been used to develop LSER for reversed phase liquid chromatography [23-25]. However, there are no literature studies of gradient methods to develop LSER in normal phase.

This thesis studies fundamental theories of normal phase high performance liquid chromatography (HPLC), including the displacement model and LSERs. The goal of the work is to achieve a better understanding of the HC-Tol and DNAP columns, and of the theories used to characterize these columns. In **Chapter 2**, the normal phase retention on the HC-Tol column is investigated using the Snyder–Soczewiñski model. In **Chapter 3**, HC-Tol is characterized by LSERs and compared to amino and 5-HGN columns. In **Chapters 4** and **5**, the slope of the linear relationship between retention and the mobile phase composition (Snyder-Soczewiñski model) in normal phase liquid chromatography (NPLC) is studied with bonded and charge-transfer phases. In **Chapter 6**, a gradient method is developed to build a LSER for normal phase chromatography.

1.2 Chromatography

1.2.1 High performance liquid chromatography (HPLC) history

Classical column chromatography was invented by the Russian botanist Mikhail Tswett [26, 27] in the early 1900s. Colored samples were poured on top of a glass cylinder packed with a fine powder (column), and then a solvent was poured into the glass cylinder. The colored pigments separated in the column could be directly viewed. In 1941, Martin and Synge [28] started their work in liquid-liquid chromatography (partition

chromatography) to separate amino acids. They also developed the plate theory of chromatography in the same paper [28]. In 1952, Martin and Synge won the Nobel Prize for their invention of partition chromatography. In those days, chromatography was time consuming and labor intensive because it had to be carried out manually. Amino acid analyzers developed in 1958 [29, 30] and gel permeation chromatographs [31, 32] invented in 1964 were important precursors to modern HPLC. They were the first automated liquid chromatographs and very close in construct to later HPLC instruments. In the 1960s, Csaba Horváth developed the first modern general purpose HPLC [33]. HPLC as a modern chromatography is characterized by the use of a high pressure pump and reusable columns. The first commercial HPLC (the ALC-100 analytical liquid chromatograph manufactured by Waters Associates) was formally introduced at the 1968 Pittsburgh Conference [32]. Since then HPLC has seen steady improvements and has become a mature and widely used technique.

1.2.2 Basic concepts of chromatography

Figure 1-1A shows a schematic of an HPLC system. A small volume (microliters) of sample is injected into the mobile phase through the injection valve. The mobile phase driven by the pump starts from the solvent reservoir goes to the column, carrying the injected sample with it. Separation takes places in the column. An HPLC column is usually packed with porous solid particles, which have a rigid support and a covalently attached stationary phase. Sample components distribute between the mobile phase and stationary phase. When a sample component stays in (on) the stationary phase, it does not move. A sample component only moves when in the mobile phase. A thermodynamic equilibration of a solute is established between the stationary phase and mobile phase. Components that are retained less by the stationary phase come off (*elute* from) the column earlier, while others held more by the stationary phase elute later. The eluted components are detected by an on-line detector, *e.g.*, ultraviolet absorption (UV) or mass spectrometry (MS). As shown in **Figure 1-1B**, the graph of detector response versus time

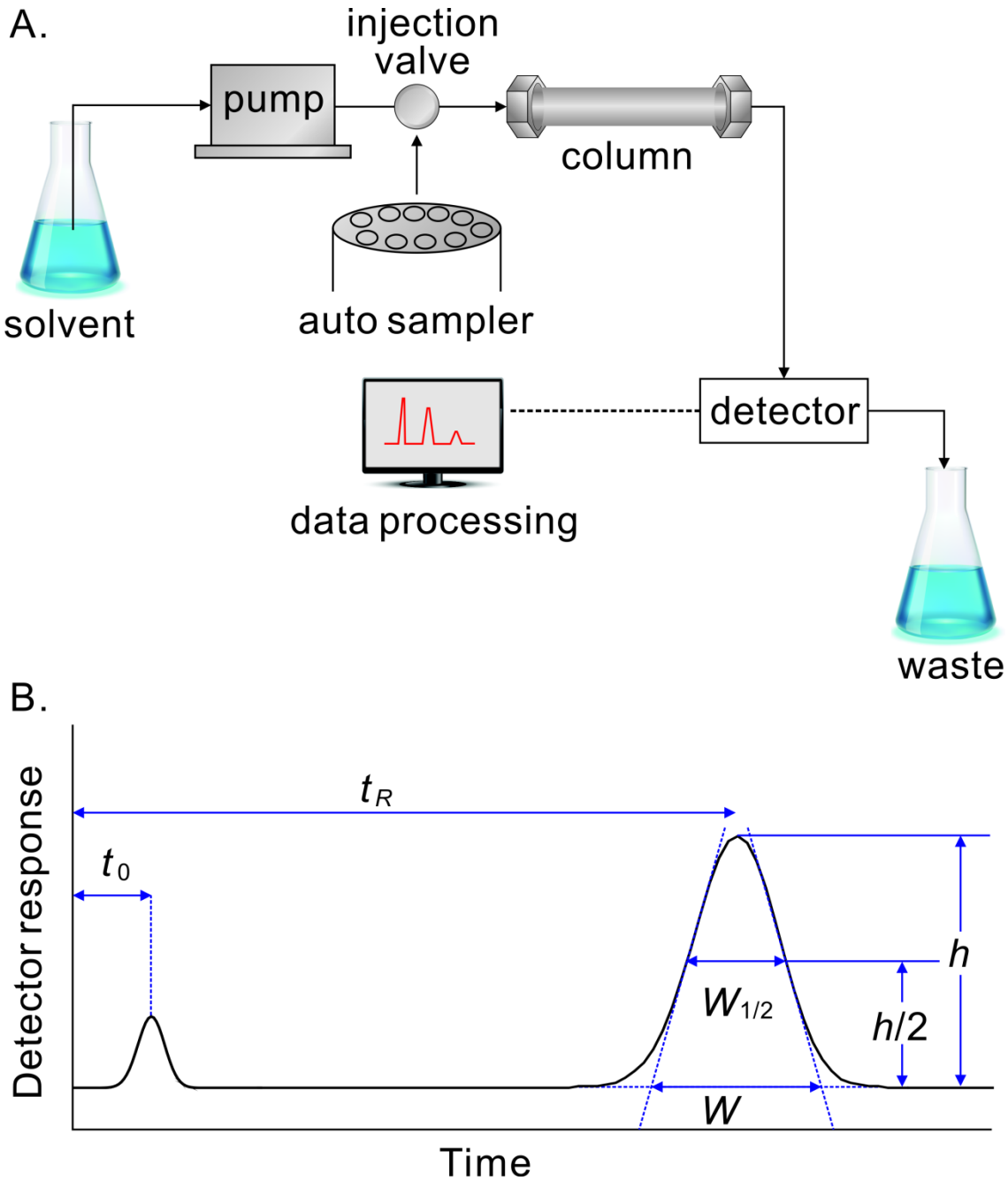

Figure 1-1A) Schematic of an HPLC instrument. **B)** Chromatogram and some basic chromatography measures.

since injection is a *chromatogram*.

The time a solute takes to travel from the injector to the detector is the *retention time*, t_R (**Figure 1-1B**) which is when the peak maximum appears in the chromatogram. The retention time of an unretained solute or mobile phase is the *dead time*, t_0. I participated in the conception of a study of methods to measure the dead time in normal phase chromatography [34], but that study is not included in this thesis.

Since retention time is affected by the instrument configuration (length of tubing, column geometry etc.), the term *retention factor* (previously referred to as the *capacity factor*) *k* is more useful. The retention factor is the time a solute spends in the stationary phase versus the time the sample spends in the mobile phase, which is:

$$k = \frac{t_R - t_0}{t_0} \tag{1-1}$$

We also have [35]:

$$\frac{\text{Time solute spends in stationary phase}}{\text{Time solute spends in mobile phase}} = \frac{\text{moles of solute in stationary phase}}{\text{moles of solute in mobile phase}} = k \tag{1-2}$$

The moles of solute in each phase equals its concentration (c_s or c_m, respectively) times the volume of each phase (v_s *or* v_m, respectively), where subscript *s* and *m* refer to the stationary phase and mobile phase, respectively. The mobile phase volume v_m is also known as the dead volume [34]. So **Eq. 1-2** gives:

$$k = \frac{c_s v_s}{c_m v_m} = K\frac{v_s}{v_m} = K\beta \tag{1-3}$$

Here *K* is the *solute distribution constant* between the stationary phase and mobile phase, and β is the *phase ratio* which is the volume ratio between the stationary phase and mobile phase. **Eq. 1-1** is typically used to calculate retention factor from a chromatogram, while **Eq. 1-3** is a theoretical guide for adjusting retention.

The injected solute band spreads out as it moves along the column which is referred to as *band broadening*. Broad peaks usually give poor separation. *Column efficiency*

reflects the ability of a column to give narrow peaks. Column efficiency can be measured by either plate number *N* or plate height *H*:

$$N = \frac{t_R^2}{\sigma^2} \tag{1-4}$$

$$H = \frac{L}{N} \tag{1-5}$$

where σ is the standard deviation of the peak and *L* is the length of the column. A chromatogram with an idealized Gaussian peak is graphed in **Figure 1-1B**. *W* is the baseline peak width and $W_{1/2}$ is the half height peak width. For a Gaussian peak:

$$W = 4\sigma \quad \text{and} \quad W_{1/2} = 2.35\sigma \tag{1-6}$$

Substituting for σ in **Eq. 1-4** gives:

$$N = 16\left(\frac{t_R}{W}\right)^2 = 5.54\left(\frac{t_R}{W_{1/2}}\right)^2 \tag{1-7}$$

Peaks are separated because of their difference in retention. The relative retention between two solutes can be quantified by *selectivity factor* α:

$$\alpha = \frac{k_m}{k_n} \tag{1-8}$$

where k_m is the retention factor of the later eluting solute, while k_n is the retention factor of the earlier eluting solute. So selectivity factor is always no less than 1. The selectivity factor can be adjusted by chromatographic conditions such as the type of stationary phase and the type of mobile phase.

How well peaks are separated can be expressed by the *resolution*, R_s, which is defined as:

$$R_s = \frac{\Delta t_R}{W_{av}} \tag{1-9}$$

where Δt_R is the difference between the retention times of two peaks, and W_{av} is the average of their baseline peak widths. So narrower peaks and larger differences in peak retention times both yield better resolution (R_s). The higher the resolution, the better the separation between two peaks. If the resolution is equal to or greater than 1.5 (*i.e.*, 6σ), two Gaussian peaks of the similar size are *baseline resolved*, which means that the signal

intensity between the two peaks returns to the baseline. Baseline resolution is complete separation of two peaks and so is favored by quantitative analysis. When peaks are not Gaussian or do not have similar size, there may be overlap of peaks even when the resolution is larger than 1.5. In this case, resolution is required to be larger than 2, especially when a tailing large peak is followed by a small peak or when a small peak is followed by a large fronting peak. **Eq. 1-9** is useful for calculating the resolution from a chromatogram, but it gives little guidance for improving and understanding resolution. So for method development purposes, another alternative equation can be expressed if it is assumed that the two peaks have the same widths:

$$R_s = \frac{N^{0.5}}{4}\frac{k_n}{1+k_n}(\alpha - 1) \qquad (1\text{-}10)$$

So improving column efficiency (N), increasing retention (k) or increasing the selectivity factor (α) can increase resolution. Among these three factors, selectivity factor (α) is the best way to improve resolution.

1.3 Normal phase liquid chromatography (NPLC)

When chromatography was first invented in early 1900s [26, 27], the stationary phase was polar while the mobile phase was less polar. This system was the most common way to run chromatography for more than a half century, and so was named *normal phase*. In 1950, *reversed phase chromatography* using a nonpolar stationary phase and a polar mobile phase was developed [36]. Beginning in 1970 with the commercialization of modern HPLCs, reversed phase liquid chromatography (RPLC) became the dominant HPLC mode because RPLC has better efficiency, quicker equilibration and is compatible with aqueous samples. However, normal phase still finds utility in thin layer chromatography, preparative chromatography and achiral isomer separations [37].

1.3.1 Normal phase retention theory

In NPLC the column is more polar than the mobile phase. Thus more polar

compounds are preferentially retained versus less polar compound in NPLC. The retention mechanism of NPLC can be described by the displacement (Snyder–Soczewiñski) model [38]. Solvent molecules are adsorbed onto the surface of the stationary phase to form a monolayer. A solute *X* must displace previously adsorbed solvent molecules *Y* to be retained. The retention equilibrium is given by:

$$X_m + nY_s \rightleftharpoons X_s + nY_m \tag{1-11}$$

where X_m and X_s refer to a solute molecule in the mobile phase and on the stationary phase respectively, and Y_s and Y_m refer to a solvent molecule on the stationary phase and in the mobile phase, respectively. In **Eq. 1-11** a certain number *n* solvent molecules leave the adsorbent surface to make room for one adsorbing solute molecule. The area required by the solute molecule is the same as *n* solvent molecules. The net free energy of retention can be written as:

$$\Delta E = E_{Xs} + nE_{Ym} - E_{Xm} - nE_{Ys} \tag{1-12}$$

The terms E_{Xs}, E_{Ym}, E_{Xm} *and* E_{Ys} are the free energies of solute (*X*) and solvent (*Y*) in the stationary phase (*s*) or mobile phase (*m*) respectively. The solute and solvent molecules interact more strongly with the more polar stationary phase than with the less polar mobile phase. Thus, to a first approximation, interactions in the mobile phase are not important. So in **Eq. 1-12** the mobile phase terms nE_{Ym} and E_{Xm} cancel, leaving

$$\Delta E = E_{Xs} - nE_{Ys} \tag{1-13}$$

Eq. 1-13 leads to the important relationship between retention factor *k* and mobile phase solvent strength ε, which is a measurement of adsorption energy on the adsorbent:

$$\log k = \log k_0 - A_S \varepsilon \tag{1-14}$$

Here k_0 is the retention factor in pure nonpolar mobile phase such as hexane, and A_S is area on the adsorbent surface required by the solute when adsorbed. The derivation and characteristics of the Snyder–Soczewiñski model are discussed in detail in **Section 2.2** and **Section 4.2**.

1.3.2 Normal phase stationary phase

The column stationary phase is the essential part of an HPLC system. Stationary phase dominates retention and selectivity. Prior to 1970, inorganic stationary phases such as alumina, silica and magnesium silicate (Florisil) were mainly used. While bare silica is still used in normal phase, polar bonded phases (*i.e.*, silica bonded with different ligands) have emerged over time. Three polar bonded phases were introduced for NPLC during the 1970s: cyano columns (**Figure 1-2A**), diol columns (**Figure 1-2B**), and amino columns (**Figure 1-2C**). Polar bonded phases are advantageous relative to silica because of their better reproducibility, faster equilibration, and less sensitivity to water. Retentivity (column strength) on the four commonly used NPLC phases are in the order [37]:

$$\text{cyano} < \text{diol} < \text{amino} \ll \text{silica} \qquad (1\text{-}15)$$

Besides the column strength, these three bonded phases all have their unique selectivity. The amino phase is the most basic stationary phase among all three bonded phases, and preferentially retains proton-donor solutes [39, 40]. The cyano phase retains dipolar compounds more strongly compared to the amino and diol phases [41].

Besides the three common polar bonded phases, this thesis studies the dinitroanilinopropyl (DNAP) phase (**Chapters 5** and **6**) and two hypercrosslinked polystyrene stationary phases (5-HGN and HC-Tol, **Chapters 2**, **3** and **5**). A DNAP column has a dinitroanilinopropyl group bonded to silica substrate (**Figure 1-2D**). DNAP column is a commercialized charge transfer bonded phase. Further details about the DNAP phase are in **Section 5.1**. The 5-HGN is a pure polymer phase (**Figure 1-3A**) while HC-Tol is a silica based hypercrosslinked phase (**Figure 1-3B**). A detailed discussion of the development and usage of the 5-HGN and HC-Tol columns can be found in **Section 3.1**.

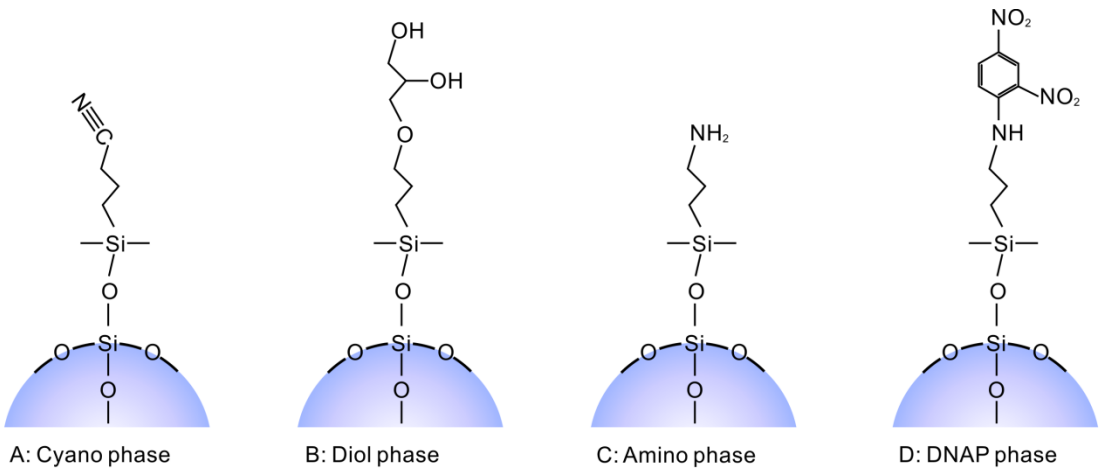

Figure 1-2 Structures of the polar bonded phases used in this work.

A: hypercrosslinked polystyrene

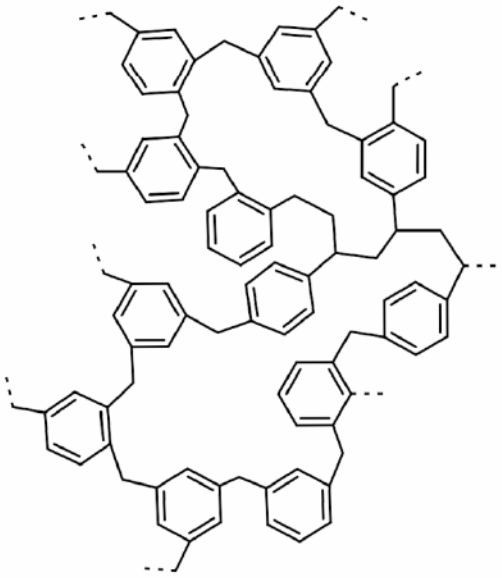

B: HC-Tol phase

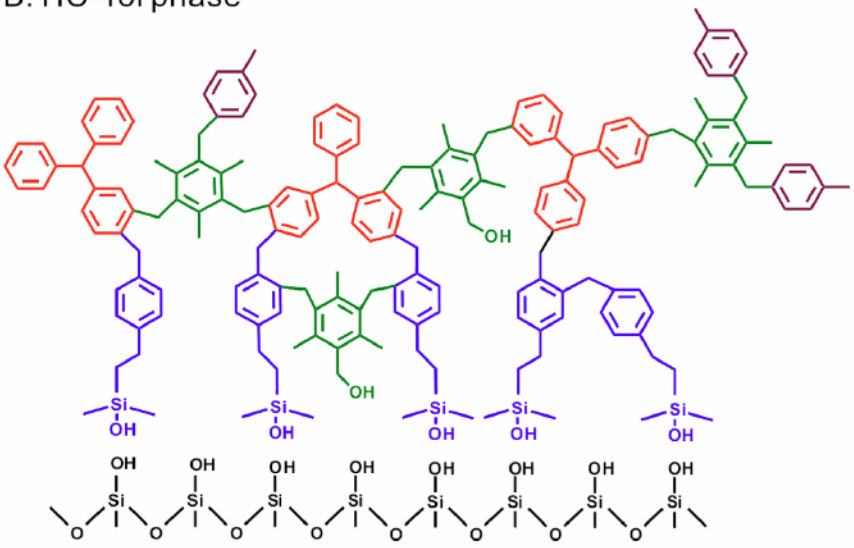

Figure 1-3 Structure of the hypercrosslinked polystyrene and HC-Tol phase. The colors reflect the individual components and steps within the synthesis. Black signifies the underlying silica, blue means the silanization step, red indicates the primary crosslinking step, green is the secondary crosslinking, and purple is the final derivatization with toluene. A adapted from Ref [42], B adapted from Ref. [43].

1.4 Linear solvation energy relationships (LSERs)

Retention is due to the equilibrium of solute between the stationary phase and the mobile phase. The energetics of the transfer of a solute into a solvent can be divided into three steps. First, a suitable size and shape of cavity is formed in the solvent. Second, the cavity is inserted with the non-interacting solute. Third, the solute–solvent interactions are activated [15]. Thus, to understand chromatography, solvent-solute interactions and transfer between phases need to be understood. This thesis uses linear solvation energy relationships (LSERs) to explain and rationalize the processes responsible for retention. LSERs intentionally include terms to account for the various intermolecular interactions governing solute transfer between two phases, and thus governing retention.

1.4.1 *Intermolecular interactions*

Intermolecular forces between uncharged molecules described in LSERs are relatively weak compared to the covalent and ionic bonds. However, these intermolecular interactions control chromatographic retention. Intermolecular interactions between uncharged molecules include dipole-dipole interactions ("Keesom"), dipole-induced dipole interactions ("Debye"), dispersion ("London") forces and hydrogen bond interactions [15, 44, 45]. The unsymmetrical distributions of positive and negative charges on different atoms of a molecule can cause a bond containing a positive end (pole) and negative end (pole) which are termed a *dipole*. Interactions between molecules with permanent dipoles (*i.e.*, polar molecules) are called dipole-dipole interactions. In such cases, the molecules interact with one another based on the attraction between the positive end of one polar molecule and the negative end of the other polar molecule. Of a particular note, hydrogen bonding is often considered as a special dipole-dipole interaction, where the attraction only happens between a hydrogen atom that is covalently bonded to a highly electronegative atom (usually N, O, or F) and electron pairs on another atom. Compared to ordinary dipole-dipole interactions, hydrogen bonding is directional, stronger, and has shorter interatomic distances. The electric field of a polar

molecule with permanent dipole can induce a change in the electron distribution of a nearby molecule (induction of a dipole). The interactions between the permanent dipole and induced dipole are called dipole-induced dipole interactions, which are often observed between a polar molecule and a nonpolar molecule. Dispersion ("London") forces arise from attraction between temporary dipoles with temporary dipoles, which offers the predominant contribution to the interactions between nonpolar molecules. The temporary dipoles occur due to the random fluctuations of the local electron density of the nonpolar molecule. This kind of intermolecular interaction is universal, which means it is present between all chemical groups, and usually is sensitive to the size of the nonpolar molecules (*i.e.*, larger molecules exhibit stronger dispersion forces than smaller ones). The term "van der Waals forces" refers to the combined effects of the Keesom, Debye and London forces.

1.4.2 Chromatographic interpretation of LSER terms

The LSER has evolved and switched its emphasis from understanding solvent interactions to solute behavior over the decades 1[15, 46, 47]. Currently, LSERs have the following symbolic representation [46]:

$$\mathrm{SP} = c + eE + sS + aA + bB + vV \tag{1-16}$$

In this equation, SP can be any free energy related measurement, and is usually log k in chromatography. c is the intercept term. The letters E, S, A, B, and V are the solute dependent parameters. The coefficients e, s, a, b, and v are obtained from regression of **Eq. 1-16**. The A parameter is related to the solute's hydrogen bond donating ability. So the a coefficient is a measurement of the difference in hydrogen bond accepting ability between two phases (the stationary phase and the mobile phase). The B parameter characterizes the solute's hydrogen bond accepting ability, meaning b reflects the difference in hydrogen bond donating between the two phases. The S parameter is a mixture of the solute's dipolarity and polarizability. Thus the coefficient s reflects differences in the two phases' abilities to interact with the solute through dipole-dipole,

dipole-induced dipole or dispersion forces. The parameter *E* is the solute's polarizability abilities that are not accounted for in the *S* parameter. Thus, the coefficient *e* reflects the difference in the two phases' abilities to interact with solute through polarizability/induction effects. The parameter *V* is a molecule volume term, so the coefficient *v* reflects the difference in the two phases' abilities to form a cavity. For example, it is easier for hexane to make a cavity than water, which is an organized, cohesive solvent. *vV* accounts for the cavity formation step in the three-step solute partition process. Imaging a solute with *V* equal to zero would mean that the solute does not occupy any space in the solvent, and so it would require no cavity formation to accommodate it. In the LSER, the *vV* reflects an unfavorable process, while the rest of the terms represent favorable intermolecular interactions. The coefficients (*a, b, s, e,* and *v*) reflect differences in the properties of the two phases.

1.5 Thesis Content

This thesis uses the displacement model and linear solvation energy relationships (LSERs) to get a better understanding of the normal phase HPLC process and of columns including HC-Tol and DNAP. In **Chapter 2**, the normal phase retention on the HC-Tol column is investigated using the Snyder–Soczewiñski model. In **Chapter 3**, HC-Tol is characterized by LSERs and compared to the amino and 5-HGN columns. In **Chapters 4** and **5**, the slope of the linear relationship between retention and mobile phase composition (Snyder-Soczewiñski model) in normal phase liquid chromatography (NPLC) is studied with bonded and charge-transfer phases. In **Chapter 6**, a gradient method is developed to build a LSER for normal phase chromatography.

1.6 References

[1] R.P. Rodgers, T.M. Schaub, A.G. Marshall, Petroleomics: MS returns to its roots, Anal. Chem. 77 (2005) 20A-27A.

[2] R.E. Paproski, J. Cooley, C.A. Lucy, Fast supercritical fluid chromatography hydrocarbon group-type separations of diesel fuels using packed and monolithic columns, Analyst 131 (2006) 422-428.

[3] R.E. Paproski, C. Liang, C.A. Lucy, Zirconia, titania, silica, and carbon columns for the group-type characterization of heavy gas oils using high temperature normal phase liquid chromatography, Energy Fuels 25 (2011) 4469-4478.

[4] N.E. Oro, C.A. Lucy, Comparison of hypercrosslinked polystyrene columns for the separation of nitrogen group-types in petroleum using high performance liquid chromatography, J. Chromatogr. A 1217 (2010) 6178-6185.

[5] N.E. Oro, C.A. Lucy, High performance liquid chromatographic separations of gas oil samples and their hydrotreated products using commercial normal phases, J. Chromatogr. A 1218 (2011) 7788-7795.

[6] J.L. Glajch, L.R. Snyder, Solvent strength of multicomponent mobile phases in liquid-solid chromatography: Mixtures of three or more solvents, J. Chromatogr. 214 (1981) 21-34.

[7] L.R. Snyder, J.L. Glajch, Solvent strength of multicomponent mobile phases in liquid-solid chromatography: Binary-solvent mixtures and solvent localization, J. Chromatogr. 214 (1981) 1-19.

[8] L.R. Snyder, J.L. Glajch, Solvent strength of multicomponent mobile phases in liquid-solid chromatography: Further study of different mobile phases and silica as adsorbent, J. Chromatogr. 248 (1982) 165-182.

[9] L.R. Snyder, H. Poppe, Mechanism of solute retention in liquid-solid chromatography and the role of the mobile phase in affecting separation - competition versus sorption, J. Chromatogr. 184 (1980) 363-413.

[10] L.R. Snyder, T.C. Schunk, Retention mechanism and the role of the mobile phase in normal-phase separation on amino-bonded-phase columns, Anal. Chem. 54 (1982) 1764-1772.

[11] L.R. Snyder, Linear elution adsorption chromatography: V. Silica as adsorbent. Adsorbent standardization, J. Chromatogr. 11 (1963) 195-227.

[12] L.R. Snyder, Linear elution adsorption chromatography: IV. Group localization in the adsorbate. Extension of the role of solute structure in separations over alumina, J. Chromatogr. 8 (1962) 319-342.

[13] L.R. Snyder, Linear elution adsorption chromatography: III. Further delineation of the eluent role in separations over alumina, J. Chromatogr. 8 (1962) 178-200.

[14] J.W. Li, Prediction of internal standards in reversed-phase liquid chromatography: III. Evaluation of an alternative solvation parameter model to correlate and predict the retention of ionizable compounds, J. Chromatogr. A 982 (2002) 209-223.

[15] M. Vitha, P.W. Carr, The chemical interpretation and practice of linear solvation energy relationships in chromatography, J. Chromatogr. A 1126 (2006) 143-194.

[16] A.A. D'Archivio, A. Giannitto, M.A. Maggi, F. Ruggieri, Cross-column retention prediction in reversed-phase high-performance liquid chromatography by artificial neural network modelling, Anal. Chim. Acta 717 (2012) 52-60.

[17] L. Szepesy, Effect of molecular interactions on retention and selectivity in reversed-phase liquid chromatography, J. Chromatogr. A 960 (2002) 69-83.

[18] J.W. Li, T. Robison, Application of linear solvation energy relationships to guide selection of polar modifiers in normal-phase liquid chromatographic separations, Anal. Chim. Acta 395 (1999) 85-99.

[19] J.W. Li, D.A. Whitman, Characterization and selectivity optimization on diol, amino, and cyano normal phase columns based on linear solvation energy relationships, Anal. Chim. Acta 368 (1998) 141-154.

[20] J.H. Park, M.H. Yoon, Y.K. Ryu, B.E. Kim, J.W. Ryu, M.D. Jang, Characterization of some normal-phase liquid chromatographic stationary phases based on linear solvation energy relationships, J. Chromatogr. A 796 (1998) 249-258.

[21] L.R. Snyder, J.W. Dolan, P.W. Carr, The hydrophobic-subtraction model of

reversed-phase column selectivity, J. Chromatogr. A 1060 (2004) 77-116.

[22] L.R. Snyder, J.W. Dolan, P.W. Carr, A new look at the selectivity of RPC columns. The hydrophobic subtraction model evaluates the selectivity of HPLC reversed-phased columns so that researchers can choose a suitable substitute or a sufficiently orthogonal second column, Anal. Chem. 79 (2007) 3254-3262.

[23] J. Li, B. Cai, Evaluation of the retention dependence on the physicochemical properties of solutes in reversed-phase liquid chromatographic linear gradient elution based on linear solvation energy relationships, J. Chromatogr. A 905 (2001) 35-46.

[24] K. Valko, S. Espinosa, C.M. Du, E. Bosch, M. Roses, C. Bevan, M.H. Abraham, Unique selectivity of perfluorinated stationary phases with 2,2,2-trifluoroethanol as organic mobile phase modifier, J. Chromatogr. A 933 (2001) 73-81.

[25] C.M. Du, K. Valko, C. Bevan, D. Reynolds, M.H. Abraham, Characterizing the selectivity of stationary phases and organic modifiers in reversed-phase high-performance liquid chromatographic systems by a general solvation equation using gradient elution, J. Chromatogr. Sci. 38 (2000) 503-511.

[26] M. Tswett, Adsorptionanalyse und chromatographische methode. Anwendung auf die chemie des chlorophylls, Ber. Dtsch. Bot. Ges. 24 (1906) 384-393.

[27] M. Tswett, Physikalisch-chemische studien über das chlorophyll. Die adsorption, Ber. Dtsch. Bot. Ges. 24 (1906) 316-326.

[28] A.J. Martin, R.L. Synge, A new form of chromatogram employing two liquid phases: A theory of chromatography. 2. Application to the micro-determination of the higher monoamino-acids in proteins, Biochem. J. 35 (1941) 1358-1368.

[29] S. Moore, D.H. Spackman, W.H. Stein, Chromatography of amino acids on sulfonated polystyrene resins - an improved system, Anal. Chem. 30 (1958) 1185-1190.

[30] D.H. Spackman, W.H. Stein, S. Moore, Automatic recording apparatus for use in the chromatography of amino acids, Anal. Chem. 30 (1958) 1190-1206.

[31] J.C. Moore, Gel permeation chromatography. I. New method for molecular weight

distribution of high polymers, J. Polym. Sci. Part A 2 (1964) 835-843.

[32] L.S. Ettre, Jim Waters: The development of GPC and the first commercial HPLC instruments, LCGC North Am. 23 (2005) 752-761.

[33] C.G. Horvath, S.R. Lipsky, Use of liquid ion exchange chromatography for separation of organic compounds, Nature 211 (1966) 748-749.

[34] P. Jiang, D. Wu, C.A. Lucy, Determination of void volume in normal phase liquid chromatography, J. Chromatogr. A 1324 (2014) 63-70.

[35] D.C. Harris, Quantitative chemical analysis, 7th ed., W. H. Freeman, New York, 2006.

[36] G.A. Howard, A.J.P. Martin, The separation of the C12-C18 fatty acids by reversed-phase partition chromatograhy, Biochem. J 46 (1950) 532-538.

[37] L.R. Snyder, J.J. Kirkland, J.W. Dolan, Introduction to modern liquid chromatography, 3rd ed., Wiley, Hoboken, N.J., 2010.

[38] L.R. Snyder, Principles of adsorption chromatography; the separation of nonionic organic compounds, Marcel Dekker, New York, 1968.

[39] A.W. Salotto, E.L. Weiser, K.P. Caffey, R.L. Carty, S.C. Racine, L.R. Snyder, Relative retention and column selectivity for the common polar bonded-phase columns: The diol-silica column in normal-phase high-performance liquid-chromatography, J. Chromatogr. 498 (1990) 55-65.

[40] P.L. Smith, W.T. Cooper, Retention and selectivity in amino, cyano and diol normal bonded phase high-performance liquid-chromatographic columns, J. Chromatogr. 410 (1987) 249-265.

[41] L.R. Snyder, J.J. Kirkland, J.L. Glajch, Practical HPLC method development, 2nd ed., Wiley, New York, 1997.

[42] C.S. Sychov, M.M. Ilyin, V.A. Davankov, K.O. Sochilina, Elucidation of retention mechanisms on hypercrosslinked polystyrene used as column packing material for high-performance liquid chromatography, J. Chromatogr. A 1030 (2004) 17-24.

[43] Y. Zhang, Y. Huang, P.W. Carr, Optimization of the synthesis of a hyper-crosslinked stationary phases: a new generation of highly efficient, acid-stable hyper-crosslinked materials for HPLC, J. Sep. Sci. 34 (2011) 1407-1422.

[44] V.L. McGuffin, Chapter 1 Theory of chromatography, in: E. Heftmann (Ed.) Chromatography : fundamentals and applications of chromatography and related differential migration methods, Elsevier, Amsterdam; Boston, 2004, pp. 1-88.

[45] C. Reichardt, T. Welton, Solvents and solvent effects in organic chemistry, 4th ed., Wiley-VCH, Weinheim, Germany, 2011.

[46] M.H. Abraham, D.S. Ballantine, B.K. Callihan, Revised linear solvation energy relationship coefficients for the 77-phase McReynolds data set based on an updated set of solute descriptors, J. Chromatogr. A 878 (2000) 115-124.

[46] P.C. Sadek, P.W. Carr, R.M. Doherty, M.J. Kamlet, R.W. Taft, M.H. Abraham, Study of retention processes in reversed-phase high-performance liquid-chromatography by the use of the solvatochromic comparison method, Anal. Chem. 57 (1985) 2971-2978.

[47] M.H. Abraham, A. Ibrahim, A.M. Zissimos, Determination of sets of solute descriptors from chromatographic measurements, J. Chromatogr. A 1037 (2004) 29-47.

Chapter Two. Retention mechanism of hypercrosslinked polystyrene silica hybrid phase in normal phase chromatography[1]

2.1 Introduction

Macroporous polystyrene–divinylbenzene (DVB) columns have been developed [1, 2] to circumvent the pH stability and other limitations of traditional silica phases [3, 4]. However, macroporous polystyrene-DVB stationary phase have poor adsorption capacity and efficiency compared to silica based columns [2]. Later, a new generation of homogeneous and rigid stationary phase called hypercrosslinked (HC) polystyrenes was synthesized [5-10]. HC polystyrene phases possess long polystyrene chains that are extensively crosslinked by connecting phenyl groups with methylene groups [11]. HC polystyrene phases have large inner surface area (up to 1000–1500m^2/g), shows better efficiency and adsorption capacity than macroporous polystyrene DVB [4, 8]. HC polystyrene phases are pH stable and compatible with polar, nonpolar and aqueous mobile phases. These properties have resulted in HC polystyrene phases becoming very promising new stationary phases that have been used for solid-phase extraction [12, 13], and both reversed and normal phase liquid chromatography (LC) [10, 14].

Normal phase liquid chromatography (NPLC) separations have been performed with fully polymeric hypercrosslinked polystyrene [5, 8] and with silica particles possessing a thin layer of highly crosslinked aromatic network [15-22]. The Carr group developed these polymer-silica hybrid phases as acid and thermal stable phases for reversed phase [15-22]. The highly crosslinked aromatic network prevents loss of stationary phase under extreme conditions. HC polystyrene silica hybrid phases can provide orthogonal

[1] A version of this chapter has been published as: D. Wu, G.K. Nedev, C.A. Lucy, "Retention mechanism of hypercrosslinked polystyrene silica hybrid phase in normal phase chromatography", J. Chromatogr. A 1370 (2014) 50-55. I was responsible for the experiments and data analysis, as well as preparation of the manuscript. George K. Nedev was responsible for column synthesis and packing.

selectivity in ultra-fast, 2D-LC[16]. A wide array of HC polystyrene silica hybrid phases have been developed, including HC-COOH [19], HC-C_8 [19], and HC-Tol [22]. Recently, our group observed that the HC-Tol phase provided unique and useful group-type selectivity for the nitrogen containing compounds under normal phase conditions [23]. In the HC-Tol phase, the silanized silica is primarily cross-linked, secondary crosslinked and finally derivatized with toluene [22]. Despite the good reproducibility, high efficiency and better acid stability than most of the commercialized acid stable phases, these silica-base HC phases are not widely used [16]. This lack of usage may be due in part to the lack of understanding of the retention mechanism.

Davankov and co-workers [4, 5, 8] referred to normal phase LC on HC polystyrene phases as *quasi-normal phase* to reflect the lack of discrete polar groups (i.e., adsorption sites) in the structure of HC polystyrene. HC-Tol column also does not have polar sites on the surface. This work seeks an understanding of the quasi-normal phase retention on the HC-Tol column. Hopefully, to promote the use of silica-base HC phases.

2.2 Theory

NPLC uses a polar stationary phase and a less polar mobile phase. NPLC stationary phases usually possess discrete polar sites, such as silanols, amines or cyano groups [24]. NPLC mobile phases are mixture of a nonpolar solvent A such as hexane and a polar solvent B such as dichloromethane (DCM). The latter one acts as the strong mobile phase component.

To understand the quasi-normal phase retention of HC-Tol column, it is important to understand the dependence of the retention factor on the mobile phase composition and solvent strength. In this chapter, we use the widely accepted Snyder–Soczewiński model [25-29]. In the 1960s, Snyder developed a model for liquid solid chromatography [30-33]. Later, Soczewiński and co-workers [34] suggested an alternative model. The two models are equivalent [35] and so are generally referred to as the Snyder–Soczewiński

displacement model. The Snyder–Soczewiński model fit and explained normal phase retention data better than the other models [25, 36], and has provided understanding of retention on silica [31], alumina[32], bonded phases [29] and other phases [37] under normal phase conditions.

According to the Snyder–Soczewiński displacement model [25-29], a solvent monolayer is present on the surface of the stationary phase. Solutes must replace adsorbed solvent molecules of comparable size to be retained. Solvent-solute interactions are lost in the mobile phase but the same interactions are gained on stationary phase, and so the net effect balances out and is ignored. The relative retention of a solute under two mobile phase conditions is [26]:

$$\log\left(\frac{k_j}{k_i}\right) = \alpha A_S(\varepsilon_i - \varepsilon_j) \tag{2-1}$$

where k is the retention factor, ε is the solvent strength parameter, α is the stationary phase activity factor, and A_S is the relative area of interaction between the solute and the adsorbent surface.

A_S is the area occupied by an adsorbed molecule on the adsorbent. For flatwise adsorption, A_S can be calculated from the van der Waal's radii of the atoms corrected for the less efficient arrangement of molecules on a chromatographic surface than in a crystalline phase (*i.e.,* an 0.5 Å increase in the van der Waal's radius of all atoms) [30]. A_S for benzene was defined as 6 in units of 8.5 $Å^2$ [30].

Expressions for retention in reversed phase LC usually substitute the composition of the strong mobile phase B% for the solvent strength [24]. Such a substitution is not possible in normal phase because the solvent strength is not linearly related to B% [24]. For a binary mobile phase of A and B in normal phase LC, the solvent strength ε_{AB} of the mixture may be determined from the solvent strengths of pure A (ε_A) and pure B (ε_B):

$$\varepsilon_{AB} = \varepsilon_A + \frac{\log(N_B 10^{\alpha A_B(\varepsilon_B - \varepsilon_A)} + 1 - N_B)}{\alpha A_B} \tag{2-2}$$

where N_B is the mole fraction of B in the mobile phase, A_B is the relative area of the stationary phase occupied by solvent B (A_S of solvent B). Combining **Eq. 2-1** and **Eq. 2-2** provides an expression for the dependence of log k on the logarithm of the mole fraction of polar solvent B N_B.

An important aspect of the Snyder–Soczewiñski model is the *localization* of the solute and solvent on the stationary phase surface [26, 38-40]. **Figure 2-1a** represents *non-localized* retention, where a less polar solute and a less polar mobile phase adsorb in a non-oriented fashion to the stationary phase. There is not a specific one-to-one interaction formed between the solute or eluent molecules with the stationary phase. Rather there are multiple transient interactions between the solvent/solute and stationary phase. Retention of solute involves replacement of an appropriate number of mobile phase molecules necessary to occupy the same area. For instance, as depicted in **Figure 2-1a**, adsorption of bromobenzene would displace two DCM molecules.

Figure 2-1b schematically represents a *localized* interaction. There is a distinct interaction (indicated by a bold double-headed arrow) between a specific functional group of a polar molecule and a discrete polar site (e.g. silanol) on the stationary phase surface. Retention of the solute involves disruption of the one-to-one interaction between the eluent and stationary phase, and formation of a one-to-one interaction between the solute and stationary phase. Mobile phase and solute compete directly for a polar site on the surface of stationary phase. Retention of solute involves replacement with an appropriate number of mobile phase molecules to occupy the same number of polar sites.

2.3 Experimental

2.3.1 Apparatus

All experiments were performed on an Agilent 1260 Infinity LC (Agilent, Santa Clara, CA, USA) consisting of a quaternary pump, an on-line degasser, an auto-sampler performing a 1 μL partial loop injection, a column heater at 35°C, and a variable

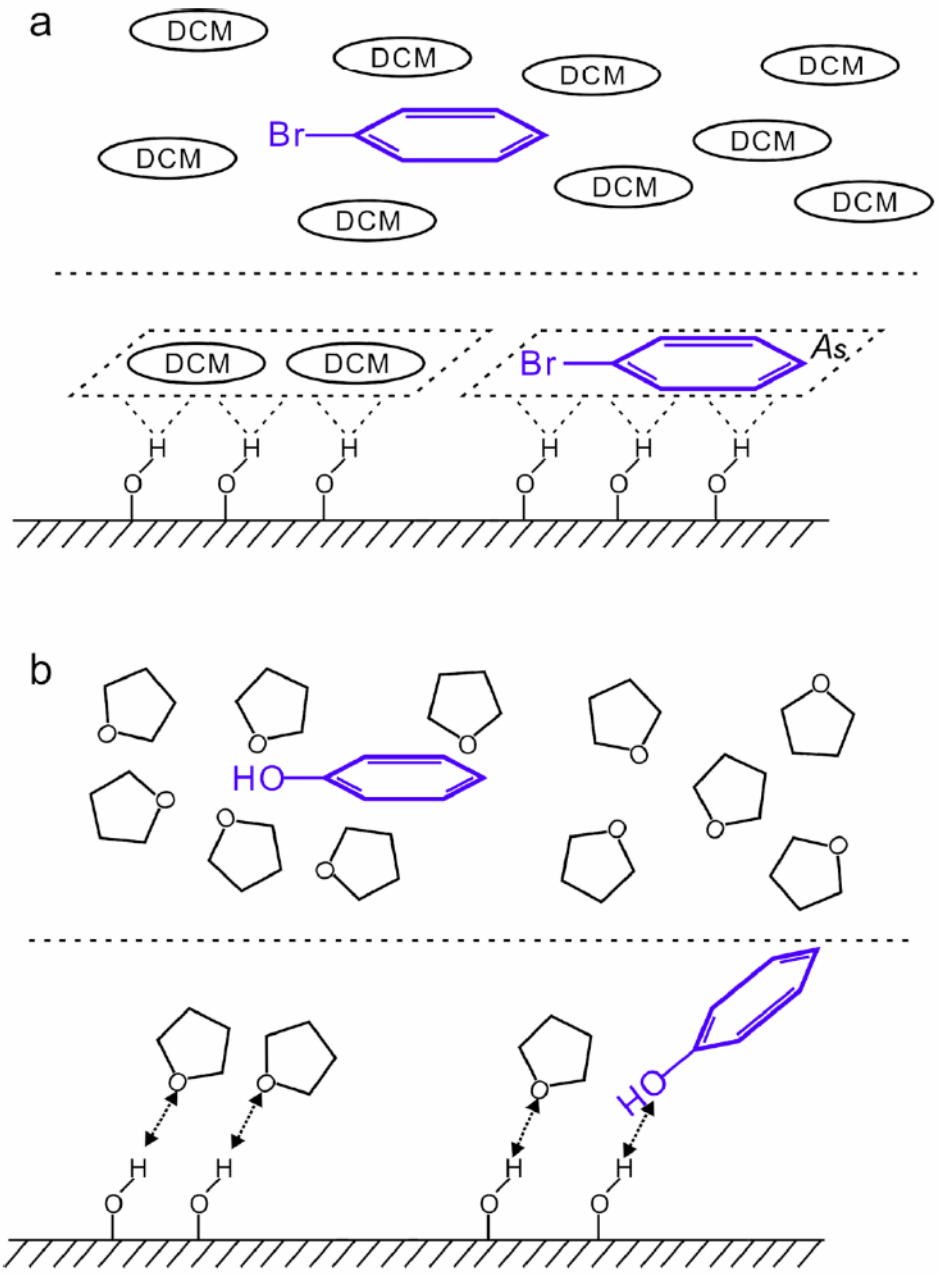

Figure 2-1 Illustration of solute and solvent localization: a) nonlocalizing solvent dichloromethane (DCM) and nonlocalizing solute bromobenzene; and b) localizing solvent tetrahydrofuran (THF) and localizing solute phenol. Adapted from [39].

wavelength detector set at 254 nm (280 nm when benzene was used as mobile phase) with a response time of 1 s. Data acquisition at 10 Hz was controlled using Agilent Chemstation software. All tubing and fittings were stainless steel (0.17 mm ID). The length of all connecting tubing was minimized.

The retention factors were calculated using the dead time t_0 based on the first peak caused by injection of pure hexane [41].

2.3.2 Chemicals

All solutes were >90% purity. Optima grade hexane, DCM, THF, benzene were purchased from Thermo Fisher Scientific Inc. (Fairlawn, NJ, USA). Chrysene and picene were from K & K Laboratories (Carlsbad, CA, USA). All other solutes were from Sigma–Aldrich (St. Louis, MO, USA). Solute solutions were 0.05 to 5 mg/mL, and filtered through 0.20 μm Millex syringe filters (EMD Millipore Corporation, Billerica, MA, USA) prior to injection.

2.3.3 Column

The HC-Tol phase was synthesized according to reference [22, 42]. Silanization and crosslinking were carried out on the surface of Zorbax RX-Sil Type B silica (5 μm, 180 m^2/g, 80 Å pore size, Agilent Technologies Inc., Wilmington, DE, USA). The substrate silica was first silanized with dimethyl-chloromethylphenylethylchlorosilane, primary cross-linked by triphenylmethane, then secondary cross-linked by 2,4,6-tris-(bromomethyl)-mesitylene, and finally derivatized with toluene.

After synthesis, the HC-Tol phase was slurry packed into a 50×4.6 mm i.d. stainless steel column with 2 μm frits (Grace Davison Discovery Science, Deerfield, IL, USA) using a Haskel nitrogen-driven fluid pump (Burbank, CA, USA). One gram of HC-Tol particles was sonicated in 10 mL isopropanol for 15 min to wet the pores. The slurry was transferred into a 10 mL stainless steel reservoir (Lab Alliance, State College, PA, USA) and packed downward into the column jacket. The packing pressure was increased from 0 to 6000 psi (414 bar) over 30 s and then maintained at 6000 psi until 200 mL of

isopropanol was driven through the column.

After packing, the column was acid washed for increased stability under low pH reversed phase conditions [22, 42]. Previous research in our group showed that this acid treatment does not affect the behavior of HC-Tol under normal phase conditions [43].

2.4 Results and discussion

Unique and useful selectivity has been observed on HC polystyrene under normal phase conditions [4-12, 14]. Retention on HC polystyrene under normal phase conditions has been termed *quasi-normal phase*, as the HC phase possesses no discrete adsorption sites [4, 5, 8]. In this paper, the Snyder–Soczewiñski model [25-29] is used to gain fundamental understanding about what the term quasi-normal phase means. Of the hypercrosslinked phases, the HC-Tol is useful for group type separations of polar petroleum compounds [23]. Therefore, it was chosen as the sample column for these studies. Solvent strengths of different mobile phase compositions on the HC-Tol column were fit by the Snyder–Soczewiñski model. This enabled other solvent strengths on HC-Tol column to be related to the mobile phase composition. Access to solvent strength values facilitates optimizing retention and selectivity. Localization and adsorption sites on the HC-Tol surface were also studied.

2.4.1 Dependence of solvent strength on mobile phase composition

Polycyclic aromatic hydrocarbons (PAHs) have been used as model nonlocalizing solutes for the determination of the solvent strength on alumina [30], silica [30], and amino [29] NPLC columns. Therefore these solutes were used to determine the solvent strength of DCM/hexane mixtures on the HC-Tol column. The activity factor α of HC-Tol in **Eq. 2-1** was assumed to be one, as recommended by Snyder for preliminary studies of new adsorbents [29, 30]. The solvent strength of the weak solvent (pure hexane) ε_A was defined to be 0 [29]. **Table 2-1** shows the solvent strengths for DCM/hexane mixtures determined using **Eq. 2-1** based on PAH retention from 0-50% DCM (**Table**

2-2). Solvent strength increases with increasing %DCM, consistent with general behavior in normal phase/quasi-normal phase [5, 24, 30]. The solvent strengths in **Table 2-1** are the same regardless of the PAH used, consistent with expectation that eluent strength is independent of solute.

The solvent strength of pure DCM (ε_B) was determined by fitting the solvent strength (ε_{AB}) from **Table 2-1** to **Eq. 2-2**. The interaction area of DCM (A_B) was 4.1 (relative to an area of benzene of 6) [30]. The resultant solvent strength for pure DCM (ε_B) on HC-Tol is 0.159±0.005. With the solvent strength of pure DCM, **Eq. 2-2** can be used to predict the solvent strength of any DCM/hexane mixture. **In Figure 2-2**, the solvent strength values predicted by **Eq. 2-2** (solid line) are compared to the experimental values (blue dots) from **Table 2-1**. The overall standard deviation is 0.008 which is comparable to that observed for DCM/hexane mobile phases on an amino column [29]. The fit between **Eq. 2-2** and the data in **Figure 2-2** improves if activity factor is greater than 1. However, solvent strength for pure DCM (ε_B) on HC-Tol remains in the experimental error of the value obtained with activity factor equal to 1. Therefore, we used the simple assumption that activity factor equal to 1. As a secondary check, the log k values of PAHs were regressed versus the solvent strength (ε_{AB}) (**Table 2-2**). The coefficients of determination (R^2) were ≥0.991 and the residuals were randomly scattered.

To verify that the solvent strengths (ε_{AB}) determined using PAHs were generally applicable for other solutes and to validate **Eq. 2-1**, **Figure 2-3** plots the log k of five solutes not used to determine ε_{AB} versus the solvent strength determined using the PAHs. The coefficients of determination (R^2) were ≥0.993 and the residuals were randomly scattered. Thus it is appropriate to apply **Eq. 2-1** to the HC-Tol column. The solvent strengths determined using the non-localizing PAHs are generally applicable to solute retention on the hypercrosslinked HC-Tol column, as has been observed for traditional NPLC phases such silica [30], alumina [30] and an amino bonded phase [29].

Table 2-1 Solvent strength of DCM/hexane on HC-Tol[a].

	3% DCM	5% DCM	7% DCM	10% DCM	20% DCM	30% DCM	40% DCM	50% DCM
N_B [b]	0.060	0.098	0.134	0.186	0.340	0.469	0.579	0.673
naphthalene	0.031	0.048	0.056	0.067	0.091	0.102	0.109	0.114
anthracene	0.028	0.044	0.051	0.062	0.085	0.099	0.108	0.117
pyrene	0.025	0.039	0.046	0.057	0.080	0.094	0.109	0.117
chrysene	0.030	0.044	0.052	0.062	0.085	0.101	0.115	0.121
picene	0.028	0.044	0.051	0.062	0.087	0.103	0.115	0.125
average	0.028±0.003	0.044±0.003	0.051±0.003	0.062±0.004	0.086±0.004	0.099±0.004	0.111±0.004	0.119±0.004

a. Conditions: column, HC-Tol, 50×4.6 mm i.d.; temperature, 35 ^{o}C; flow rate, 1.0 mL/min; detection, 254 nm; injection volume, 1 μL. Retention in 0% DCM/100% hexane was used as the reference point for calculation of the solvent strengths of DCM/hexane mixtures.

b. Mole fraction =DCM%$\times d_{DCM}$/[DCM%$\times d_{DCM}$+(1- DCM%)$\times d_{hexane}$].

d_{DCM}= density of DCM/molar mass of DCM=1.327 g mL^{-1} (20^{o}C) [44,45] /84.93 g mol^{-1}=0.01562 mol mL^{-1} (20^{o}C).

d_{hexane}= density of hexane/molar mass of hexane=0.6547 g mL^{-1} (24.99 ^{o}C) [46] / 86.18 g mol^{-1}=0.007597 mol mL^{-1}.

Table 2-2 Logarithm of retention factor of DCM/hexane on HC-Tol column[a].

Solute	0% DCM	3% DCM	5% DCM	7% DCM	10% DCM	20% DCM	30% DCM	40% DCM	50% DCM
naphthalene	-0.051	-0.305	-0.443	-0.501	-0.592	-0.787	-0.878	-0.933	-0.972
anthracene	0.343	0.053	-0.103	-0.177	-0.284	-0.525	-0.665	-0.763	-0.850
pyrene	0.458	0.195	0.039	-0.038	-0.147	-0.392	-0.546	-0.709	-0.794
chrysene	0.783	0.418	0.239	0.149	0.021	-0.268	-0.457	-0.638	-0.711
picene	1.241	0.843	0.612	0.502	0.345	-0.005	-0.238	-0.419	-0.553

a. Conditions as in **Table 2-1**

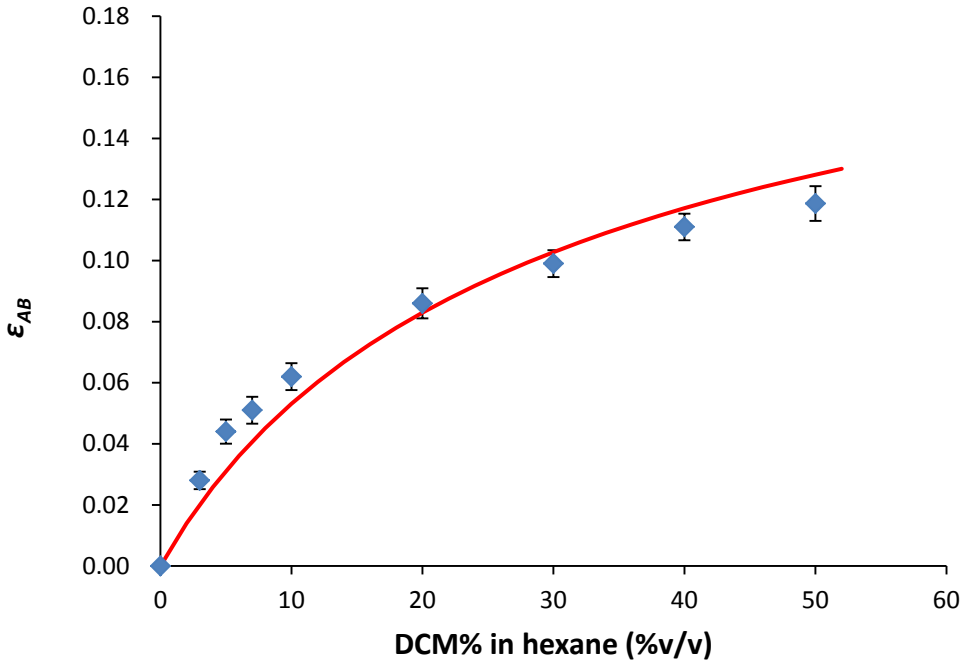

Figure 2-2 Dependence of solvent strength on mobile phase composition. Conditions: column, HC-Tol, 50×4.6 mm i.d.; temperature, 35 ^{o}C; flow rate, 1.0 mL/min; detection, 254 nm; injection volume, 1 µL. Error bar is 95% confidence interval. (◆) experimental; (—) predicted by **Eq. 2-2**.

2.4.2 Methodology to test for localization on a column

Traditional NPLC stationary phases such as silica and amine bonded phases have discrete polar sites. Thus all NPLC columns can be considered to be inherently localizing. Hypercrosslinked polystyrene phases do not have discrete polar sites. Davankov and coworkers used the term *quasi-normal phase* to reflect their expectation that the hypercrosslinked polystyrene would be non-localizing in its interactions [4, 5, 8]. Localization has traditionally been a descriptor for only solvent and solute, since all supports in normal phase could be considered localizing. In this section, we review the behavior of non-localizing solvents, and then apply similar methodologies with localizing solvents to reveal whether a hypercrosslinked polystyrene phase is indeed non-localizing or actually a localizing phase.

As shown in **Figure 2-1**, interactions of a solute or solvent with the stationary phase may either be localized or non-localized. Polar solutes (e.g., phenol and 2-nitroanisole) and polar solvents (e.g., THF and acetonitrile) localize on stationary phases that possess discrete polar adsorption sites [24, 39]. Less polar solutes (e.g., bromobenzene and chlorobenzene) and solvents (e.g., DCM and benzene) adsorb in a less oriented fashion [24, 39].

For non-localizing solvents and any solutes, retention follows:

$$\log k = \log k_0 - A_S \varepsilon \tag{2-3}$$

where k_0 is the solute retention factor in pure weak (nonpolar) mobile phase (e.g., hexane), and ε is the mobile-phase strength determining using non-localizing PAHs. Thus, plots of log k vs. mobile-phase strength (ε) should show linear dependence on ε, regardless of whether the solutes are localizing (**Figure 2-3**) or non-localizing (**Figure 2-4**).

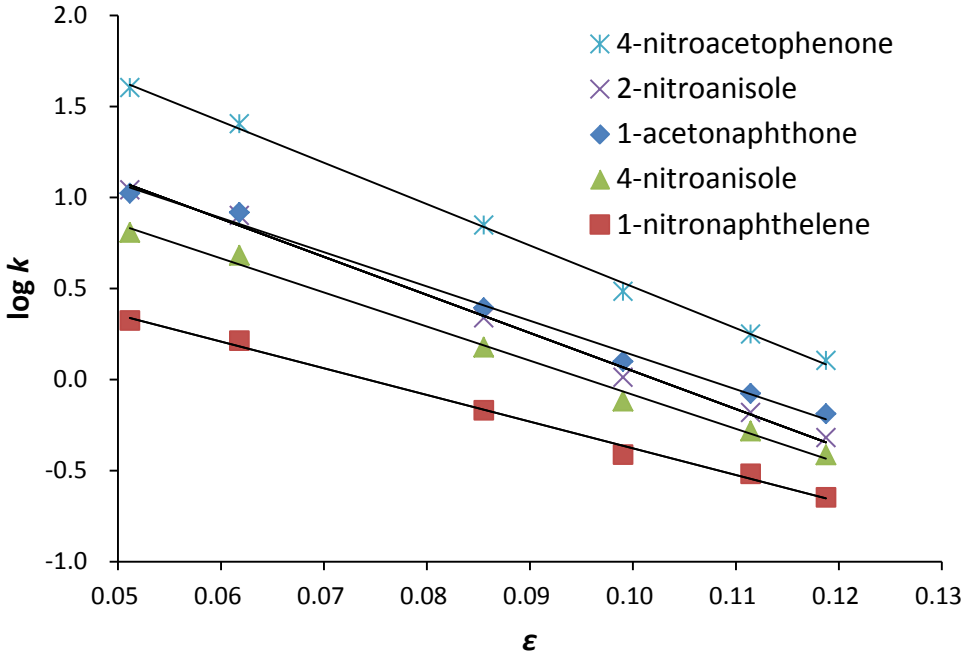

Figure 2-3 Dependence of log k on solvent strength of DCM/hexane mixtures for localizing compounds not used to determine ε_{AB}. Conditions as in **Figure 2-2**.

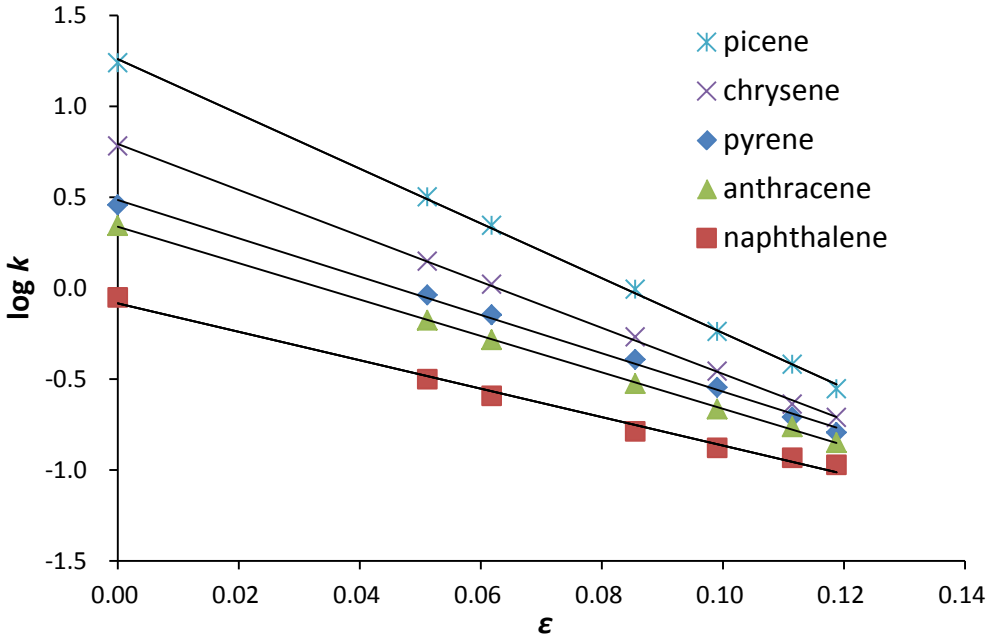

Figure 2-4 Dependence of log k on solvent strength of DCM/hexane mixtures for the PAHs (**Table 2-2**) that were used to establish the solvent strength. Conditions as in **Figure 2-2**.

Use a different non-localizing mobile phase (e.g., benzene/hexane in place of DCM/hexane) should yield the same retention for all compounds for a given ε_{AB} [39]. Thus for a given $\varepsilon_{AB,}$ a plot of log k_i versus the log k_j for a variety of solutes should be linear if non-localizing eluents are used [39]. **Figure 2-5** shows such a plot. Benzene is a non-localizing solvent [39]. Retention of PAHs with benzene/hexane mobile phases enabled determination of the solvent strength of pure benzene on HC-Tol ($\varepsilon_{benzene}$ = 0.127±0.008). 17% benzene/hexane has a similar solvent strength (ε_{AB} = 0.065±0.005) to 10% DCM/hexane. The solutes studied in **Figure 2-5** are very strongly localizing [30]. However, since both mobile phases are non-localizing, no complications from the competition of localizing solutes and solvents would be expected, regardless of the stationary phase. The strong correlation in **Figure 2-5** confirms this expectation.

We now extend this argument to the stationary phase. If a stationary phase were truly non-localizing, as the term quasi-normal phase implies, a plot such as **Figure 2-5** would be linear regardless of the mobile phases used. The experiment in **Figure 2-5** was repeated using a localizing strong mobile phase component (THF). Solvent strength values of THF/hexane mixtures **(Table 2-3)** enable determination of the pure solvent strength of THF on HC-Tol (ε_{THF} =0.22±0.01). 7% THF in hexane has the same ε_{AB} as 10% DCM in hexane. **Figure 2-6** shows the retention of the localizing test solutes with a non-localizing solvent (DCM) vs. a localizing solvent (THF). The plot shows substantial scatter, indicating that localized retention is occurring on the HC-Tol column. As shown in **Figure 2-7** and **Figure 2-8**, small changes in the %THF had no effect on the scatter observed in **Figure 2-6**. Due to localization, replacing a localizing B solvent with a less polar nonlocalizing B solvent causes a higher net adsorption energy, and thus preferential retention of the more polar solutes [39].

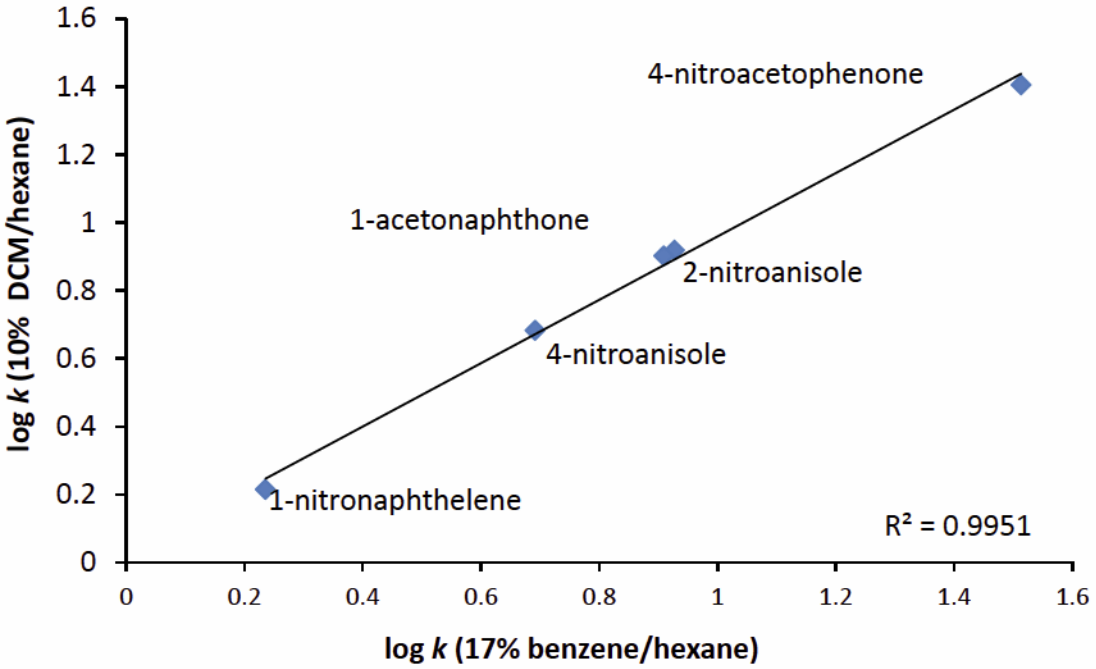

Figure 2-5 log *k*-log *k* plot for two nonlocalizing solvents ($\varepsilon_{AB} = 0.06$). Conditions as in **Figure 2-2** except detector was at 280 nm when benzene was used as mobile phase.

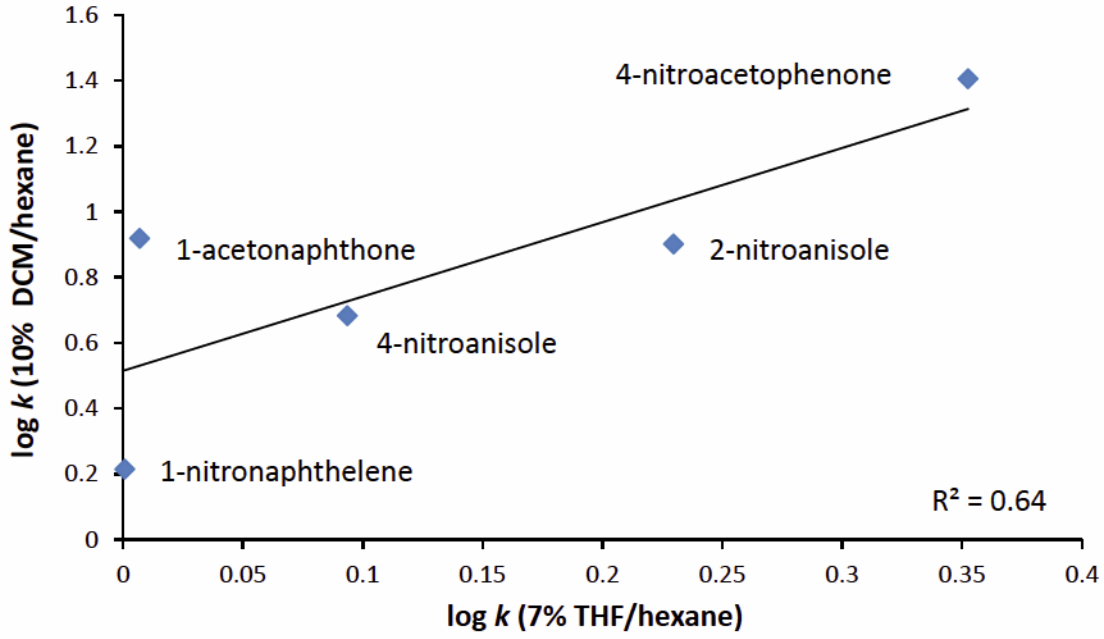

Figure 2-6 log *k*-log *k* plot for one nonlocalizing solvent DCM and one localizing solvent THF. Conditions as in **Figure 2-2**.

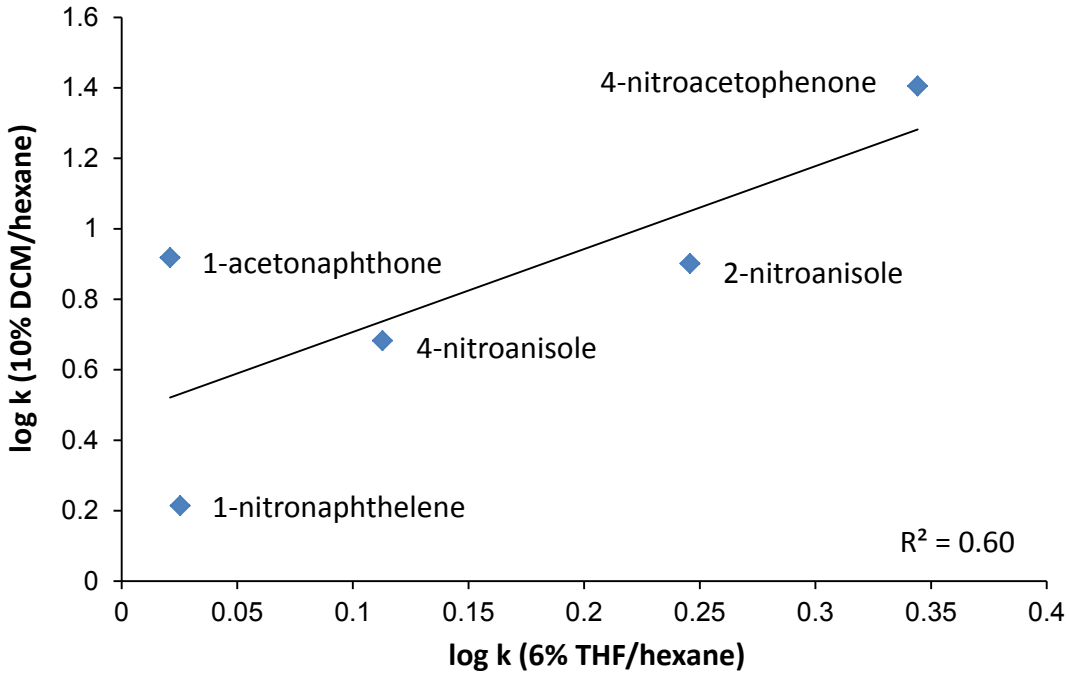

Figure 2-7 log *k*-log *k* plot for 6% THF/hexane and 10% DCM/hexane. Conditions as in **Figure 2-2.**

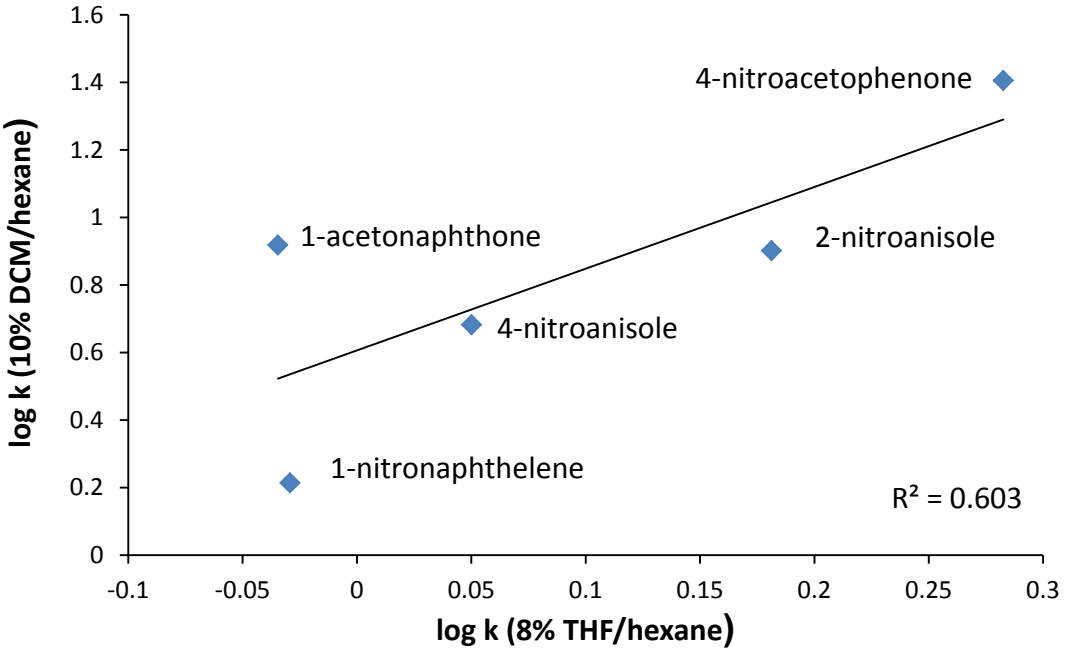

Figure 2-8 log *k*-log *k* plot for 8% THF/hexane and 10% DCM/hexane. Conditions as in **Figure 2-2.** .

Table 2-3 Solvent strength ε of THF/hexane on HC-Tol column[a] .

Solute	0% THF	1% THF	2% THF	3% THF	4% THF	5% THF	6% THF	7% THF	8% THF
Average	0	0.045	0.047	0.051	0.054	0.056	0.059	0.062	0.063
naphthalene	0	0.057	0.059	0.063	0.066	0.069	0.071	0.074	0.074
anthracene	0	0.047	0.049	0.052	0.055	0.057	0.060	0.062	0.063
pyrene	0	0.039	0.040	0.044	0.047	0.049	0.051	0.054	0.055
chrysene	0	0.043	0.045	0.049	0.052	0.054	0.057	0.059	0.061
picene	0	0.041	0.043	0.046	0.050	0.053	0.056	0.058	0.61

a. Conditions as in **Figure 2-2**

2.4.3 Nature of the sorption sites on HC-Tol

Figure 2-6 shows that localized adsorption occurs on HC-Tol. **Figure 2-1b** suggests that the area of interaction for a localized solute would be less than that for a nonlocalized solute (A_S). However when a solute localizes on the stationary phase, a solvent molecule may simultaneously interact with the same polar site – an effect known as *site-competition delocalization* [28]. There is site-competition delocalization on the silica [28] and amino column [29]. Site-competition delocalization has the effect of increasing the effective area of interaction.

To determine if site-competition delocalization occurs on the HC-Tol phase, experimental values of A_S can be compared with calculated values [28, 29]. Experimental A_S values are calculated from the slopes of **Figure 2-3** and **Figure 2-4** According to **Eq. 2-1**, slope equals $-A_S$. The calculated A_S values for a compound adsorbed flat on the surface were determined by summing Snyder's increment values for the components of the molecule [30].

Table 2-4 summarizes the experimental and calculated A_S for nonlocalizing and localizing solutes. For the nonlocalizing solutes there is good agreement between the observed and calculated interaction areas, as would be expected. For the localizing solutes, the observed and calculated interaction areas do not agree, consistent with the conclusion above that HC-Tol is a localizing stationary phase. Moreover the experimental A_S are larger than the calculated values. This means site-competition delocalization is occurring on the HC-Tol stationary phase. Site-competition delocalization only happens when the adsorption sites extend above the surface, e.g., silanols on silica [39]. Site-competition delocalization is not observed on alumina because its adsorption sites are buried under the surface and so cannot participate in lateral interactions. That site-competition delocalization occurs on HC-Tol indicates that whatever its adsorption groups are, they must extend above the surface.

Table 2-4 Experimental and calculated interaction area.

Compounds	A_S (experimental)[a]	A_S (calculated)[b]
Nonlocalizing compounds		
picene	15.1±0.2	14.4
chrysene	12.6±0.1	12.3
pyrene	10.5±0.3	10.7
anthracene	10.02±0.09	10.2
naphthalene	7.8±0.03	8.1
Localizing compounds		
1-acetonaphthone	18.8±0.8	9.6
1-nitronaphthelene	14.7±0.5	9.4
4-nitroanisole	18.7±0.7	10.5
2-nitroanisole	20.9±0.7	10.5
4-nitroacetophenone	22.7±0.5	10.9

a. Experimental A_S are determined from the slopes of **Figure 2-3** and **Figure 2-4**.

b. Calculated A_S are determined by summing Snyder's increment values for the components of the molecule.

2.5 Conclusions

Hypercrosslinked polystyrene phases have been described as quasi-normal phase, because there is no explicit polar site in their structure. The Snyder–Soczewiñski model of adsorptive chromatography was used to gain fundamental understanding about retention on the HC-Tol column. The term quasi-normal phase suggests that hypercrosslinked polystyrene phases should behave as nonlocalizing stationary phases. However, experiments demonstrate that HC-Tol is a localizing stationary phase which suggests HC-Tol has polar adsorption sites on its surface. Polar compounds are more retained on HC-Tol. Also, site-competition delocalization demonstrates that the adsorption groups on the HC-Tol stationary phase must extend above the surface. Thus, HC-Tol is actually a normal phase stationary phase, with localized retention on discrete extended adsorption sites.

2.6 References

[1] M. Galia, F. Svec, J.M.J. Frechet, Monodisperse polymer beads as packing material for high-performance liquid-chromatography - effect of divinylbenzene content on the porous and chromatographic properties of poly-n-styrene-co-divinylbenzene) beads prepared in presence of linear polystyrene as a porogen, J. Polym. Sci. A Polym. Chem. 32 (1994) 2169-2175.

[2] J. Zhang, S.L. Wu, J. Kim, B.L. Karger, Ultratrace liquid chromatography/mass spectrometry analysis of large peptides with post-translational modifications using narrow-bore poly(styrene-divinylbenzene) monolithic columns and extended range proteomic analysis, J. Chromatogr. A 1154 (2007) 295-307.

[3] J.L. Glajch, J.J. Kirkland, J. Kohler, Effect of column degradation on the reversed-phase high-performance liquid chromatographic separation of peptides and proteins, J. Chromatogr. 384 (1987) 81-90.

[4] V.A. Davankov, M.P. Tsyurupa, Hypercrosslinked polymeric networks and adsorbing

materials : synthesis, properties, structure, and applications, 1st ed., Elsevier, Amsterdam ; Boston, 2011.

[5] V. Davankov, C.S. Sychov, M.M. Ilyin, K.O. Sochilina, Hypercrosslinked polystyrene as a novel type of high-performance liquid chromatography column packing material - Mechanisms of retention, J. Chromatogr. A 987 (2003) 67-75.

[6] V.A. Davankov, M.P. Tsyurupa, N.N. Alexienko, Selectivity in preparative separations of inorganic electrolytes by size-exclusion chromatography on hypercrosslinked polystyrene and microporous carbons, J. Chromatogr. A 1100 (2005) 32-39.

[7] V. Davankov, M. Tsyurupa, Preparative frontal size-exclusion chromatography of mineral ions on neutral hypercrosslinked polystyrene, J. Chromatogr. A 1087 (2005) 3-12.

[8] C.S. Sychov, M.M. Ilyin, V.A. Davankov, K.O. Sochilina, Elucidation of retention mechanisms on hypercrosslinked polystyrene used as column packing material for high-performance liquid chromatography, J. Chromatogr. A 1030 (2004) 17-24.

[9] M.P. Baya, P.A. Siskos, V.A. Davankov, Evaluation of a hypercrosslinked polystyrene, MN-200, as a sorbent for the preconcentration of volatile organic compounds in air, J. AOAC Int. 83 (2000) 579-583.

[10] S.V. Prokopov, E.V. Tyrina, V.A. Davankov, M.M. Il'in, S.V. Kurbatova, Quasi-normal phase chromatography of nitrogen-containing adamantane derivatives, Russ. J. Phys. Chem. A 87 (2013) 114-119.

[11] V.A. Davankov, M.P. Tsyurupa, Structure and properties of hypercrosslinked polystyrene - the 1st representative of a new class of polymer networks, React. Polym. 13 (1990) 27-42.

[12] N. Fontanals, J. Cortes, M. Galia, R.M. Marce, P.A.G. Cormack, F. Borrull, D.C. Sherrington, Synthesis of Davankov-type hypercrosslinked resins using different isomer compositions of vinylbenzyl chloride monomer, and application in the solid-phase extraction of polar compounds, J. Polym. Sci. A Polym. Chem. 43 (2005) 1718-1728.

[13] N. Fontanals, M. Galia, P.A.G. Cormack, R.M. Marce, D.C. Sherrington, F. Borrull, Evaluation of a new hypercrosslinked polymer as a sorbent for solid-phase extraction of polar compounds, J. Chromatogr. A 1075 (2005) 51-56.

[14] S.V. Prokopov, S.V. Kurbatova, V.A. Davankov, M.A. Il'in, Chromatographic retention of adamantylamidrazones and triazoles by octadecyl silica gel and hypercrosslinked polystyrenes from water-acetonitrile solutions, Russ. J. Phys. Chem. A 86 (2012) 852-859.

[15] L.J. Ma, H. Luo, J. Dai, P.W. Carr, Development of acid stable, hyper-crosslinked, silica-based reversed-phase liquid chromatography supports for the separation of organic bases, J. Chromatogr. A 1114 (2006) 21-28.

[16] Y. Zhang, H. Luo, P.W. Carr, Silica-based, hyper-crosslinked acid stable stationary phases for high performance liquid chromatography, J. Chromatogr. A 1228 (2012) 110-124.

[17] H. Luo, L. Ma, Y. Zhang, P.W. Carr, Synthesis and characterization of silica-based hyper-crosslinked sulfonate-modified reversed stationary phases, J. Chromatogr. A 1182 (2008) 41-55.

[18] B.C. Trammell, L. Ma, H. Luo, M.A. Hillmyer, P.W. Carr, An ultra acid stable reversed stationary phase, J. Am. Chem. Soc. 125 (2003) 10504-10505.

[19] B.C. Trammell, L. Ma, H. Luo, M.A. Hillmyer, P.W. Carr, Synthesis and characterization of hypercrosslinked, surface-confined, ultra-stable silica-based stationary phases, J. Chromatogr. A 1060 (2004) 61-76.

[20] B.C. Trammell, L. Ma, H. Luo, D. Jin, M.A. Hillmyer, P.W. Carr, Highly cross-linked self-assembled monolayer stationary phases: an approach to greatly enhancing the low pH stability of silica-based stationary phases, Anal. Chem. 74 (2002) 4634-4639.

[21] Y. Zhang, P.W. Carr, Novel ultra stable silica-based stationary phases for reversed phase liquid chromatography--study of a hydrophobically assisted weak acid cation

exchange phase, J. Chromatogr. A 1218 (2011) 763-777.

[22] Y. Zhang, Y. Huang, P.W. Carr, Optimization of the synthesis of a hyper-crosslinked stationary phases: a new generation of highly efficient, acid-stable hyper-crosslinked materials for HPLC, J. Sep. Sci. 34 (2011) 1407-1422.

[23] N.E. Oro, C.A. Lucy, Comparison of hypercrosslinked polystyrene columns for the separation of nitrogen group-types in petroleum using high performance liquid chromatography, J. Chromatogr. A 1217 (2010) 6178-6185.

[24] L.R. Snyder, J.J. Kirkland, J.W. Dolan, Introduction to modern liquid chromatography, 3rd ed., Wiley, Hoboken, N.J., 2010.

[25] L.R. Snyder, H. Poppe, Mechanism of solute retention in liquid-solid chromatography and the role of the mobile phase in affecting separation - competition versus sorption, J. Chromatogr. 184 (1980) 363-413.

[26] J.L. Glajch, L.R. Snyder, Solvent strength of multicomponent mobile phases in liquid-solid chromatography: Mixtures of three or more solvents, J. Chromatogr. 214 (1981) 21-34.

[27] L.R. Snyder, J.L. Glajch, Solvent strength of multicomponent mobile phases in liquid-solid chromatography: Binary-solvent mixtures and solvent localization, J. Chromatogr. 214 (1981) 1-19.

[28] L.R. Snyder, J.L. Glajch, Solvent strength of multicomponent mobile phases in liquid-solid chromatography: Further study of different mobile phases and silica as adsorbent, J. Chromatogr. 248 (1982) 165-182.

[29] L.R. Snyder, T.C. Schunk, Retention mechanism and the role of the mobile phase in normal-phase separation on amino-bonded-phase columns, Anal. Chem. 54 (1982) 1764-1772.

[30] L.R. Snyder, Principles of adsorption chromatography; the separation of nonionic organic compounds, Marcel Dekker, New York, 1968.

[31] L.R. Snyder, Linear elution adsorption chromatography: V. Silica as adsorbent.

Adsorbent standardization, J. Chromatogr. 11 (1963) 195-227.

[32] L.R. Snyder, Linear elution adsorption chromatography: IV. Group localization in the adsorbate. Extension of the role of solute structure in separations over alumina, J. Chromatogr. 8 (1962) 319-342.

[33] L.R. Snyder, Linear elution adsorption chromatography: III. Further delineation of the eluent role in separations over alumina, J. Chromatogr. 8 (1962) 178-200.

[34] Soczewiński.E, Solvent composition effects in thin-layer chromatography systems of type silica gel-electron donor solvent, Anal. Chem. 41 (1969) 179–182.

[35] L.R. Snyder, Role of solvent in liquid-solid chromatography - review, Anal. Chem. 46 (1974) 1384-1393.

[36] M. Waksmundzka-Hajnos, A. Petruczynik, E. Soczewiński, A. Hawryl, Retention mechanism of model compounds on polar bonded stationary phases in normal phase systems, Chem. Anal. (Warsaw) 47 (2002) 483-505.

[37] J.L. Robinson, W.J. Robinson, M.A. Marshall, A.D. Barnes, K.J. Johnson, D.S. Salas, Liquid-solid chromatography on amberlite xad-2 and other styrene-divinylbenzene adsorbents .1. development of a solvent eluotropic scale, J. Chromatogr. 189 (1980) 145-167.

[38] L.R. Snyder, Localization in adsorption chromatography, J. Planar Chromatogr. 25 (2012) 184-189.

[39] L.R. Snyder, Solvent selectivity in normal-phase TLC, J. Planar Chromatogr. 21 (2008) 315-323.

[40] L.R. Snyder, J.L. Glajch, J.J. Kirkland, Theoretical basis for systematic optimization of mobile phase selectivity in liquid-solid chromatography - solvent-solute localization effects, J. Chromatogr. 218 (1981) 299-326.

[41] P. Jiang, D. Wu, C.A. Lucy, Determination of void volume in normal phase liquid chromatography, J. Chromatogr. A 1324 (2014) 63-70.

[42] M.H. Abraham, J.R.M. Gola, J. Gil-Lostes, W.E. Acree, Jr., J.E. Cometto-Muniz,

Determination of solvation descriptors for terpene hydrocarbons from chromatographic measurements, J. Chromatogr. A 1293 (2013) 133-141.

[43] G. Nedev, Mixed-mode retetnion on a hypercrosslinked silica-based column, Msc. thesis, University of Alberta, September 28th, 2012.

[44] D. Nurok, R.M. Kleyle, K.B. Lipkowitz, S.S. Myers, M.L. Kearns, Dependence of retention and separation quality in planar chromatography on properties of the mobile-phase, Anal. Chem. 65 (1993) 3701-3707.

[45] G.V.S.M. Carrera, C.A.M. Afonso, L.C. Branco, Interfacial properties, densities, and contact angles of task specific ionic liquids, J. Chem. Eng. Data 55 (2010) 609-615.

[46] M. Dominguez-Perez, E. Rilo, L. Segade, C. Franjo, O. Cabeza, Surface tension deviations and excess molar volumes on the ternary system propyl propanoate plus hexane plus p-xylene at 298.15 K, J. Chem. Eng. Data 55 (2010) 1317-1321.

Chapter Three. Linear solvation energy relationship (LSER) characterization of the normal phase retention mechanism on hypercrosslinked polystyrenes[1]

3.1 Introduction

Hypercrosslinked (HC) polystyrene phases are prepared from pre-formed polystyrene chains that are subsequently extensively (>40%) crosslinked, preferably by connecting the phenyl rings with methylene bridges [1-7]. Hypercrosslinked polystyrene is a rigid, extended 3-dimensional network with large surface area. Hypercrosslinked polystyrene is compatible with nonpolar, polar and even aqueous mobile phases [1, 2, 6]. Hypercrosslinked polystyrene materials have been used for solid-phase extraction [8, 9] and as high performance liquid chromatography stationary phases [7, 10]. Surprisingly, hypercrosslinked polystyrene has also been used under normal phase conditions [1, 2, 11]. Davankov and co-workers [1, 2] termed these separations *quasi-normal phase* to reflect the lack of discrete polar groups (*i.e.*, adsorption sites) in the structure of hypercross-linked polystyrene.

Quasi-normal phase HPLC separations have been performed with fully polymeric hypercrosslinked polystyrene (*e.g.*, Chromalite 5-HGN [1, 2]). Chromalite 5-HGN is 5 μm hypercrosslinked (H), gel type (G) and nonactivated (N) beaded polystyrene. Quasi-normal phase has also performed with silica particles possessing a thin highly crosslinked polystyrene layer developed by the Carr group [11]. The Carr group were not actually interested in normal phase chromatography. Rather they were developing an acid stable phase for reversed phase liquid chromatography [12-19]. This new generation of HC phases have a thin highly crosslinked polystyrene layer on the surface of a porous

[1] My colleague Ping Jiang was involved with the conception phase of this chapter and Georgi Nedev synthesized the HC-Tol column. I did all chromatographic experiments, data analysis, and writing.

silica particle. In the HC-Tol phase, porous silica is silanized with dimethylchloromethylphenylethylchlorosilane (blue in **Figure 1-3B**), then primarily crosslinked with triphenylmethane (red in **Figure 1-3B**), next secondarily crosslinked with 2,4,6-tris-(bromomethyl)-mesitylene (green in **Figure 1-3B**) and finally derivatized with toluene (purple in **Figure 1-3B**) [19].

Previous studies in our group demonstrated the group type separation of polycyclic aromatic hydrocarbons (PAHs), pyrroles and pyridines on HC-Tol using a step gradient [11]. *Group type separation* means that the separation contained essentially three peaks; with all PAHs in one peak, all pyrroles in a second peak, and all pyridines in a third peak. Group type separations are valuable in the petroleum industries, as they provide information about the composition and behavior of the petroleum.

While the HC-Tol phase was effective for these group type separations under normal phase conditions, its retention mechanism was unclear. Once the retention mechanism of these specific columns is understood, better modification of the stationary phase of these columns will be viable.

Linear solvation energy relationships (LSERs, **Section 1.4**) [20-26] are widely used to characterize the fundamental molecular interactions giving rise to retention and selectivity in chromatography. Interactions between solutes, solvents and stationary phase cannot be detected directly. But these intermolecular interactions can be understood by analyzing the chromatographic behavior using LSERs. Solvent parameters relevant to LSERs were first introduced by Kamlet, Taft and Abboud [27-29]. Abraham and Carr further developed this model [30, 31]. The latest notation of LSERs in chromatography presented by Abraham can be written as [32]:

$$\log k = c + eE + sS + aA + bB + vV \qquad (3\text{-}1)$$

where k is the retention factor, c is an intercept, and E, S, A, B and V are the solute dependent parameters accounting for intermolecular interactions:

E = solute excess polarizability

S = solute dipolarity plus some polarizability

A = solute hydrogen bond acidity

B = solute hydrogen bond basicity

V = solute McGowan [33] volume

Abraham and his coworkers calculated the parameters *(E*, *S*, *A*, *B*, *V*) for thousands of solutes [32, 34-36]. Abraham's solute parameters may also be obtained from commercial software such as ACD/ADME suite 5.0 from Advanced Chemistry Development, Inc. (Toronto, Canada), as was done in this study.

The coefficients *e*, *s*, *a*, *b*, and *v* are the differences between the stationary and mobile phases' excess polarizability, polarizability/dipolarity, hydrogen bond accepting ability, hydrogen bond donating ability, and cavity formation ability. These coefficients can be obtained by multivariable linear regression of solute parameters which are the input values. The coefficients are the complementary properties of the solute parameters. The sign of the coefficient reveals whether the interaction has a positive or negative impact on retention. The magnitude of the coefficient reveals the relative importance of the interaction to retention. Retention of a solute is determined by differences in the interactions between the solute and the stationary phase versus the solute and the mobile phase.

This chapter characterizes the retention mechanism of the hypercrosslinked polystyrene phase HC-Tol column under normal phase conditions. LSERs have been widely used to characterize solute partitioning between two bulk phases, such as in reversed phase chromatography [21-23]. LSER studies in normal phase chromatography are less common, but a few have been performed [24-26, 37]. Here I apply LSERs to retention on HC-Tol to elucidate the type and relative importance of molecular interactions between model solutes and the HC-Tol stationary phase. The results of this work will be very useful in guiding the design of improved hypercrosslinked polystyrene columns and enable HC phases to address important questions in petroleum science.

3.2 Experimental

3.2.1 Apparatus

An Agilent 1260 Infinity LC system (Agilent, Santa Clara, CA, USA) was used. The Agilent 1260 system includes a quaternary low pressure pump (1.0 mL/min), an on-line degasser, an auto-sampler (1 μL partial loop injection), a temperature controlled (35°C) column compartment, and a variable wavelength detector (254 nm). A wavelength of 269 nm was used to detect nitromethane.

3.2.2 Chemicals

Optima grade hexane, dichloromethane (DCM) and tetrahydrofuran (THF) were from Fisher (Thermo Fisher Scientific Inc., Fairlawn, NJ, USA). **Table 3-1** lists the model solutes and their source. All were analytical grade. Standard solutions containing each of the solutes were prepared at concentrations of 0.05 to 5 mg/mL, and passed through 0.20 μm Millex syringe driven filters (EMD Millipore Corporation, Billerica, MA, USA).

3.2.3 Columns

A Waters Spherisorb amino column (3 μm, 80 Å, 150 mm long × 4.6 mm ID, Waters Limited, Mississauga, ON, Canada) was used as a model NPLC stationary phase.

The HC-Tol phase was synthesized by my colleague Georgi Nedev according to the reference procedure [19, 36]. Silanization and crosslinking were carried out on the surface of Zorbax RX-Sil Type B silica (5 μm, 180 m^2/g surface area, 80 Å, Agilent Technologies Inc., Wilmington, DE, USA). The substrate silica was first silanized with dimethyl-chloromethylphenylethyl chlorosilane, then primary crosslinked with triphenylmethane, followed by secondary crosslinking with 2,4,6-tris-(bromomethyl)-mesitylene, and finally derivatized by toluene.

After synthesis, the HC-Tol phase was slurry packed into a 50 mm long × 4.6 mm ID stainless steel column with a 2 μm frit (Grace Davison Discovery Science, Deerfield, IL, USA) using a Haskel nitrogen-driven fluid pump (Burbank, CA, USA). Prior to

packing, one gram of HC-Tol particles was sonicated in 10 mL isopropanol for 15 min to wet the pores. The slurry was transferred into a 10 mL stainless steel reservoir (Lab Alliance, State College, PA, USA) and packed downward into the column jacket using isopropanol. The packing pressure was increased from 0 to 6000 psi (414 bar) in 30 s, and then was maintained at 6000 psi until 200 mL of isopropanol had passed through the column.

The 5-HGN particles were a gift from Purolite (Purolite International Limited, Wales, UK and Bala Cynwyd, PA, USA). The particles have a mean diameter of 5 μm, and their surface area is 1100–1500 m^2/g. The 5-HGN phase was home-packed in a 50 mm long × 4.6 mm ID stainless steel column using the same procedure as for the HC-Tol column.

3.2.4 Data analysis

The parameters of the solutes (solute descriptors) were obtained from ACD/ADME suite (ACD/Labs, Toronto, ON, Canada) [23]. If there was an Exact Match (*i.e.*, literature value), the Exact Match value was used. Otherwise, values estimated by the software were used.

Linear regression of log *k* versus the solute parameters was used to obtain the coefficients *c*, *e*, *s*, *a*, *b*, and *v* in **Eq. 3-1**. Multiple linear regression (MLR) was performed using the Data Analysis function in Excel. Partial least square (PLS) regression was performed using the PLS_tool box software (Eigenvector Research, Inc., Wenatchee, WA, USA). All data were mean centered during the PLS regression process. Due to the number of solutes, the leave-one-out method was used for cross validation, as recommended by Vitha and Carr [10].

3.2.5 Retention factor determination

For most solutes, the retention factor *k* was determined using:

$$k = \frac{t_R - t_0}{t_0} \tag{3-2}$$

where t_R is the retention time as determined by the peak maximum and t_0 is the dead time.

Dead time was determined using the first peak caused by injecting pure hexane [38].

Under weaker mobile phase conditions (*e.g.*, 5% DCM), some solutes (*e.g.*, 2-naphthol) were too strongly retained to allow direct measurement of their retention time. Previous studies had demonstrated that retention on HC-Tol was adsorptive in nature [11]. Therefore, the Snyder–Soczewiñski equation [39] was used to extrapolate the retention factor observed at ≥15% of the strong mobile phase to that predicted under the weak mobile phase conditions. The Snyder–Soczewiñski equation is:

$$\log k_{AB} = \log k_1 - n\log N_{\mathrm{B}} \tag{3-3}$$

where k_{AB} is the retention factor in a mobile phase consisting of mixture of a weak solvent (A) and a strong solvent (B), k_1 is the retention factor in pure strong solvent, n is a constant for a given solute assumed to be related to the solute area (Snyder model) or the number of polar substituents in the molecules (Soczewiñski model), and N_{B} is the mole fraction of solvent B in mobile phase. The nature of the slope n is discussed in detail in **Chapters 4** and **5**. N_{B} can usually be approximated by the volume fraction of strong solvent B (ϕ) to get **Eq. 3-4** [40]:

$$\log k_{AB} = \log k_1 - n\log \phi \tag{3-4}$$

In cases where retention was too strong to measure in weaker mobile phases (*e.g.*, 5% DCM), the retention under a series of stronger mobile phase conditions was extrapolated back to 5% DCM using **Eq. 3-4**. Examples of such extrapolations are shown in **Appendix A**.

3.3 Results and Discussion

Hypercrosslinked polystyrene is an inert, pH stable and highly porous material which is compatible with both organic and aqueous solvents [1, 2, 6]. These properties make hypercrosslinked polystyrene a good sorbent for HPLC. Hypercrosslinked polystyrene is prepared by crosslinking long polystyrene chains in solution. Hypercrosslinked polystyrene consists of extended, rigid three dimensional networks as

in **Figure 1-3A**. 5-HGN is a commercial hypercrosslinked polystyrene phase from Purolite International.

In contrast to the fully polymeric 5-HGN, HC-Tol has a hypercrosslinked polystyrene phase on the surface of porous silica particles (**Figure 1-3B**) [19, 20]. Within the silica-hypercrosslinked phases, HC-Tol is distinguished in that the last synthesis step is to derivatize the hypercrosslinked polystyrene with toluene (purple in **Figure 1-3B**). HC-Tol was designed as a reversed phase column with high tolerance to acidic conditions [19]. Subsequently, our group discovered that HC-Tol was capable of group-type separations of nitrogen compounds under normal phase conditions [11].

Under normal phase conditions, retention on 5-HGN and HC-Tol [11] is an adsorption process. However, the structure of hypercrosslinked phases such as 5-HGN and HC-Tol (**Figure 1-3**) do not possess discrete polar sites for adsorption. Hence, Davankov and co-workers refer to normal phase retention on hypercrosslinked phases as *quasi-normal phase* [1].

In this chapter, I construct Linear Solvation Energy Relationships (LSERs) for the 5-HGN and HC-Tol columns to elucidate the properties of the stationary phases. LSERs have been widely used to characterize gas-liquid chromatography [20, 41] and reversed phase liquid chromatography [21-23]. LSERs are based on general solute parameters, and characterize general intermolecular interactions. While, LSERs have been most widely used to describe bulk phase partition behavior [21-23], LSER studies of normal phase liquid chromatography have also been performed [24-26, 37].

3.3.1 Test solute selection and model development

To generate a robust LSER, the test solutes should be selected intentionally to cover a wide range in each of the solvatochromic parameters [20]. Practically, all test solutes must be soluble in the mobile phase (*i.e.*, in hexane or hexane with a small amount of polar modifier in our case) to avoid injection solvent effects [42]. Also, test solutes must

Table 3-1 Test solutes and their solvatochromic parameters.[a]

Solute	*A*	*B*	*S*	*E*	*V*
benzene	0.0	0.1	0.5	0.61	0.716
n-propylbenzene[c]	0.0	0.1	0.5	0.60	1.139
dibenzofuran	0.0	0.1	1.0	1.40	1.274
dibenzothiophene	0.0	0.2	1.3	1.95	1.379
naphthalene	0.0	0.2	0.9	1.34	1.085
1,3,5-tri-tert-butylbenzene[b,d,e]	0.0	0.2	0.3	0.57	2.407
Pyrene	0.0	0.2	1.5	2.60	1.584
anthracene	0.0	0.2	1.3	2.29	1.454
nitrobenzene	0.0	0.2	1.1	0.87	0.890
anisole	0.0	0.2	0.7	0.70	0.916
1-nitronaphthalene	0.0	0.2	1.5	1.60	1.259
dodecanophenone[b]	0.0	0.4	1.1	0.78	2.282
ethyl benzoate	0.0	0.4	0.8	0.68	1.213
acetophenone	0.0	0.4	1.0	0.81	1.013
1-acetonaphthone	0.0	0.5	1.4	1.51	1.382
acetone[c,e]	0.0	0.4	0.7	0.17	0.547
nitromethane	0.0	0.3	0.9	0.31	0.423
carbazole[d]	0.1	0.0	2.0	1.78	1.315
cinnamyl alcohol[f]	0.3	0.6	1.0	1.09	1.154
benzyl alcohol	0.3	0.5	0.8	0.80	0.916
Indole	0.4	0.2	1.1	1.20	0.946
phenol[d]	0.6	0.3	0.8	0.80	0.775
2-naphthol[c,d]	0.6	0.4	1.0	1.52	1.144

a. From the ACD/ADME suite software, ACD/Labs, Toronto, ON, Canada

b. No Exact Match in the ACD/ADME suite database. Therefore, the calculated parameters were used.

c. Not used for the amino column due to too high or too low retention

d. Not used for 5-HGN column due to too high or too low retention

e. Not used for HC-Tol column due to too high or too low retention

f. Used for amino and 5-HGN column as a substitution of 2-naphthol

be compatible with the detection mode used (UV absorbance herein). Based on these criteria, the test solutes in **Table 3-1** were chosen. The solvatochromic parameters of these test solutes are also given in the table.

In selecting test solutes for LSER analysis, the covariance between the solute parameters should be reviewed [20]. Strong covariance between the solvatochromic parameters indicates that these parameters represent the same interaction. The greater the covariance between two parameters, the larger the uncertainties there will be in the corresponding multi-linear regression coefficients [20]. **Table 3-2** summarizes the correlation coefficients between the parameters for the test solutes in **Table 3-1**.

Table 3-2 Correlation matrix for the LSERs parameters of solutes listed in **Table 3-1**.

	A	***B***	***S***	***E***	***V***
A	1.00				
B	0.23	1.00			
S	0.032	-0.08	1.00		
E	-0.02	-0.25	0.75	1.00	
V	-0.25	-0.03	0.15	0.33	1.00

The correlations in **Table 3-2** are low between most of the solute parameters. The most significant correlation in **Table 3-2** is the +0.75 between *S* (solute dipolarity plus some polarizability) and *E* (solute excess polarizability), which is due to both of these parameters being related to the solute polarizability [20]. This means that an LSER model would be highly unstable if multilinear regression (MLR) is used to build the LSER model [20]. A small perturbation in the input data may cause huge differences in the regression results.

In the studies below, two procedures were used to assess the impact of the covariance between *S* and *E*. First, both MLR and PLS regression were used to build

LSER models based on all of the solute parameters in **Table 3-1**. PLS does not regress to the *X* variables, *i.e*., the solute parameters herein. Rather, in PLS regression the *X* (solute parameters) and *Y* (log *k*) matrixes are projected into a new space where the fundamental relations (latent variables) between them are found. Then, PLS regresses to find the latent variables which correlate the *X* and *Y* matrix the most, and at the same time capture the maximum of the variance in *X* matrix. Thus, PLS regression has a higher tolerance to collinear solute parameters and small solute numbers [43, 44]. The second method to assess the impact of the covariance between *S* and *E* was to construct the LSER models based on all of the solute parameters in **Table 3-1**, and compare the LSER with those obtained with *E* and *V* parameters omitted (discussed below).

Our final validation step was to construct LSER models for amino phases. Such phases are widely used in normal phase chromatography, and have been the subject of past LSER studies [25, 26, 37]. Only after our data analysis procedures were valid for the amino column, did we start exploring the behavior of the novel hypercrosslinked polystyrene phases.

3.3.2 Amino NPLC stationary phases

Amino column is a commonly used NP stationary phase [45, 46]. To validate our modeling, LSER will first be constructed for a Spherisorb NH_2, consisting of porous silica with bonded amino propyl functionality (**Figure 1-2**), using the test solutes in **Table 3-1**.

Table 3-3 shows the regression results for the amino column. As noted in **Section 3.3.1**, MLR becomes unstable when there is significant co-variance between input variables [20]. Therefore, both MLR and PLS regression were used to create LSERs for the retention of the solutes in **Table 3-1** on the amino column using 5% DCM as mobile phase. Five % DCM was used because this is the appropriate mobile phase for the hypercrosslinked phases that are the primary focus of this study. The top two rows in **Table 3-3** show the LSER parameters for MLR and PLS regression based on all of the

solute parameters. The leave-one-out was used as a cross-validation method. Leave-one-out is an appropriate cross-validation method for small sample sets [47]. Four latent variables were chosen for the PLS regression, which give the smallest RMSECV (root mean square error of cross-validation), and capture >90% of the variance of the *X* (solute parameters) and *Y* (log *k*) matrix. PLS_tool box cannot provide a standard error for each coefficient. Thus, only the coefficients from MLR are presented with standard errors. The relative magnitude and sign of the coefficients derived from PLS regression and MLR using all solute parameters (**Table 3-3**, top two lines) agree well. All values from the PLS regression are within the 95% confidence interval of the MLR values. So according to the PLS results, the extent of collinearity noted in **Table 3-2** does not cause problems in the MLR [20].

To further evaluate the collinearity, unimportant variables were excluded from regression to test the robustness of the model. Since *v* is statistically equal to zero, it should have an insignificant effect on the regression model. Regression coefficients without *v* (**Table 3-3**, third line) agree well with the all parameter fit using MLR (**Table 3-3**, top line). The variable *e* is the next smallest of the LSER coefficients in **Table 3-3**, top line. So *e* was further excluded to avoid any possible collinearity problem (*S* and *E* have a correlation coefficient of 0.75, **Table 3-2**). The LSER coefficients excluding *e* and *v* (**Table 3-3** fourth line) still agree with the all parameter MLR fit (**Table 3-3** top line). Thus, the LSER model using MLR with the test solutes in **Table 3-1** is robust. Further discussions will focus on the MLR results.

A residual analysis **(Figure 3-1)** was done as suggested in Ref. [20]. **Figure 3-1** shows the standardized log *k* residual *vs*. the measured log *k.* All residuals in **Figure 3-1** are within three standard deviations of the fit, and distribute symmetrically around zero. These attributes indicate that the LSER coefficients are reliable. Most of the test solutes are well represented by the LSERs. Nitromethane shows a large standardized residual which means the nitromethane is not modeled entirely correctly.

Table 3-3 LSER coefficients for the amino column using a DCM/hexane mobile phase.[a]

Mobile phase	*a*	*b*	*s*	*e*	*v*	No. of solutes	R	Standard Error
5% DCM								
MLR, all parameter fit[b]	2.98±0.39	3.48±0.50	1.37±0.27	-0.47± 0.18	0.18±0.16	20	0.96	0.30
PLS	3.42	3.26	1.41	-0.50	0.24	20	0.96	0.25
MLR, excluding *V*	2.84±0.38	3.59±0.49	1.32±0.28	-0.41±0.17	—	20	0.96	0.30
MLR, excluding *E* and *V*	2.98±0.42	3.88±0.54	0.84±0.21	—	—	20	0.94	0.34
Literature								
Hexane [25]	1.58	3.89	1.46	—	-1.00	23	0.987	0.139
Hexane [25]	1.65	3.81	1.40	—	-0.85			
Hexane [37]	—	2.25	1.23	-0.55	—	36	0.909	0.30
Hexane/ethyl acetate [37]	1.60	0.60	1.10	-0.38	—	42	0.871	0.30

a. Conditions: column, Spherisorb amino; flow rate, 1.0 mL/min; injection volume, 1 μL; column temperature, 35 °C; detector wavelength, 254 nm.

b. Standard error

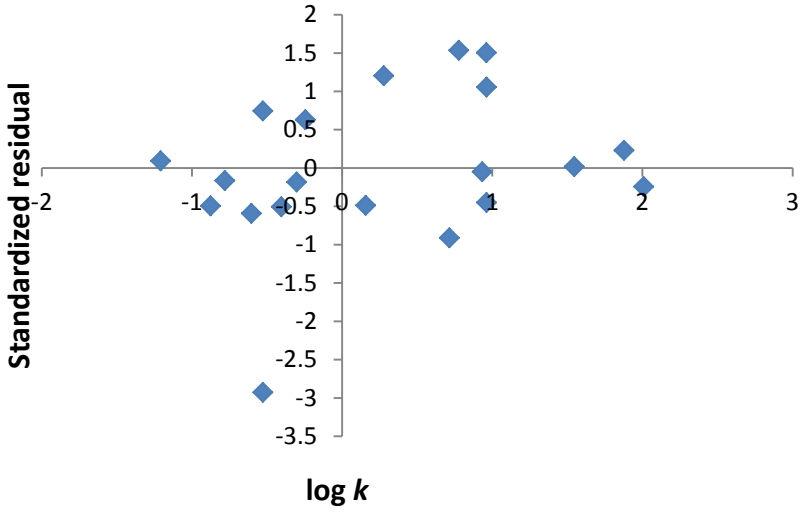

Figure 3-1 Standardized residual analysis as a function of log *k* for the amino column using a 5% DCM mobile phase. The standardized residual is the measured log *k* minus the predicted log *k*, divided by the standard error. The standardized residual was calculated using the Excel data analysis function.

The MLR using all of the solute parameters in **Table 3-1** yields an LSER **(Table 3-3** top row) in which both the *a* and *b* coefficients are large and positive. This means that for the amino column, the hydrogen bond acidity and basicity of the solutes are the predominant factors governing retention. The *s* coefficient is moderate in magnitude and positive in sign, while *e* is small and negative and *v* is insignificant.

For comparison, **Table 3-3** also summarizes literature LSER studies of amino columns under normal phase conditions. The correlation coefficient achieved herein (R=0.96) is comparable with that achieved previously [25, 37]. This indicates the goodness of fit is comparable to literature studies. Unfortunately, the coefficients cannot be directly compared with the literature values, because different mobile phases/ parameters were used [37]. Also the literature [25] did not use the recommended [20]

Abraham's parameters [32]. Nonetheless some general comparisons can be made. All the coefficients except *v* determined herein have the same sign as the literature. According to literature [37], the amino phase acts like an organic solvent when solutes transfer between mobile phase and organic phase. Under such circumstances, the value of *v* should be zero. The Student-*t* test shows our *v* coefficient value is statistically equal to zero.

3.3.3 5-HGN stationary phase

The 5-HGN stationary phase consists of polymeric hypercrosslinked polystyrene (**Figure 1-3A**), which is very similar to the polystyrene part of HC-Tol (**Figure 1-3B**). As a commercial pure polymer HC phase, 5-HGN was used as a reference column. **Table 3-4** shows the LSER coefficients obtained on the 5-HGN column by an MLR all parameter fit, PLS, and MLR excluding *e* and *v*. As on the amino column (**Table 3-3**), leave-one-out was used for cross-validation. Two latent variables were chosen to build the PLS model which gives the smallest RMSECV and captures about 80% of the variance of the *X* (solute parameters) and *Y* (log *k*) matrix. Also, the less important coefficients *e* and *v* were excluded to test the robustness of the MLR model. PLS and MLR excluding *e* and *v* are free from covariance problems, as discussed in **Section 3.3.1** and **3.3.2**. The coefficients from these two models (PLS and MLR excluding *e* and *v*) agree well with the coefficients from MLR with all parameters. Thus, the LSER model using MLR is robust.

The correlation coefficient for all 5-HGN models is 0.89, which is slightly worse than observed for the amino (**Section 3.3.2**) and the HC-Tol (**Section 3.3.4**) columns. Residual analysis was also done on 5-HGN (**Figure 3-2)**. All residuals in **Figure 3-2** are within three standard deviations of the fit, which indicates that the LSER coefficients are reliable. Nitromethane (at the bottom in **Figure 3-2**) shows a large standardized residual which means the nitromethane is not modeled entirely correctly.

Table 3-4 LSER coefficients for the 5-HGN and HC-Tol columns using a 5% DCM/hexane mobile phase.[a]

	a	***b***	***s***	***e***	***v***	**No. of solutes**	**R**	**Standard Error**
5-HGN								
MLR, all parameter fit [b]	1.45±0.51	1.19±0.61	0.93±0.043	0.22±0.21	-0.03±0.21	19	0.89	0.29
PLS	1.12	1.15	1.17	0.15	-0.13	19	0.89	0.25
MLR, excluding *E* and *V*	1.54±0.46	0.89±0.47	1.25±0.22	—	—	19	0.89	0.28
HC-Tol								
MLR, all parameter fit [b]	2.10±0.40	3.13±0.64	1.51±0.33	-0.42±0.21	-0.38±0.27	20	0.93	0.34
PLS	2.32	1.43	1.79	-0.53	-0.48	20	0.89	0.37
MLR, excluding *E* and *V*	2.33±0.45	3.21±0.70	0.79±0.27	—	—	20	0.89	0.42

c. Conditions: flow rate, 1.0 mL/min; injection volume, 1 μL; column temperature, 35 °C; detector wavelength, 254 nm

a. Standard error

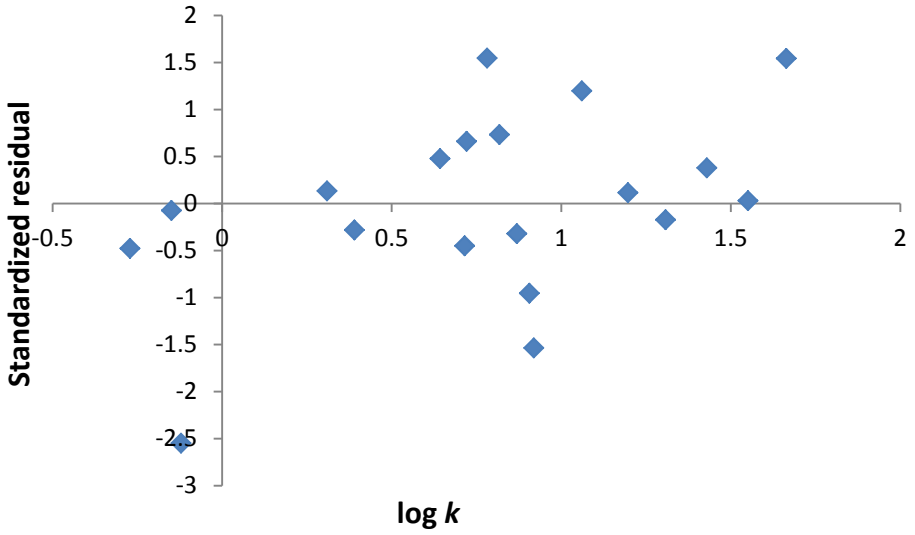

Figure 3-2 Standardized residual analysis as a function of log *k* for the 5-HGN column using a 5% DCM mobile phase.

3.3.4 HC-Tol column

The LSER coefficients for fits of retention data on the HC-Tol column are also shown in **Table 3-4**. As on the amino and the 5-HGN phases, PLS regression and MLR excluding *e* and *v* were used to validate the MLR model. Two latent variables were chosen for PLS regression because around 80% of the variance in the solute parameters and *log k* were captured and RMSECV was relatively small. The results from the three regression methods (MLR, PLS and MLR excluding *e* and *v*) generally agree based on the sign and magnitude of the LSER coefficients. This indicates that collinearity is not too severe as to cause a problem in the regression, in agreement with **Section 3.3.2** for the amino column and **Section 3.3.3** for the 5-HGN column. Thus, the LSER model using MLR with the chosen test solutes (**Table 3-1**) is robust. The following discussion will use only the MLR parameters, as they have an associated uncertainty.

The regression between log *k* and solute parameters has a correlation coefficient of 0.93 (**Table 3-4**, first line of HC-Tol). This is lower than typically observed for RPLC

(typically R = 0.98-0.99), but consistent with literature LSER studies in NPLC [24-26, 37]. **Figure 3-3** shows the standardized log *k* residual *vs*. the measured log *k*. **Figure 3-3** shows there is no obvious outlier within the data. All residuals in **Figure 3-3** are within three standard deviations of the fit, and distribute symmetrically around zero. These attributes indicate that the LSER coefficients are reliable. Benzyl alcohol (at the bottom in **Figure 3-3**) shows a large standardized residual which means the benzyl alcohol is not modeled entirely correctly.

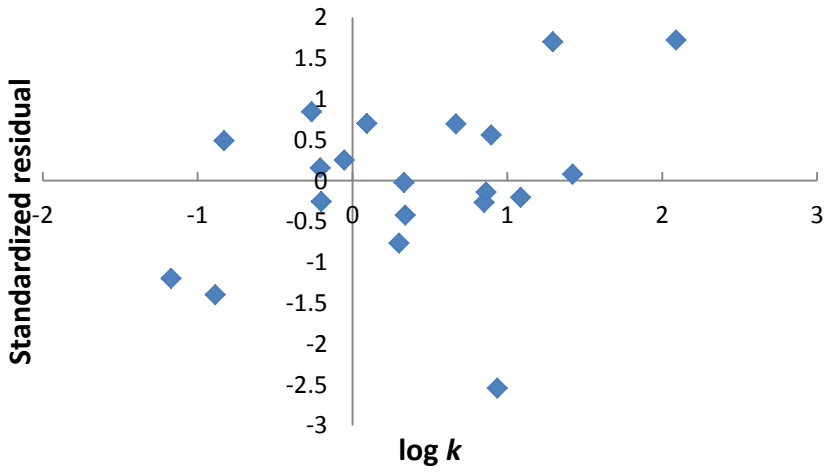

Figure 3-3 Standardized residual analysis as a function of log *k* for HC-Tol using a 5% DCM mobile phase.

Amongst the coefficients in **Table 3-4**, *a*, *b* and *s* are large and positive. This indicates that the solute hydrogen bonding acidity *A*, basicity *B* and polarity/ polarizability *S* are the predominant factors determining retention. Retention increases with the increasing solute's *A*, *B* and *S*. Thus, we can conclude that hydrogen bonding plays an important role in retention, with the stationary phase having much more hydrogen bond acidity and basicity than the DCM/hexane mobile phase. Residual silanol groups can be hydrogen bond donors [48]. Unfortunately, because *S* is a blend of polarity and polarizability effects, the influence of *S* is hard to explain. Regardless, the

coefficients *a, b* and *s* are all related to polar interactions, and based on theory are expected to be positive in NPLC, as has been previously observed [24-26, 37]. Thus, HC-Tol displays typical normal phase behavior.

It is hard to determine whether polarizability has a positive or negative impact on retention. Both *s* and *e* are related to polarizability interactions, but *s* is positive and *e* is negative for HC-Tol in **Table 3-4**. The *v* coefficient is also small and negative, meaning that the solute volume *V* has a small but negative impact on retention.

3.3.5 Comparison of LSERs for amino, 5-HGN and HC-Tol columns

To better illustrate the LSER coefficients for the HC-Tol column, the coefficients for the amino, 5-HGN and HC-Tol columns are compared in **Figure 3-4**. The NH_2 column has similar properties as the HC-Tol column. That is, the coefficients *a, b, s* and *e* all have the same sign and similar magnitude. On both columns, polar interactions predominate and contribute to retention. They are both a better hydrogen bonding acid than hydrogen bonding base.

The primary difference between the amino and HC-Tol columns is with the volume *v*. For the amino column, *v* is insignificant, while *v* is small (but statistically different than zero) and negative for the HC-Tol column. The significance of this subtle difference will be discussed in **Section 3.3.6**.

The HC-Tol column is a hydrogen bonding base and a hydrogen bonding acid. Characterization of the HC-Tol column under reversed phase conditions using the hydrophobic subtraction model suggested that the hydrogen bonding acidity is due to the intrinsic acid activity of the silica substrate [19]. The hydrogen bond acidity and basicity of HC-Tol may also be caused by the underlying silica substrate. To trace down the source of hydrogen bond acidity and basicity of HC-Tol, the LSERs coefficients on HC-Tol and 5-HGN were compared (**Figure 3-4**). 5-HGN has smaller *a* and *b* values than HC-Tol, which means that 5-HGN does not have as strong hydrogen bond characteristics

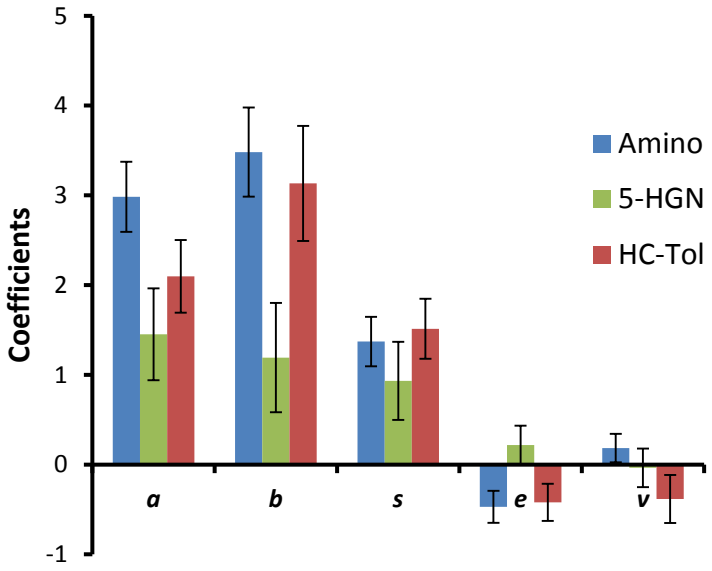

Figure 3-4 Comparison of LSER coefficients for the amino, 5-HGN and HC-Tol stationary phases using 5% DCM in hexane as mobile phase. The error bars indicate one standard deviation.

as HC-Tol. This suggests that the hydrogen bond acidity and basicity of HC-Tol is caused by the silica substrate. Generally, 5-HGN is not as polar as the amino and HC-Tol phases, as indicated by the smaller *a*, *b*, and *s*.

3.3.6 Why the HC-Tol phase works for group type separation of petroleum

Previous work from our group demonstrated that the HC-Tol phase could separate PAHs, pyrroles and pyridines according to their group type [11]. That is, all PAHs, regardless of their size, co-elute as a single peak. Likewise, all pyrroles elute as a second peak, and all pyridines as a third peak.

Table 3-5 compares the solvatochromic parameters for the three groups of model petroleum compounds separated on HC-Tol. The *a*, *b* and *s* coefficients are positive and large on the HC-Tol column, with *b* being the largest. Thus, the solute hydrogen bonding acidity *A*, basicity *B* and polarity/polarizability *S* are the predominant factors determining retention. PAHs have the smallest *A*, *B* and *S* parameters among the three groups, so PAHs are the first group to elute. Pyridines are basic compounds with largest *B* parameters which can contribute dramatically to retention so they are the last to elute. The primary difference between the amino and HC-Tol columns is *v*.

For the amino column, *v* is insignificant, while *v* is small (but statistically different than zero) and negative for the HC-Tol column. Thus, a solute's *V* value has no impact on retention on the amino column, while *V* has a slightly negative influence on retention for the HC-Tol column. The difference in coefficient *v* might explain why HC-Tol is capable of group type separation. A solute's polarity/polarizability *S* usually increases with solute size. Solute volume *V* also increases with the solute size. However, for the HC-Tol (**Table 3-4** and **Figure 3-4**) *s* is positive while *v* is negative. Thus the effects of solute size from *S* and *V* cancel each other out.

Table 3-5 Solvatochromic parameters of group separation compounds.

Solute	Compound Group	*A*	*B*	*S*	*E*	*V*
benzene		0	0.14	0.52	0.61	0.7164
anthracene	PAH	0	0.2	0.92	1.34	1.4544
pyrene		0	0.2	0.92	1.34	1.5846
indole		0.44	0.22	1.12	1.2	0.9464
carbazole	pyrroles	0.18	0.08	2.01	1.787	1.3154
1h-benzo indole		0.31	0.39	1.43	1.94	1.3154
quinoluine		0	0.54	0.97	1.268	1.0443
phenanthridine	pyridines	0	0.5	1.23	1.73	1.4565
acridine		0	0.54	0.97	1.268	1.4133

3.4 Conclusions

On both the HC-Tol and amino columns, the solute acidity (*A*), basicity (*B*) and polarity (*S*) all contribute significantly to retention while solute excess polarizability *E* has small but negative effect to retention. Solute volume *V* has no impact on retention on the amino column, while *V* has a slightly negative influence on retention for HC-Tol column. The difference in coefficient *v* between the amino and HC-Tol columns might explain why HC-Tol is capable of group type separation. 5-HGN has smaller *a* and *b* values which means 5-HGN is not as basic or acidic as HC-Tol. So the hydrogen bonding character of the HC-Tol phase arises from its silica substrate. To double check whether the silica substrate is the source of hydrogen bond character of HC-Tol column, HC-Tol column can be endcapped and characterized by LSERs again.

3.5 References

[1] V. Davankov, C.S. Sychov, M.M. Ilyin, K.O. Sochilina, Hypercrosslinked polystyrene as a novel type of high-performance liquid chromatography column packing material -

Mechanisms of retention, J. Chromatogr. A 987 (2003) 67-75.

[2] C.S. Sychov, M.M. Ilyin, V.A. Davankov, K.O. Sochilina, Elucidation of retention mechanisms on hypercrosslinked polystyrene used as column packing material for high-performance liquid chromatography, J. Chromatogr. A 1030 (2004) 17-24.

[3] V.A. Davankov, M.P. Tsyurupa, N.N. Alexienko, Selectivity in preparative separations of inorganic electrolytes by size-exclusion chromatography on hypercrosslinked polystyrene and microporous carbons, J. Chromatogr. A 1100 (2005) 32-39.

[4] V. Davankov, M. Tsyurupa, Preparative frontal size-exclusion chromatography of mineral ions on neutral hypercrosslinked polystyrene, J. Chromatogr. A 1087 (2005) 3-12.

[5] M.P. Baya, P.A. Siskos, V.A. Davankov, Evaluation of a hypercrosslinked polystyrene, MN-200, as a sorbent for the preconcentration of volatile organic compounds in air, J. AOAC Int. 83 (2000) 579-583.

[6] V.A. Davankov, M.P. Tsyurupa, Hypercrosslinked polymeric networks and adsorbing materials : synthesis, properties, structure, and applications, 1st ed., Elsevier, Amsterdam ; Boston, 2011.

[7] S.V. Prokopov, E.V. Tyrina, V.A. Davankov, M.M. Il'in, S.V. Kurbatova, Quasi-normal phase chromatography of nitrogen-containing adamantane derivatives, Russ. J. Phys. Chem. A 87 (2013) 114-119.

[8] N. Fontanals, J. Cortes, M. Galia, R.M. Marce, P.A.G. Cormack, F. Borrull, D.C. Sherrington, Synthesis of Davankov-type hypercrosslinked resins using different isomer compositions of vinylbenzyl chloride monomer, and application in the solid-phase extraction of polar compounds, J. Polym. Sci. A Polym. Chem. 43 (2005) 1718-1728.

[9] N. Fontanals, M. Galia, P.A.G. Cormack, R.M. Marce, D.C. Sherrington, F. Borrull, Evaluation of a new hypercrosslinked polymer as a sorbent for solid-phase extraction of polar compounds, J. Chromatogr. A 1075 (2005) 51-56.

[10] S.V. Prokopov, S.V. Kurbatova, V.A. Davankov, M.A. Il'in, Chromatographic

retention of adamantylamidrazones and triazoles by octadecyl silica gel and hypercrosslinked polystyrenes from water-acetonitrile solutions, Russ. J. Phys. Chem. A 86 (2012) 852-859.

[11] N.E. Oro, C.A. Lucy, Comparison of hypercrosslinked polystyrene columns for the separation of nitrogen group-types in petroleum using high performance liquid chromatography, J. Chromatogr. A 1217 (2010) 6178-6185.

[12] L.J. Ma, H. Luo, J. Dai, P.W. Carr, Development of acid stable, hyper-crosslinked, silica-based reversed-phase liquid chromatography supports for the separation of organic bases, J. Chromatogr. A 1114 (2006) 21-28.

[13] Y. Zhang, H. Luo, P.W. Carr, Silica-based, hyper-crosslinked acid stable stationary phases for high performance liquid chromatography, J. Chromatogr. A 1228 (2012) 110-124.

[14] H. Luo, L. Ma, Y. Zhang, P.W. Carr, Synthesis and characterization of silica-based hyper-crosslinked sulfonate-modified reversed stationary phases, J. Chromatogr. A 1182 (2008) 41-55.

[15] B.C. Trammell, L. Ma, H. Luo, M.A. Hillmyer, P.W. Carr, An ultra acid stable reversed stationary phase, J. Am. Chem. Soc. 125 (2003) 10504-10505.

[16] B.C. Trammell, L. Ma, H. Luo, M.A. Hillmyer, P.W. Carr, Synthesis and characterization of hypercrosslinked, surface-confined, ultra-stable silica-based stationary phases, J. Chromatogr. A 1060 (2004) 61-76.

[17] B.C. Trammell, L. Ma, H. Luo, D. Jin, M.A. Hillmyer, P.W. Carr, Highly cross-linked self-assembled monolayer stationary phases: an approach to greatly enhancing the low pH stability of silica-based stationary phases, Anal. Chem. 74 (2002) 4634-4639.

[18] Y. Zhang, P.W. Carr, Novel ultra stable silica-based stationary phases for reversed phase liquid chromatography--study of a hydrophobically assisted weak acid cation exchange phase, J. Chromatogr. A 1218 (2011) 763-777.

[19] Y. Zhang, Y. Huang, P.W. Carr, Optimization of the synthesis of a hyper-crosslinked stationary phases: a new generation of highly efficient, acid-stable hyper-crosslinked materials for HPLC, J. Sep. Sci. 34 (2011) 1407-1422.

[20] M. Vitha, P.W. Carr, The chemical interpretation and practice of linear solvation energy relationships in chromatography, J. Chromatogr. A 1126 (2006) 143-194.

[21] A.A. D'Archivio, A. Giannitto, M.A. Maggi, F. Ruggieri, Cross-column retention prediction in reversed-phase high-performance liquid chromatography by artificial neural network modelling, Anal. Chim. Acta 717 (2012) 52-60.

[22] J.W. Li, Prediction of internal standards in reversed-phase liquid chromatography: III. Evaluation of an alternative solvation parameter model to correlate and predict the retention of ionizable compounds, J. Chromatogr. A 982 (2002) 209-223.

[23] L. Szepesy, Effect of molecular interactions on retention and selectivity in reversed-phase liquid chromatography, J. Chromatogr. A 960 (2002) 69-83.

[24] J.W. Li, T. Robison, Application of linear solvation energy relationships to guide selection of polar modifiers in normal-phase liquid chromatographic separations, Anal. Chim. Acta 395 (1999) 85-99.

[25] J.W. Li, D.A. Whitman, Characterization and selectivity optimization on diol, amino, and cyano normal phase columns based on linear solvation energy relationships, Anal. Chim. Acta 368 (1998) 141-154.

[26] J.H. Park, M.H. Yoon, Y.K. Ryu, B.E. Kim, J.W. Ryu, M.D. Jang, Characterization of some normal-phase liquid chromatographic stationary phases based on linear solvation energy relationships, J. Chromatogr. A 796 (1998) 249-258.

[27] M.J. Kamlet, R.W. Taft, The solvatochromic comparison method. I. The .beta.-scale of solvent hydrogen-bond acceptor (HBA) basicities, J. Am. Chem. Soc. 98 (1976) 377-383.

[28] R.W. Taft, M.J. Kamlet, Solvatochromic comparison method. 2. Alpha-scale of solvent hydrogen-bond donor (hbd) acidities, J. Am. Chem. Soc. 98 (1976) 2886-2894.

[29] M.J. Kamlet, J.L. Abboud, R.W. Taft, Solvatochromic comparison method. 6. Pi-star scale of solvent polarities, J. Am. Chem. Soc. 99 (1977) 6027-6038.

[30] M.J. Kamlet, M.H. Abraham, P.W. Carr, R.M. Doherty, R.W. Taft, Solute solvent interactions in chemistry and biology. 7. An analysis of mobile phase effects on high-pressure liquid-chromatography capacity factors and relationships of the latter with octanol water partition-coefficients, Journal of the Chemical Society-Perkin Transactions 2 (1988) 2087-2092.

[31] L.C. Tan, P.W. Carr, M.H. Abraham, Study of retention in reversed-phase liquid chromatography using linear solvation energy relationships 1. The stationary phase, J. Chromatogr. A 752 (1996) 1-18.

[32] M.H. Abraham, A. Ibrahim, A.M. Zissimos, Determination of sets of solute descriptors from chromatographic measurements, J. Chromatogr. A 1037 (2004) 29-47.

[33] M.H. Abraham, J.C. Mcgowan, The use of characteristic volumes to measure cavity terms in reversed phase liquid-chromatography, Chromatographia 23 (1987) 243-246.

[34] M.H. Abraham, Y.H. Zhao, Determination of solvation descriptors for ionic species: Hydrogen bond acidity and basicity, J. Org. Chem. 69 (2004) 4677-4685.

[35] T.W. Stephens, M. Loera, M. Calderas, R. Diaz, N. Montney, W.E. Acree, M.H. Abraham, Determination of Abraham model solute descriptors for benzoin based on measured solubility ratios, Phys. Chem. Liq. 50 (2012) 254-265.

[36] M.H. Abraham, J.R.M. Gola, J. Gil-Lostes, W.E. Acree, Jr., J.E. Cometto-Muniz, Determination of solvation descriptors for terpene hydrocarbons from chromatographic measurements, J. Chromatogr. A 1293 (2013) 133-141.

[37] F.Z. Oumada, M. Roses, E. Bosch, M.H. Abraham, Solute-solvent interactions in normal-phase liquid chromatography: a linear free-energy relationships study, Anal. Chim. Acta 382 (1999) 301-308.

[38] P. Jiang, D. Wu, C.A. Lucy, Determination of void volume in normal phase liquid chromatography, J. Chromatogr. A 1324 (2014) 63-70.

[39] E. Soczewiñski, Mechanistic molecular model of liquid-solid chromatography retention-eluent composition relationships, J. Chromatogr. A 965 (2002) 109-116.

[40] L.R. Snyder, Solvent selectivity in normal-phase TLC, J. Planar Chromatogr. 21 (2008) 315-323.

[41] N. Ulrich, J. Muhlenberg, H. Retzbach, G. Schuurmann, W. Brack, Linear solvation energy relationships as classifiers in non-target analysis - A gas chromatographic approach, J. Chromatogr. A 1264 (2012) 95-103.

[42] B.J. VanMiddlesworth, J.G. Dorsey, Quantifying injection solvent effects in reversed-phase liquid chromatography, J. Chromatogr. A 1236 (2012) 77-89.

[43] S. Wold, A. Ruhe, H. Wold, W.J. Dunn, The collinearity problem in linear-regression - the partial least-squares (Pls) approach to generalized inverses, SIAM J. Sci. Comput. 5 (1984) 735-743.

[44] P. Geladi, B.R. Kowalski, Partial least-squares regression - a tutorial, Anal. Chim. Acta 185 (1986) 1-17.

[45] L.R. Snyder, J.J. Kirkland, J.W. Dolan, Introduction to modern liquid chromatography, 3rd ed., Wiley, Hoboken, N.J., 2010.

[46] L.R. Snyder, T.C. Schunk, Retention mechanism and the role of the mobile phase in normal-phase separation on amino-bonded-phase columns, Anal. Chem. 54 (1982) 1764-1772.

[47] K. Varmuza, P. Filzmoser, Introduction to multivariate statistical analysis in chemometrics, CRC Press, Boca Raton, 2009.

[48] R. West, R.H. Baney, Hydrogen bonding studies. II. The acidity and basicity of silanols compared to alcohols, J. Am. Chem. Soc. 81 (1959) 6145-6148.

Chapter Four. Study of the slope of the linear relationship between retention and mobile phase composition (Snyder-Soczewiñski model) in normal phase liquid chromatography with classic bonded phases[1]

4.1 Introduction

Classical normal phase liquid chromatography (NPLC) used bare adsorbents such as silica and alumina. Detailed models for adsorption retention were developed for such phases. Currently much of the NPLC is done with bonded phase adsorbents such as cyano propyl, diol and amino phases. However, there has been limited evaluation [1-5] of these bonded phase columns using the classical models for adsorption.

This chapter explores the classical bonded phases in the context of the Snyder-Soczewiñski model. In particular, we focus on the slope of the log k *vs*. log N_B (mole fraction of strong solvent) plots, as this parameter governs changes in selectivity in NPLC.

4.2 Theory

The Snyder-Soczewiñski (S-S) model is a well-known model for normal phase chromatography [6-10]. The S-S model expresses the relationship between the retention factor k_{AB} in a mobile phase consisting of mixture of a weak solvent (A) and a strong solvent (B) as:

$$\log k_{AB} = \log k_1 - n\log N_B \tag{4-1}$$

where k_1 is the retention factor in pure strong solvent, N_B is the mole fraction of strong

[1] A version of this chapter has been accepted by Journal of Chromatography A as part of Di Wu and Charles A. Lucy , " Study of the slope of the linear relationship between retention and mobile phase composition (Snyder-Soczewiñski model) in normal phase liquid chromatography with bonded and charge-transfer phases", 2016. I conducted all experiments and wrote the manuscript.

solvent. The meaning of the *n*-slope is slightly different between the Snyder model [7, 8, 11] and the Soczewiñski model [6, 8, 9]. This difference arose from the different initial conditions considered by each investigator. Soczewiñski started from the consideration that polar solutes and polar solvents adsorbed in a 1:1 fashion with the adsorption sites on silica [6]. Soczewiñski considered *n* as (*nominally*) the number of polar substituent groups in the solute molecule, N_{Polar} [8, 9, 12]:

$$n_{Soczewiñski} = N_{Polar} \tag{4-2}$$

For example, the *n*-slope for a mono-functional solute such as phenol would be 1. Soczewinski and co-workers noted several exceptions to this simple assumption. The *n*-slope may be larger than predicted by Eq. 4-2 if there are strong solvation effects in the mobile phase [13-15] or if the solute is large in size [16]. Conversely, the *n*-slope may be smaller than predicted by **Eq. 4-2** if the solvent is self-associating, such as ethanol [8, 14]. For solutes with two polar substituents, the *n*-slope depends on the position of the two groups (whether the distance of the two polar groups is greater than the distance of adsorption sites on the adsorbent surface or not) [8, 17, 18]. Other factors such as presence of certain polar groups and internal hydrogen bonding also affect the *n*-slope of multi-functional solutes [14, 17, 18]. A third or even fourth polar group in the solute do not increase the *n*-slope [8, 18]. A particular limitation of the Soczewiñski assumption is that aromatic rings are not considered to contribute to the *n*-slope. This deficiency is particularly apparent in considering charge transfer columns such as DNAP (discussed in **Chapter 5**) which are specifically used for separations based on ring number [19, 20].

Snyder's model was initially constructed to consider adsorption of less polar (weaker adsorbing) solutes and solvents on alumina, where flat adsorption may be assumed [21]. Snyder's model can be expressed as:

$$\log\ k_{AB} = \log k_0 - \alpha\varepsilon_{AB}A_S \tag{4-3}$$

where k_0 is the retention factor in the pure nonpolar solvent, α is an activity factor, ε_{AB} is the solvent strength of the mobile phase, and A_S is the molecular area of the solute

required when adsorbed on stationary phase. The activity factor α is typically initially assumed to be 1 for uncharacterized phases [2], and usually ranges from 0.5 to 1.5. For the remainder of the theory discussion, the activity factor is assumed to be 1 and omitted from the following equations.

Snyder expressed *n* in **Eq. 4-1** as ideally the ratio of the molecular area of the solute (A_S) required when adsorbed on stationary phase *vs*. the molecular area of the strong solvent (A_B) on the adsorbent surface [7, 8, 11].

$$n_{Snyder} = A_S/A_B \tag{4-4}$$

If flat adsorption is assumed, the molecular areas can be calculated according to the group contributions to molecular area, such as in Table 8-4 in Ref. [11]. These group contributions allow for the less compact arrangement of the solute on the adsorbent than in a crystalline state. However, there are many exceptions to this simplest assumption. Firstly, very polar solutes and solvents may exhibit distinct one-to-one interaction with an adsorption site on the stationary phase, which is called *localization* [12, 22]. Thus polar solvents such as tetrahydrofuran (THF) are said to be *localizing solvents*. Conversely, less polar solvents such as dichloromethane (DCM) adsorb to the stationary phase in a non-oriented fashion, and so are referred to as *non-localizing solvents*. A third term is *delocalization*, which refers to adsorption at a site which could localize, but for whatever reason does not. For instance, for compounds with more than one polar group, the polar group with largest adsorption energy in the analyte can localize. The analyte is anchored by this localization, such that the remaining polar groups cannot achieve a preferred position with respect to the other adsorption sites on the stationary phase surface [10]. These remaining groups are said to be *delocalized*. The more strongly the primary polar group is localized, the more delocalized the remaining polar groups will be. This localized/delocalized adsorption can result in larger molecular interaction areas than that predicted by flat adsorption [23].

Secondly, systems involving hydrogen bonding (*e.g*., proton donor-acceptor solvent

systems such as alcohols) are less understood and harder to predict. Snyder added a secondary term Δ_{eas} to **Eq. 4-3** to correct for hydrogen bonding and any other secondary solvent effects not considered in the simplest equation [24]:

$$\log\ k_{AB} = \log k_0 - \varepsilon_{AB} A_s + \Delta_{easAB} \tag{4-5}$$

Δ_{eas} depends on both the solute and solvent. From **Eq. 4-5**, we can get

$$\log \frac{k_{AB}}{k_1} = (\varepsilon_B - \varepsilon_{AB}) A_S + (\Delta_{easAB} - \Delta_{easB}) \tag{4-6}$$

where k_1 is retention factor in pure strong solvent. **Eq. 4-6** can also be written as

$$\log k_{AB} = \log k_1 + (\varepsilon_B - \varepsilon_{AB}) A_S + (\Delta_{easAB} - \Delta_{easB}) \tag{4-7}$$

Except in the case of very diluted solvent B, the solvent strength of the mixture AB is [10]:

$$\varepsilon_{AB} = \varepsilon_B + \frac{\log N_B}{A_B} \tag{4-8}$$

Substituting **Eq. 4-8** into **Eq. 4-7** yields:

$$\log k_{AB} = \log k_1 - \frac{A_S}{A_B} \log N_B + (\Delta_{easAB} - \Delta_{easB}) \tag{4-9}$$

Eq. 4-9 has the same form as **Eq. 4-1**.

The simplest relationship (**Eq. 4-1**) is most widely used, and is used in this paper to compare the Snyder and Soczewiñski models. The *n*-slope is discussed in relation to the solute, mobile phase and stationary phase characteristics. The *n*-slope relates retention to molecular structure. Knowing *n* is important for retention prediction, mobile phase adjustment, and even column selection. Previously these two models have been compared on silica, and were both found to provide predicted values of *n* reasonably close to experimental values [7]. In this chapter, the *n* values derived from literature studies [1, 2, 4, 15, 25] with an extended set of solutes on variety of conventional NPLC bonded phases (cyano, diol, amino) with solvent systems are first analyzed.

4.3 Experimental

4.3.1 Procedures

Molecular topological polar surface area (TPSA) was calculated using the Molinspiration software [26].

Our initial investigations of the factors governing the *n*-slope in **Eq. 4-1** will use the data of Soczewiñski [3], as summarized in **Table 4-1**. Retention of sixteen compounds on cyano, diol and amino stationary phases were investigated with heptane plus methyl ethyl ketone (MEK), isopropyl alcohol (IPA), ethyl acetate (EA) and tetrahydrofuran (THF) as mobile phases. Soczewiñski collected this extensive data set to evaluate the Snyder-Soczewiñski model, the Scott-Kucera equation and the Jaroniec model [27, 28]. However, Soczewiñski did not systematically relate the molecular properties of the analytes with the observed *n*, which is the objective of this chapter.

Table 4-1 shows the experimental *n* values for the various solute/stationary phase/mobile phase combinations from Ref. [3]. We observed some inconsistencies within the values reported by Soczewiñski [3]. In Ref. [3] Soczewiñski regressed the retention data *vs*. **Eq. 4-1** and *vs*. the Scott-Kucera model [29, 30]:

$$\frac{1}{k} = A' + B'\phi \tag{4-10}$$

where *A'* and *B'* are constants, ϕ is volume fraction of polar solvent in the eluent. The log *k* was calculated using regression parameters from Ref. [3] for both **Eq. 4-1** and **4-10**. Generally the retention factors predicted by the two equations agreed to within 30%. If the calculated *k* by the two equations differed by greater than a factor of 10, we assumed that there was an error in the reported regression parameters, and so the *n* value for that compound was excluded from **Table 4-1**. Also some original *n* values from Ref. [3] were reported as negative for regressions *vs*. **Eq. 4-1**, but were clearly positive based on the **Eq. 4-10**. These *n* values were corrected to positive in **Table 4-1**.

In studies of the effect of the aromatic ring number, the *n*-slope was determined based on plots of the logarithm of retention factor from Ref. [1, 2, 4, 25] and our previous

Table 4-1 Experimental *n*-slope values from Soczewiñski [3][a].

Stationary phase	**Cyano**			**Diol**			**Amino**				**Polar group**	N_{polar}
Mobile phase	IPA	EA	THF	MEK	EA	THF	MEK	IPA[a]	THF	EA[b]		
Phenol	1.18	0.88	1.24	1.20	1.27	1.14	1.72	0.91	1.77	1.19	OH	1
4-Aminophenol	2.06			1.38	2.40	1.20		0.2			OH, NH_2	2
4-Nitrophenol	1.63	1.34	1.46	1.23	1.23	1.37		1.69			OH, NO_2	2
Hydroquinone	1.84	1.98	2.03	1.86	1.43	1.68		1.88			OH, OH	2
2-Hydroxyquinoline	1.57		1.82	1.19	1.21	1.39	1.71	0.86	1.76	2.05	N, OH	2
Quinoline	0.75	0.70	1.08	0.79	0.87	1.06	1.33	0.64	1.06	2.15	N	1
6-Nitroquinoline	0.85	1.07	1.25	1.19	1.17	1.34	0.80	0.73	1.37	1.11	N, NO_2	2
8-Methylquinoline	0.6	0.62	0.78	0.76	0.74	0.84	1.29	0.60	0.85	0.51	N	1
Aniline	0.89	1.15		1.05	0.99	1.29	2.23[c]	0.68	0.68	1.22	NH_2	1
1,2-Phenylenediamine	1.50			1.32		1.27	1.48	1.01	2.29	1.63	NH_2, NH_2	2
2-Nitroaniline	1.15	1.32	1.25	1.19	1.20	1.27	2.02	0.99	1.38	1.14	NH_2, NO_2	2
4-Nitroaniline	1.46		1.64	1.60	1.58	1.87	1.10	1.44	2.08	1.67	NH_2, NO_2	2
2-Iodoaniline	0.71	0.93	1.09	0.90	0.90	0.98	1.24	0.68	1.11	0.76	I, NH_2	2
4-Iodoaniline	1.02	1.07	1.17	1.02	1.03	1.10	1.93	0.82	1.28	0.96	I, NH_2	2
1,5-Diamino naphthalene	1.29		2.29	1.69	1.70	2.00	1.51	1.16	1.98	1.33	NH_2, NH_2	2
1-Aminonaphthalene	0.99	1.34	1.25	1.16	1.20	1.25	1.03	0.81	1.62	1.27	NH_2	1

a. The standard error of the regressions in [3] was typically 0.08 and ranged from 0.02 to 0.23

b. Originally negative.

c. Indicates slope values that we feel are abnormal, but cannot be discounted for cause.

Table 4-2 Molecular area of interaction *vs*. the solvent molecular area (A_S/A_B) and the topological polar surface area (TPSA) for compounds in Ref. [3].

	A_S/A_B				TPSA
Solute	**MEK**	**IPA**	**EA**	**THF**	
phenol	1.27	0.73	1.03	1.17	20.23
4-aminophenol	1.28	0.74	1.04	1.18	46.25
4-nitrophenol	1.43	1.74	1.16	1.32	66.05
hydroquinone	1.24	0.71	1.00	1.14	40.46
2-hydroxyquinoline	1.68	0.97	1.36	1.55	33.12
quinoline	1.72	0.99	1.39	1.58	12.89
6-nitroquinoline	1.88	1.08	1.52	1.73	58.72
8-methylquinoline	1.77	1.02	1.43	1.63	12.89
aniline	1.32	0.76	1.06	1.21	26.02
1,2-phenylenediamine	1.33	0.76	1.07	1.22	52.05
2-nitroaniline	1.48	0.85	1.19	1.36	71.85
4-nitroaniline	1.48	0.85	1.19	1.36	71.85
2-iodoaniline	1.48	0.85	1.19	1.36	26.02
4-iodoaniline	1.48	0.85	1.19	1.36	26.02
1,5-diamino naphthalene	1.78	1.03	1.44	1.64	52.05
1-aminonaphthalene	1.77	1.02	1.43	1.63	26.02

Table 4-3 Observed change in *n*-slope for similar compounds from Soczewiñski data [3].

Stationary phase	**Cyano**			**Diol**			**Amino**			
Mobile phase	**IPA**	**EA**	**THF**	**MEK**	**EA**	**THF**	**MEK**	**IPA**	**THF**	**EA**
Aniline	0.89	1.15		1.05	0.99	1.29	2.23	0.68	0.68	1.22
1- Amino naphthalene	0.99	1.34	1.25	1.16	1.20	1.25	1.03	0.81	1.62	1.27
Change in slope	+0.10	+0.19		+0.11	+0.21	-0.04	-1.20	+0.13	+0.94	+0.05
Change predicted based on A_S	+0.26	+0.37	+0.42	+0.45	+0.37	+0.42	+0.45	+0.26	+0.42	+0.37

paper [23] against the logarithm of the mole fraction.

4.4 Results and Discussion

To compare the Snyder model *vs.* the Soczewiñski model**, Table 4-1** presents the experimental *n*-slope, the type of polar group(s) and the number of polar substitutes. **Table 4-2** presents the molecular area of interaction *vs*. the solvent molecular area (A_S/A_B) and the topological polar surface area (TPSA) of each solute.

4.4.1 Effect of addition of aromatic rings on n-slope on classic nplc bonded phases

A first criterion to compare the two models is their prediction for the effect of the addition of an aromatic ring to a solute. Soczewiñski assumed that aromatic rings had no effect on the *n*-slope [18]. In contrast, Snyder's point of view was that the ring would impact the solute area A_S, which in turn would affect the *n*-slope.

First, we compare aniline and 1-aminonaphthalene from **Table 4-1**. These solutes possess the same polar functionality but differ in the number of aromatic rings. The Soczewiñski model predicts that the change in *n*-slope between these compounds would be 0. The Snyder model predicts that the *n*-slope will increase proportional to the solute area A_S. **Table 4-3** shows that addition of a ring can either contribute negligibly to the slope (*e.g.*, THF on the diol phase) in agreement with the Soczewiñski model, or strongly increases the slope (*e.g.*, 0.94 for THF on the amino phase), and even apparently decrease the slope (e.g., -1.20 for MEK on the amino) depending on the column and mobile phase. In general, the positive contribution due to the additional aromatic ring in **Table 4-3** agrees better with the predictions of the Snyder model. This is in agreement with other studies where the average slope based on five mobile phases on silica increasing from 1.3 for phenol to 1.5 for naphthol [7].

Second, the relative retention of polycyclic aromatic hydrocarbons (PAHs) is used to assess the effect of additional aromatic groups on the *n*-slope. PAHs may be described by their number of aromatic rings, their number of double bonds N_{double}, or their solute

Table 4-4 Experimental *n*-slope values.

SP	Mobile phase	Naph thalene	Anth racene	Phenan threne	Fluoran thene	Py rene	Chry sene	Pery lene
	N_{double}	5	7	7	8	8	9	10
	A_S	8.1	10.2	10.2	10.7	10.7	12.3	12.8
Cyano	MTBE[a]		0.16		0.17		0.19	
	MTBE[b]			0.28			0.29	0.31
	DCM[b]			0.63			0.78	0.72
	DCM [c]						0.25	0.32
	$CHCl_3$[b]			0.62			0.73	0.83
Diol	MTBE[b]			0.17			0.22	0.26
	DCM[b]			0.58			0.64	0.70
	$CHCl_3$[b]			0.42			0.57	0.59
Amino	MTBE[a]		0.37		0.38		0.42	
	MTBE[b]			0.52			0.66	0.69
	THF[d]	0.23		0.26	0.32		0.36	
	DCM[b]			0.67			0.76	0.88
	DCM[d]			0.84	1.0		1.4	1.6
	CCl_4[d]			0.54	0.58		0.66	1.0
	$CHCl_3$[b]			0.59			0.69	0.75
	$CHCl_3$[d]			0.56	0.83		0.78	0.97
	EA[d]			0.6	0.44		0.61	0.89
A_S/A_B	MTBE	1.45	1.82	1.82	1.91	1.91	2.20	2.29
	THF	1.62	1.82	1.82	1.91	1.91	2.20	2.29
	DCM	1.98	2.49	2.49	2.61	2.61	3.00	3.12
	CCl_4	1.62	2.04	2.04	2.14	2.14	2.46	2.56
	$CHCl_3$	1.62	2.04	2.04	2.14	2.14	2.46	2.56
	EA	1.41	1.79	1.79	1.88	1.88	2.16	2.25
	IPA	1.01	1.28	1.28	1.34	1.34	1.54	1.60

a. calculated from retention data in Ref. [25]

b. calculated from retention data in Ref. [4]

c. calculated from retention data in Ref. [1]

d. calculated from retention data in Ref. [2]

interaction area A_S, as summarized in **Table 4-4**. While these descriptors are roughly correlated, N_{double} and A_S are more discriminating, particularly for the larger PAHs. For example, chrysene and pyrene both have four aromatic rings but chrysene has one more double bond. Thus, they differ in number of double bonds N_{double} and their solute interaction area A_S. **Table 4-4** summarizes the *n*-slope values for PAHs on cyano, diol, and amino from the literature [1, 2, 4, 25]. **Table 4-5** summarizes the correlation between the *n*-slope and these parameters for a wide range of stationary and mobile phases. For cyano, diol and amino phases, the *n*-slope increases with all three PAH descriptors: the number of rings, number of double bonds, and A_S. The correlation is poorest for the number of rings, and comparable for the number of double bonds and A_S. The similarity in correlations for double bonds and A_S is not surprising, as the number of double bonds and A_S are linearly related (R^2=0.97) for the PAHs in **Table 4-4**. We could find no literature discussing whether in general ring number or number of aromatic double bonds is better correlated with *n*-slope. However, Ref. [27] found PAH retention on amino columns correlated better with the number of aromatic carbon atoms than with the number of aromatic rings, consistent with **Table 4-5**. In conclusion, the number of double bonds N_{double} correlates strongly with *n*-slope and is much easier to calculate than A_S, and so N_{double} is the preferred descriptor when estimating the relative *n*-slope of PAHs.

Although A_S values correlate with the *n*-slope for PAHs (**Table 4-5**), the values for the *n*-slope (**Table 4-4**) are much lower than the A_S/A_B predicted by the Snyder model for an activity factor of 1 (**Eq. 4-4**). Further, the *n*-slopes with localizing solvents (MTBE, THF, EA) are usually smaller than the *n*-slopes with non-localizing solvents (DCM, $CHCl_3$, CCl_4) on the same column. That is, increasing the concentration of a localizing solvent such as THF has less effect on retention than a non-localizing solvent such as DCM. This behavior can be rationalized if the localizing solvents interacts with residual silanols which are too large for large PAHs to access [4].

4.4.2 Effect of molecular area on n-slope on classic NPLC bonded phases

Table 4-5 Dependence of *n*-slope on PAH size.

Stationary phase	Mobile phase	R^2 for No. of rings	R^2 for N_{double}	R^2 for A_S
Cyano	MTBE[a]	0.89	0.96	0.989
	MTBE[b]	0.57	0.86	0.74
	DCM[b]	0.84	0.54	0.69
	DCM [c]	na	na	na
	$CHCl_3$[b]	0.77	0.97	0.90
Diol	MTBE[b]	0.80	0.98	0.92
	DCM[b]	0.75	0.96	0.89
	$CHCl_3$[b]	0.988	0.95	0.994
Amino	MTBE[a]	0.96	0.89	0.998
	MTBE[b]	0.97	0.97	0.9997
	THF[d]	0.82	0.92	0.91
	DCM[b]	0.68	0.93	0.83
	DCM[d]	0.91	0.97	0.99
	CCl_4[d]	0.55	0.81	0.71
	$CHCl_3$[b]	0.86	0.998	0.96
	$CHCl_3$[d]	0.37	0.80	0.60
	EA[d]	0.50	0.51	0.54

a. calculated from retention data in Ref. [25]

b. calculated from retention data in Ref. [4]

c. calculated from retention data in Ref. [1]

d. calculated from retention data in Ref. [2]

Another way of comparing the models is to evaluate the accuracy of their predicted slopes. Snyder idealized *n* as the ratio of the adjusted molecular areas of the solute to that of the solvent (A_S/A_B) at the adsorbent surface (**Eq. 4-4**) [7, 8, 11]. Alternately, Soczewiński approximated that the *n*-slope was equal to the number of polar groups (N_{polar} in **Eq. 4-2**) [8, 9], but qualified that the *n*-value could be larger if the solute was "*large enough to displace vicinal solvent molecules"* [8] or smaller for solutes with weak polar groups [8, 9]. The relative adsorption areas (A_S/A_B) for each solute/solvent pair (Snyder, **Table 4-2**) and the number of polar functionalities N_{polar} (Soczewiński, **Table 4-1**) for each solute are both tabulated. Both models have been reported to provide predictions of the *n*-slope that are close to the observed values [2].

To evaluate the effectiveness of the two predictions, Snyder [7] calculated the standard deviation of the difference between the *n*-value predicted by each model and that observed experimentally. For a perfect model, the mean difference would be zero and the standard deviation of the differences would be small. For hydroxylated solutes on a silica stationary phase, Snyder [7] observed that the standard deviation between predicted *n*-values *vs*. experimental was ±0.3 for the Soczewiński model and ±0.2 for the Snyder model. Based on this, Snyder concluded that the predictions of both models were reasonably close. However, Snyder's study was limited to a single phase (silica) with analytes having a strong polar group (*e.g.*, -OH). Further, silica does not allow differentiation between the two models, as the retention of PAHs is weak on silica [32].

To compare the models with a wider array of solutes and stationary phases, we calculated the differences between the values calculated by the Snyder model (A_S/A_B in **Table 4-2**) and the Soczewiński model (N_{polar} in **Table 4-1**) versus the experimental *n*-slope values on each stationary phase in **Table 4-1**. **Table 4-6** shows the mean differences between the model predicted *n*-slope and the experimental *n*, and their associated standard deviations. Overall, the Snyder model better predicts the *n*-slope (mean difference = 0.04) than the Soczewiński model (mean difference = 0.4). However,

both models are equally uncertain in predicting the *n*-slope for a given compound, as indicated by the large standard deviations in **Table 4-6** for a given column with a given mobile phase. The standard deviations of the predictions for individual compounds for a given column and solvent (typically ~0.5) are significantly poorer than observed previously by Snyder (0.3) [7], presumably due to the more diverse compound set in **Table 4-6** than in Ref. [7].

Based on **Table 4-6** we draw a number of conclusions. First, we observe slightly better prediction of the *n*-slope with the Snyder model, consistent with Ref. [7]. Second, on average the Soczewiñski model over-predicts the impact of the polar groups on the *n*-slope, as evidenced by the large positive mean deviation (+0.4) in the rightmost column of **Table 4-6**. Third, we conclude the two models have comparable uncertainty in predicting the *n*-slope of an individual compound for a given column and mobile phase, in agreement with Ref. [7].

Table 4-6 Difference between the predictions by the Snyder and Soczewiñski models versus the experimentally measured *n*-slope [3].

Stationary phase	**Cyano**			**Diol**			**Amino**				**Mean**
Mobile phase	**IPA**	**EA**	**THF**	**MEK**	**EA**	**THF**	**MEK**	**IPA**	**THF**	**EA**	
Snyder	-0.3 ±0.5	0.1 ±0.5	0.04 ±0.49	0.3 ±0.4	-0.02 ±0.5	0.09 ±0.37	0.08 ±0.57	-0.01 ±0.42	-0.2 ±0.5	0.1 ±0.5	0.04
Soczewiñski	0.5 ±0.4	0.4 ±0.5	0.1 ±0.7	0.5 ±0.4	0.4 ±0.5	0.4 ±0.4	0.1 ±0.7	0.7 ±0.5	0.1 ±0.5	0.3 ±0.7	0.4

Other topographical parameters have been used in quantitative structure-activity relationships. One such is the molecular polar surface area (PSA) [33], which is defined as the sum of the surfaces of the polar atoms within a molecule. PSA has been related to phenomena such as molecular passive transportation, but has not commonly been used for chromatography [34]. PSA values for each solute were calculated using TPSA by summation of the surface contributions of polar fragments [35]. The TPSA for the solutes

are listed in the rightmost column of **Table 4-2**.

The TPSA values have poor correlation with the *n*-slopes in **Table 4-1** (R^2<0.25). The cause for this poor correlation can be illustrated by comparing phenol and 4-nitrophenol. The nitro group contributes twice the TPSA as the -OH in 4-nitrophenol (45.82 *vs*. 20.23), yet the *n*-values for 4-nitrophenol is not nearly 3 times larger than that of phenol (e.g., 1.63 *vs*. 1.18). Rather, as will be discussed below, substituents such as -NO_2 contribute less to the *n*-slope than -OH. The inapplicability of TPSA to normal phase adsorption may be because TPSA is a three-dimensional parameter, whereas adsorption is a two-dimensional process.

4.4.3 Contribution of polar groups to n-slope on classic NPLC bonded phases

As suggested by the above discussion, the nature of the substituent seems to have a strong influence on the *n*-slope. To confirm this analysis of variance (ANOVA) was performed (using Excel version 2010) on the data in **Figures 4-1A** and **4-1B** to determine the relative influence of the mobile phase on each column *vs*. the solute identify. The differences within-groups (solutes) are much larger than the differences between-groups (mobile phases) on the cyano and diol phases (**Table 4-7**). This verifies that the mobile phase has less influence on the *n*-slope than does the nature of the solute. However, the mobile phase has a significant influence over the *n*-slope on the amino phase (**Figure 4-1C**). For example, the *n*-slope of 2-nitroaniline on an amino column is 0.99 with IPA mobile phase, but 2.02 with MEK mobile phase. The significant influence of the mobile phase on the *n*-slopes on the amino phase is verified by the ANOVA (**Table 4-7**), where the differences within-groups (*i.e.*, solutes) and between-groups (*i.e.*, mobile phase) are comparable. On the amino stationary phase, the mobile phase has a substantial influence on slope, so it is hard to rank the contributions of the substituents. Only the group contributions on the cyano and the diol phases are discussed below.

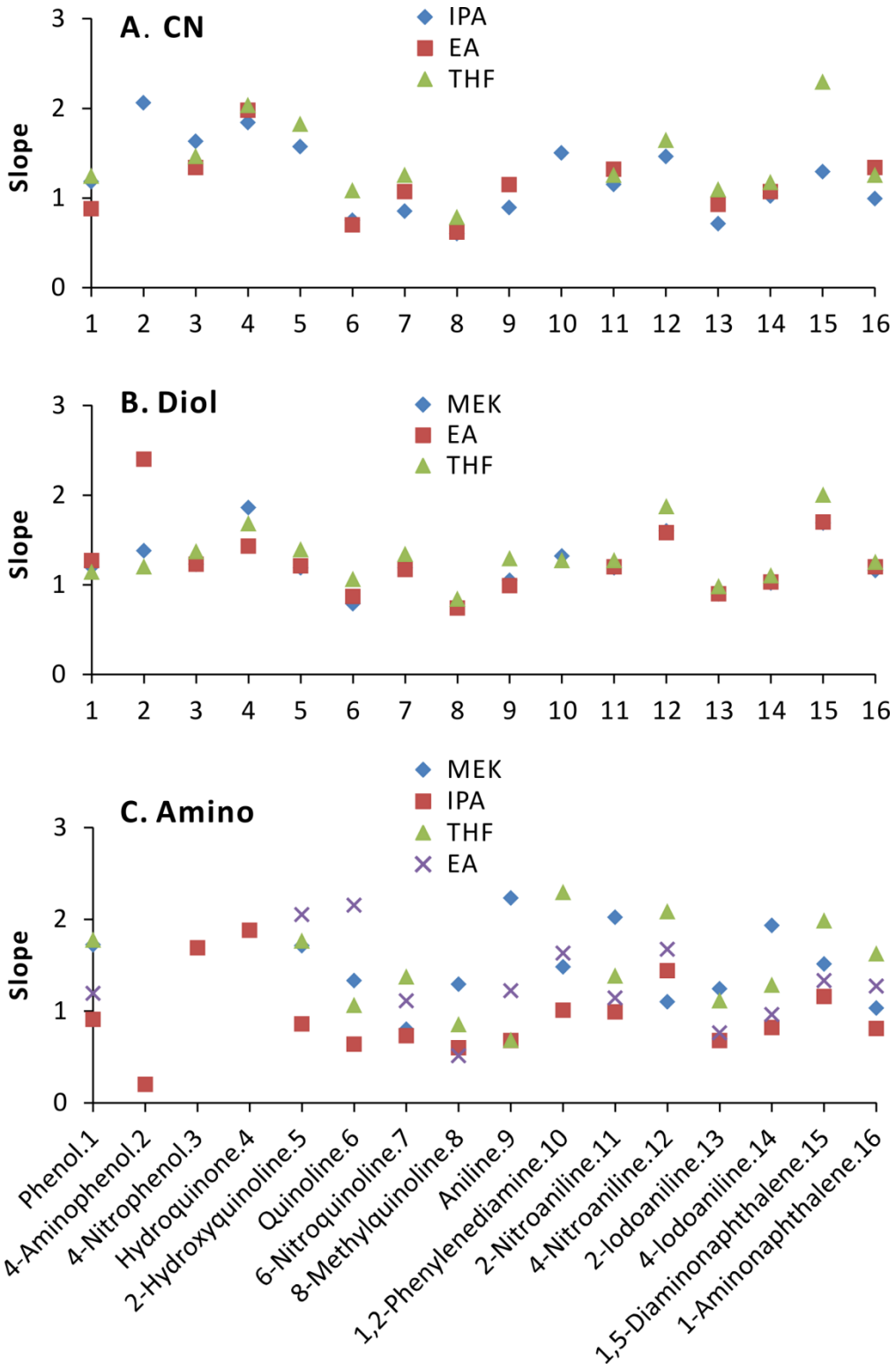

Figure 4-1 Solvent dependence of *n*-slopes for solutes on cyano (CN), diol and amino stationary phases from Soczewiński [3]. The compound numbers are as presented in Ref. [3]

Table 4-7 ANOVA analysis for influence of mobile phase.

Sum of Squares	Cyano	Diol	Amino
Within group (solutes)	0.4	0.08	3.3
Between groups (mobile phases)	3.9	5.1	8.3

a. EA data are not included due to limited number of solutes.

Initially multivariant analysis was attempted to determine the quantitative contribution of each polar group to the *n*-slope. The Solver function of Excel 2010 was used to minimize the residual between the predicted and the experimental *n*-slope. However, the complex interplay between analyte, mobile phase and stationary phase made it impossible to determine universal quantitative polar group contributions. Thus, only qualitative conclusions are drawn below.

On the cyano and diol phases, the contributions of the polar groups to the *n*-slope increase in the order:

$$\text{-I} < \text{-N} < \text{-NO}_2 < \text{-NH}_2 < \text{-OH} \quad (4\text{-}11)$$

where –N refers to heteroatom nitrogen such as in quinoline. The order in **Eq. 4-11** is more similar to the adsorption energies on alumina (**Eq. 4-12**) than on silica (**Eq. 4-13**) (**Table 4-8**) [36].

$$\text{-I} << \text{-O-R} << \text{-NO}_2 < \text{-CO}_2\text{-R} \approx \text{-CHO} < \text{-CO-R} < \text{-NH}_2 < \text{-NH-Ar} << \text{-OH} \quad \text{(alumina)} \quad (4\text{-}12)$$

$$\text{-I} << \text{-O-R} << \text{-NO}_2 < \text{-NH-Ar} < \text{-CO}_2\text{-R} \approx \text{-CHO} < \text{-OH} < \text{-CO-R} < \text{-NH}_2 \quad \text{(silica)} \quad (4\text{-}13)$$

Synder [22] has stated that the adsorption energy order parallels the "polarity" of a solute group.

Table 4-8 Group adsorption energy of substituted benzenes and naphthalene on alumina and silica [36].

Q_k^0 ($\frac{\text{kcal}}{\text{mol}}$)	-I	O-R	NO_2	-CO_2-R	-CHO	-CO-R	-NH_2	-NH-Ar	-OH
alumina	0.51	1.77	2.75	3.32	3.35	3.74	4.41	5.1	7.40
silica	-0.15	1.83	2.77	3.45	3.90	4.69	5.10	3.0	4.20

Initially Soczewiñski had assumed that each polar functionality contributes 1 to the *n*-slope (**Eq. 4-2**) [8]. Later he amended this rule such that "*weak adsorption*" functionalities (low adsorption energy) could contribute less than 1 to the *n*-slope. Such weak contributions to *n* are apparent in **Figures 4-1** and **4-2**. For example, heteroatom nitrogen (-N) is a weakly adsorbing group [9], and so -N contributes less than other polar groups on all of the stationary phases.

The contributions of two polar groups are not simply addictive, and are usually smaller than the sum of two polar groups. For example, the *n*-slope of phenol (one hydroxyl group) is 1.24 on the cyano phase with THF mobile phase, while the *n*-slope of hydroquinone (two hydroxyl groups) is 1.82 under the same conditions. Only the most polar group within the analyte can localize to an adsorption site [10, 22, 37], and so only it will contribute fully to the *n*-slope. All remaining substituents experience delocalized adsorption [10, 22, 37], and so do not contribute fully to the *n*-slope.

In addition to delocalization, the relative position of the two polar groups also affects the *n*-slope. In **Table 4-1**, the para compounds have a larger slope than their ortho isomers. There are a variety of causes for this trend. 2-Iodoaniline experiences steric hindrance between the functionalities, and so its *n*-slope is lower than that of 4-iodoaniline. For the nitroanilines, both strong intramolecular hydrogen bonding in 2-nitroaniline [10] and steric hindrance causes 2-nitroaniline to have a smaller slope than 4-nitroaniline. However, while the para compounds consistently have a larger slope than their ortho isomers in **Table 4-1**, there are many exceptions to this trend in the literature for other systems. For example, ortho compounds usually have a larger adsorption energy on alumina than their para isomers [10], which will in turn will result in a larger slope.

4.4.4 Influence of the mobile phase and stationary phase on the n-slope

As evident in **Table 4-1**, the *n*-slope depends on both the mobile phase and stationary phase. To evaluate the influence of the mobile phase, **Figure 4-1** plots the *n*-slope for 16 solutes on the cyano (**Figure 4-1A**), diol (**Figure 4-1B**), and amino (**Figure 4-1C**)

stationary phases for a variety of mobile phases. The *n*-slope strongly depends on the particular solute, ranging from 0.6 for solutes such as 8-methylquinoline to 2.29 for 1,2-phenylenediamine. Based on Soczewiñski, the *n*-slope should be constant for a given solute, independent of the mobile phase. However, most experimental *n*-slope values on the cyano and diol phases in **Table 4-1** do depend on the mobile phase. According to Snyder, the *n*-slope for a given solute with differing mobile phases should be consistently biased by a factor related to the relative adsorption areas of the solute and strong solvent (A_S/A_B, **Table 4-2**). For example, the *n*-slope values with THF (A_B = 5.0) as mobile phase should always be 1.6 times larger than the *n*-slope with IPA (A_B =8.0). However, for the solutes in **Table 4-1** the ratio between the *n*-slopes with THF *vs*. IPA are 1.2 ± 0.2 for the cyano column. The ratio between the *n*-slopes with THF *vs*. MEK are 1.1 ± 0.1 for the diol column, which should be 0.92 according to the A_S/A_B. Thus the effect of mobile phase on the *n*-slope does not agree with either model. However, the mobile phase has a relatively small effect on the *n*-slope, as had been indicated by the ANOVA result (**Table 4-7**) mentioned earlier.

Mobile phase has a strong effect on the *n*-slope on the amino stationary phase based on both the ANOVA (**Table 4-7**) and **Figure 4-1C**. The amino phase has the strongest retention compared to the diol and cyano columns [10]. According to Linear Solvation Energy Relationships (LSERs), amino phases are more basic than either diol or cyano phases [38, 39]. Its hydrogen bond acidity is similar to that for cyano phases, but less than that for silica or diol phases [38, 39]. Hydrogen bond accepting compounds (ethers, esters and ketones) are less strongly retained on amino phases, while hydrogen bond donating solutes are more strongly retained relative to other solutes [2]. Amino phases generally show more retention for acidic compounds than either the diol or cyano phases [40]. When the hydrogen bond donating solvent IPA was used as mobile phase on the amino column, the *n*-slopes are smaller than with other mobile phases (**Table 4-1**) due to the preferential adsorption of IPA. The strong preferential interactions between stationary

Table 4-9 ANOVA analysis for influence of stationary phase.

Sum of Squares	THF (Figure 4-2A)	EA (Figure 4-2B)
Within group (solutes)	0.2	0.1
Between groups (stationary phases)	6.4	2.8

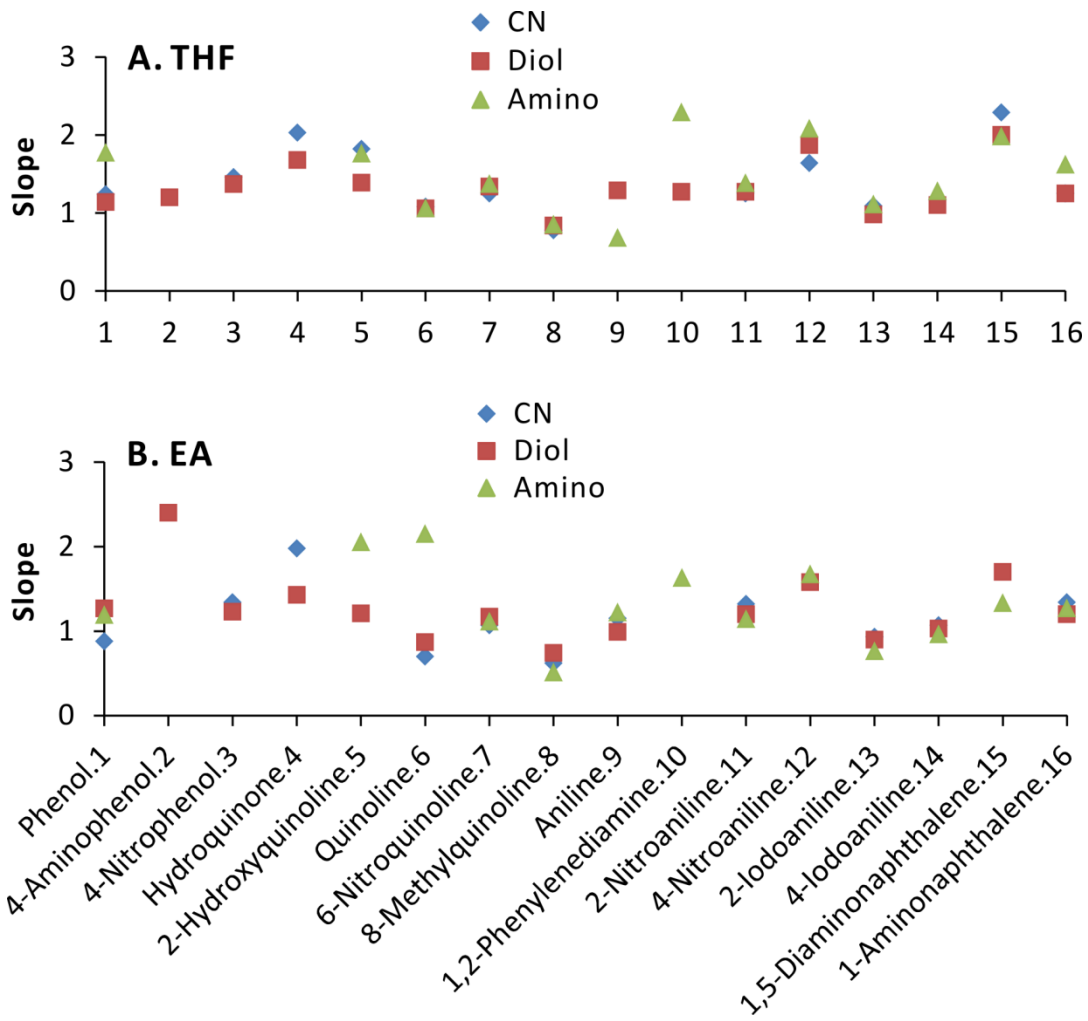

Figure 4-2 Stationary phase dependence of *n*-slopes for solutes with tetrahydrofuran (THF) and ethyl acetate (EA) mobile phases. Data from Soczewiñski [3]. The compound numbers are as presented in Ref. [3].

phase, mobile phase and solute cause retention on the amino stationary phase to be different from that of other classic NPLC bonded phases.

In analogy to **Figure 4-1**, **Figure 4-2** plots the *n*-slopes obtained with the same mobile phase for various stationary phases. The *n*-slopes on the diol, cyano and amino phases are within 30% percent for a given compound with either THF or EA as mobile phase. A few compounds show distinctly different behavior on the amino phase (*e.g.*, quinoline, for which *n* varies 85%). This is consistent with the ANOVA results (**Table 4-9**) which showed that the differences between-solutes was much greater than the differences between-stationary phases.

In summary, on all three stationary phases, the solute property is the most important factor that determines the *n*-slope.

4.5 Conclusions

On classic NPLC bonded phases, we have the following conclusions. There is a measurable contribution of an aromatic ring to the *n*-slope which agrees better with the Snyder model. The Soczewiñski model predicts no contribution to the *n*-slope. The number of aromatic double bonds is the best descriptor when estimating the relative *n*-slope of PAHs because of its good correlation and simplicity. Increasing the concentration of a localizing solvent such as IPA has less effect on retention than does increasing the concentration of a non-localizing solvent such as DCM. Overall, the Snyder model predicts the *n*-slope slightly better than the Soczewiñski model, but both models have comparable uncertainty in predicting the *n*-slope for a specific compound. On the cyano and diol phases, the contributions of the polar groups to the *n*-slope parallel the adsorption energy. For a doubly substituted aromatic, the contribution of the less polar functionality to the *n*-slope is diminished because of the delocalization caused by the localization of the more polar group. The mobile phase has a relatively small effect on the *n*-slope on the cyano and diol phase. On the amino phase, mobile phase has a strong effect on the *n*-slope. The strong preferential interactions between stationary phase,

mobile phase and solute cause retention on amino stationary phase to be different from other classic NPLC bonded phases. On all classic NPLC bonded phases, the nature of the solute is the most important factor governing the *n*-slope.

4.6 References

[1] E.L. Weiser, A.W. Salotto, S.M. Flach, L.R. Snyder, Basis of retention in normal-phase high-performance liquid-chromatography with cyano-propyl columns, J. Chromatogr. 303 (1984) 1-12.

[2] L.R. Snyder, T.C. Schunk, Retention mechanism and the role of the mobile phase in normal-phase separation on amino-bonded-phase columns, Anal. Chem. 54 (1982) 1764-1772.

[3] M. Waksmundzka-Hajnos, A. Petruczynik, E. Soczewiñski, A. Hawryl, Retention mechanism of model compounds on polar bonded stationary phases in normal phase systems, Chem. Anal. (Warsaw) 47 (2002) 483-505.

[4] P.L. Smith, W.T. Cooper, Retention and selectivity in amino, cyano and diol normal bonded phase high-performance liquid-chromatographic columns, J. Chromatogr. 410 (1987) 249-265.

[5] M. Waksmundzka-Hajnos, A. Petruczynik, A. Hawryl, Comparison of chromatographic properties of cyanopropyl-, diol- and aminopropyl- polar-bonded stationary phases by the retention of model compounds in normal-phase liquid chromatography systems, J. Chromatogr. A 919 (2001) 39-50.

[6] E. Soczewiñski, Solvent composition effects in thin-layer chromatography systems of type silica gel-electron donor solvent, Anal. Chem. 41 (1969) 179-182.

[7] L.R. Snyder, Role of solvent in liquid-solid chromatography - review, Anal. Chem. 46 (1974) 1384-1393.

[8] E. Soczewiñski, T. Dzido, W. Golkiewicz, A simple molecular model of adsorption chromatography. 11. Adsorption of aromatic nitro-compounds with various polar groups on magnesium-silicate, Chromatographia 10 (1977) 298-302.

[9] E. Soczewiñski, W. Golkiewicz, T. Dzido, A simple molecular model of adsorption chromatography. 10. Solvent composition effects in TLC of aromatic nitro-compounds using magnesium-silicate as adsorbent, Chromatographia 10 (1977) 221-225.

[10] L.R. Snyder, J.J. Kirkland, J.W. Dolan, Introduction to modern liquid chromatography, 3rd ed., Wiley, Hoboken, N.J., 2010.

[11] L.R. Snyder, Principles of adsorption chromatography; the separation of nonionic organic compounds, Marcel Dekker, New York, 1968.

[12] L.R. Snyder, Solvent selectivity in normal-phase TLC, J. Planar Chromatogr. 21 (2008) 315-323.

[13] E. Soczewinski, W. Golkiewicz, A simple molecular model for adsorption chromatography. VII. Relationship between the RM value and the composition for phenols in systems of the type (cyclohexane+polar solvent)/silica, Chromatographia 6 (1973) 269-273.

[14] E. Soczewiñski, T. Dzido, Effect of the eluent composition in HPLC on the retention of bi- and trifunctional aromatic solutes, Chromatographia 22 (1986) 25-30.

[15] E. Soczewiñski, Mechanistic molecular model of liquid-solid chromatography retention-eluent composition relationships, J. Chromatogr. A 965 (2002) 109-116.

[16] W. Gołkiewicz, A simple molecular model for adsorption chromatography. IX. Comparison of adsorption mechanisms in thin-layer chromatography and high-speed liquid chromatography, Chromatographia 9 (1976) 113-118.

[17] W. Gołkiewicz, E. Soczewiñski, A simple molecular model of adsorption chromatography. VI. RM-composition relationships of solutes with two functional groups, Chromatographia 5 (1972) 594-601.

[18] E. Soczewiñski, W. Golkiewicz, W. Markowski, A simple molecular model of adsorption chromatography. 8. Solvent composition effects in thin-layer chromatography of aromatic nitro-compounds in (cyclohexane + polar-solvent) - silica type systems, Chromatographia 8 (1975) 13-17.

[19] P.L. Grizzle, J.S. Thomson, Liquid-chromatographic separation of aromatic-hydrocarbons with chemically bonded (2,4-dinitroanilinopropyl)silica, Anal. Chem. 54 (1982) 1071-1078.

[20] J.S. Thomson, J.W. Reynolds, Separation of aromatic-hydrocarbons using bonded-phase charge-transfer liquid-chromatography, Anal. Chem. 56 (1984) 2434-2441.

[21] L.R. Snyder, Linear elution adsorption chromatography: III. Further delineation of the eluent role in separations over alumina, J. Chromatogr. 8 (1962) 178-200.

[22] L.R. Snyder, Localization in adsorption chromatography, J. Planar Chromatogr. 25 (2012) 184-189.

[23] D. Wu, G.K. Nedev, C.A. Lucy, Retention mechanism of hypercrosslinked polystyrene silica hybrid phase in normal phase chromatography, J. Chromatogr. A 1370 (2014) 50-55.

[24] L.R. Snyder, H. Poppe, Mechanism of solute retention in liquid-solid chromatography and the role of the mobile phase in affecting separation - competition versus sorption, J. Chromatogr. 184 (1980) 363-413.

[25] P. Olsson, I. Sadiktsis, J. Holmback, R. Westerholm, Class separation of lipids and polycyclic aromatic hydrocarbons in normal phase high performance liquid chromatography - A prospect for analysis of aromatics in edible vegetable oils and biodiesel exhaust particulates, J. Chromatogr. A 1360 (2014) 39-46.

[26] Molinspiration, Calculation of molecular properties and bioactivity score. http://www.molinspiration.com/cgi-bin/properties,2016 (accessed 30.03.16)

[27] M. Jaroniec, A. Patrykiejew, Theory of Adsorption from Multicomponent Liquid-Mixtures on Solid-Surfaces and Its Application to Liquid Adsorption Chromatography, J. Chem. Soc. Faraday Trans. 1 76 (1980) 2486-2495.

[28] M. Jaroniec, J.A. Jaroniec, Simple-model of liquid-solid chromatography involving solute-solvent and solvent-solvent interactions, J. Chromatogr. 210 (1981) 130-132.

[29] R.P.W. Scott, P. Kucera, Solute interactions with mobile and stationary phases in

liquid-solid chromatography, J. Chromatogr. 112 (1975) 425-442.

[30] R.P.W. Scott, P. Kucera, Solute-solvent interactions on the surface of silica-gel. 2, J. Chromatogr. 171 (1979) 37-48.

[31] S.A. Wise, S.N. Chesler, H.S. Hertz, L.R. Hilpert, W.E. May, Chemically-Bonded Aminosilane Stationary Phase for High-Performance Liquid-Chromatographic Separation of Polynuclear Aromatic-Compounds, Anal. Chem. 49 (1977) 2306-2310.

[32] L.Y. Lin, W.T. Cooper, Isocratic high-performance liquid chromatographic separation and multiple-wavelength ultraviolet detection of aldicarb and its soil degradation products. Optimization of stationary phase selectivity, J. Chromatogr. A 390 (1987) 285-295.

[33] D.E. Clark, What has polar surface area ever done for drug discovery?, Future Med. Chem. 3 (2011) 469-484.

[34] D. Nurok, R.R. Sorrell, C.L. McCain, M.C. Frost, P. Hajdu, T.C. Powell, T. Lahr, R.M. Kleyle, Prediction of retention using polar and nonpolar surface areas of single-solvent mobile phases, J. Planar Chromatogr. 12 (1999) 42-45.

[35] P. Ertl, B. Rohde, P. Selzer, Fast calculation of molecular polar surface area as a sum of fragment-based contributions and its application to the prediction of drug transport properties, J. Med. Chem. 43 (2000) 3714-3717.

[36] L.R. Snyder, Linear elution adsorption chromatography: XII. Functional group adsorption energies on metal oxide adsorbents, J. Chromatogr. 23 (1966) 388-402.

[37] L.R. Snyder, Linear elution adsorption chromatography: IV. Group localization in the adsorbate. Extension of the role of solute structure in separations over alumina, J. Chromatogr. 8 (1962) 319-342.

[38] J.W. Li, D.A. Whitman, Characterization and selectivity optimization on diol, amino, and cyano normal phase columns based on linear solvation energy relationships, Anal. Chim. Acta 368 (1998) 141-154.

[39] J.H. Park, M.H. Yoon, Y.K. Ryu, B.E. Kim, J.W. Ryu, M.D. Jang, Characterization

of some normal-phase liquid chromatographic stationary phases based on linear solvation energy relationships, J. Chromatogr. A 796 (1998) 249-258.
[40] J. Cazes, Encyclopedia of chromatography, Marcel Dekker, New York, 2001.

Chapter Five. Study of the slope of the linear relationship between retention and mobile phase composition (Snyder-Soczewiñski model) in charge-transfer and hypercrosslinked phases[1]

5.1 Introduction

Polycyclic aromatic compounds (PACs) including hydrocarbons (PAHs) and heterocycles are commonly monitored environmental pollutants. Measurement of PACs is important for petroleum and coal industry. Charge transfer liquid chromatography has been intensively used for the separation of PACs [1]. Charge transfer liquid chromatography is also very useful in separating biological compounds including amino acids, peptides, nucleosides and nucleotides [2].

Charge transfer chromatography uses the formation of labile charge transfer complexes (*i.e.*, electron donor-acceptor complexes) [3]. The complexation takes place during the separation and is part of the retention mechanism. The complexation can happen either in the stationary phase [1, 4] (most frequent, and in this chapter) or in the mobile phase [5]. The charge transfer phase can be electron donors/acceptors coated or bonded to the support [6, 7]. Since its invention in 1975 [8], chemically bonded silica phase with electron donors or acceptors have been intensively developed. Many charge transfer columns are chemically bonded phases with nitro groups, such as dinitroanilinopropyl phase (DNAP), which was invented by Thomson and co-workers [9, 10] and commercialized by ES Industries.

This chapter explores the DNAP charge transfer phase and HC-Tol (column

[1] A version of this chapter has been accepted by Journal of Chromatography A as part of Di Wu and Charles A. Lucy, "Study of the slope of the linear relationship between retention and mobile phase composition (Snyder-Soczewiñski model) in normal phase liquid chromatography with bonded and charge-transfer phases", 2016. I conducted all experiments and wrote the manuscript.

introduced in **Section 1.3.2** and **Section 2.1**) hypercrosslinked phase in the context of the Snyder-Soczewiñski model. As in **Chapter 4**, we focus on the *n*-slope of the log *k vs*. log N_B (mole fraction of strong solvent) plots. The understanding gained from classic polar bonded phases was used to interpret the *n*-slope values observed on the DNAP and hyperscrosslinked polystyrene phases.

5.2 Experimental

The theory, apparatus and procedures were similar to those in **Chapter 4**. Thus, these will only briefly be reviewed.

5.2.1 Apparatus

All experiments were performed on an Agilent 1260 Infinity LC system (Agilent, Santa Clara, CA, USA) with Agilent Chemstation Rev. B.04.03 software. The system consisted of a quaternary low pressure pump at a flow rate of 1.0 mL/min, an on-line degasser, an auto-sampler performing a 1 μL partial loop injection, a temperature controlled column compartment at 35°C, and a variable wavelength detector set at 254 nm with a response time of 1 s. Data acquisition was at 10 Hz. All tubing and fittings were stainless steel of 0.17 mm ID. The DNAP column (5 × 0.46 cm) was purchased from ES Industries (Catalog #: 1-800-356-6140, West Berlin, NJ, USA) packed with 5 μm particles of 60 Å pore size. HC-Tol column was home-packed as in **Section 2.3.3**.

5.2.2 Chemicals

All solutes were >90% purity. Optima grade hexane and dichloromethane (DCM) and isopropanol (IPA) were purchased from Thermo Fisher Scientific Inc. (Fairlawn, NJ, USA). Chrysene and picene were purchased from K & K Laboratories (Carlsbad, CA, USA). All other solutes were from Sigma–Aldrich (St. Louis, MO, USA). Solute solutions were prepared either in pure hexane or in mobile phase (0.05 to 5 mg/mL), and filtered through 0.20 μm Millex syringe filters (EMD Millipore Corporation, Billerica, MA, USA) prior to injection.

5.2.3 Procedures

The retention factors on DNAP and the hypercrosslinked phases were based on triplicate injections and calculated using the dead time t_0 based on the first peak caused by injection of pure hexane [8].

5.3 Results and Discussion

5.3.1 Charge transfer columns

Charge transfer columns (*i.e.*, separations based on the formation of charge transfer complexes) are widely used in petroleum analysis [11-13]. However there have been few fundamental studies of the retention and selectivity of these columns. In particular, the *n*-slope of plots of log *k vs*. log N_B has not been analyzed on DNAP columns. DCM is the most widely used polar solvent on DNAP columns [2, 11, 12, 14], and so was used in our studies. Plots of log *k vs*. log N_B are linear ($R^2 > 0.97$) over 20-50% DCM for the 27 solutes studied on a DNAP column (**Figure 5-1**).

5.3.1.1 Effect of addition of aromatic rings on charge transfer NPLC phases

To illustrate the effect of aromatic ring number on the *n*-slopes, compound pairs in **Table 5-1** that possessed the same polar group but differed in the number of aromatic rings were selected. These compound pairs ($n_{1\text{-nitronaphthalene}} - n_{nitrobenzene} = 1.91 - 1.58 = 0.33$, and $n_{aminonaphthalene} - n_{aniline} = 2.1 - 1.6 = 0.5$) show that the aromatic rings contribute to the *n*-slope on DNAP.

Alternately, the effect of an aromatic ring on *n*-slope with DCM can be determined based on the PAHs in **Table 5-1**. Regressing the *n*-slope *vs*. aromatic ring number (**Figure 5-2a**) yields a contribution of 0.4 per ring with an R^2 of 0.91. The correlation of the *n*-slope with the aromatic rings is consistent with the Snyder model's prediction of increased *n*-slope with increased area of interaction of the solute (A_S in **Eq. 4-4**). This agreement is not surprising given retention on DNAP would be expected to be similar to Snyder's assumption of a less polar solute adsorbing flatwise on a less polar adsorbent [15]. **Table 5-2** summarizes the contribution of the aromaticity to the *n*-slope on the

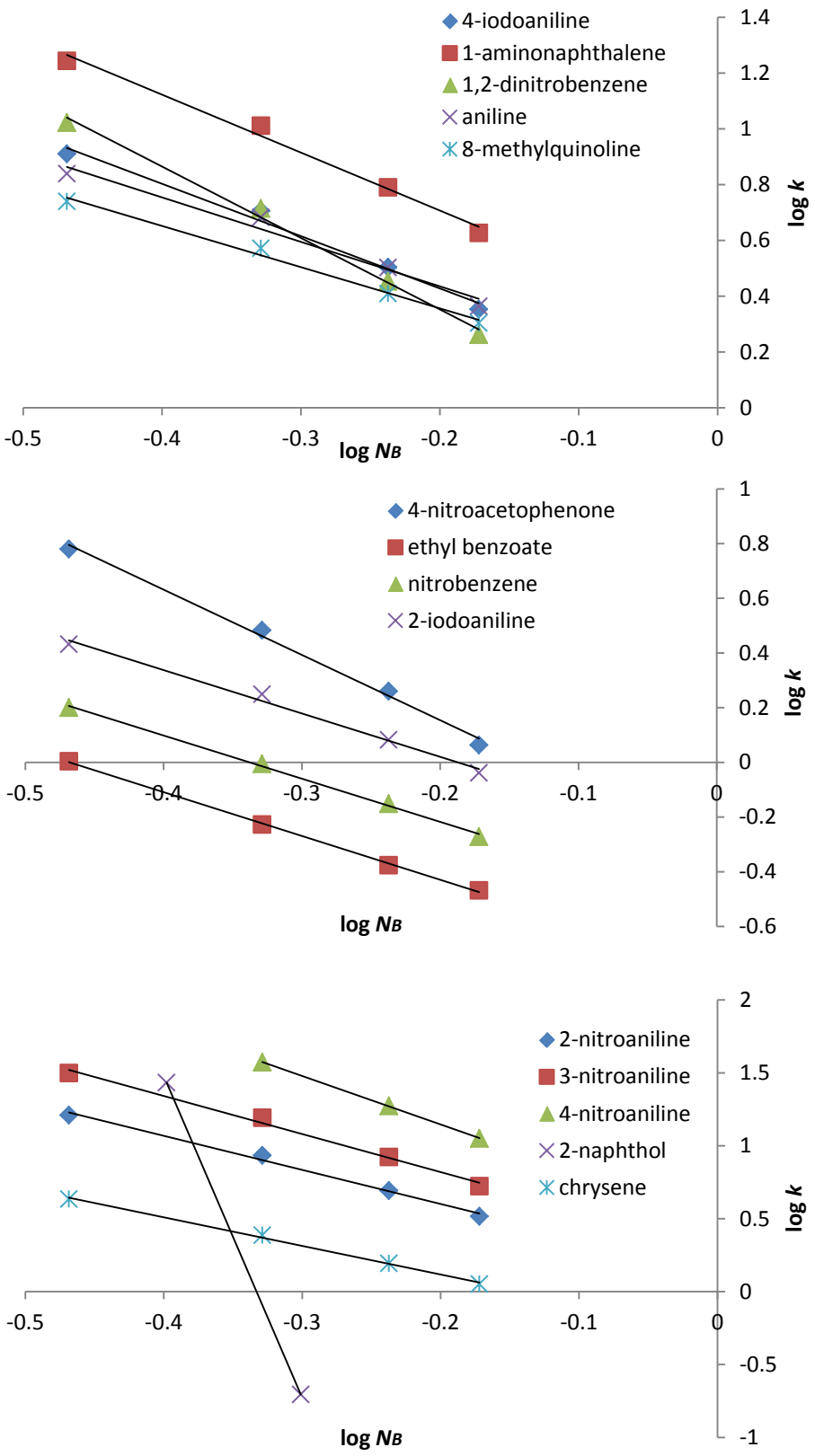

Figure 5-1a log *k*-log N_B plot on DNAP column with DCM/hexane mobile phase.

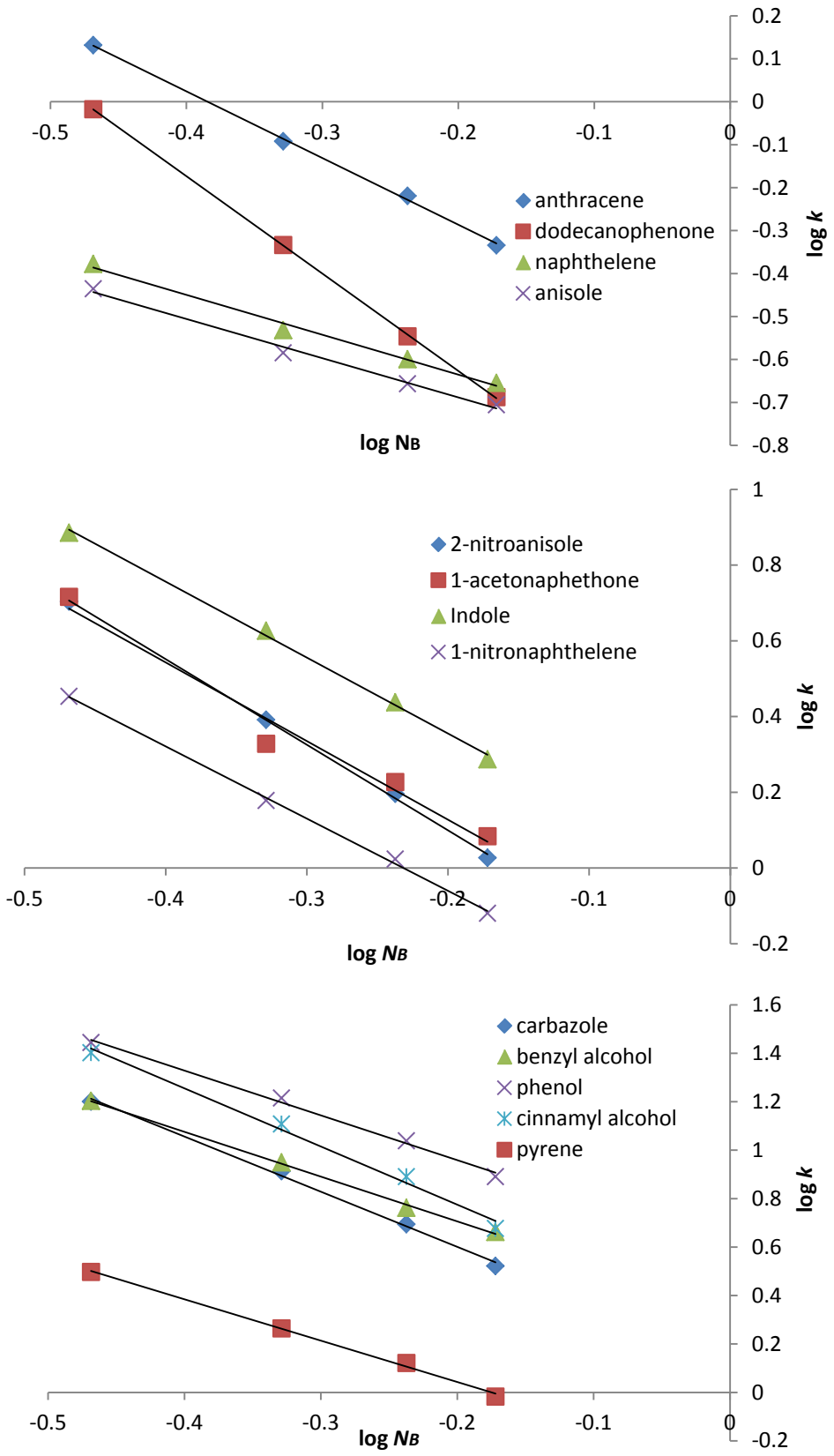

Figure 5-1b log k-log N_B plot on DNAP column with DCM/hexane mobile phase.

Table 5-1 Comparison of the predicted and experimental *n*-slope on DNAP with a hexane/DCM mobile phase.

	Observed *n*	**R^2**	**A_S/A_B**	**Polar group**	**N_{Polar}**
naphthalene	0.93±0.06	0.991	1.98	None	0
anthracene	1.55±0.04	0.999	2.49	None	0
pyrene	1.71±0.06	0.997	2.61	None	0
chrysene	2.0±0.07	0.997	3.00	None	0
benzyl alcohol	1.85±0.05	0.998	1.65	OH	1
ethyl benzoate	1.60±0.03	0.999	2.11	COO	1
nitrobenzene	1.58±0.05	0.998	1.65	NO_2	1
1-acetonaphthone	2.1±0.2	0.972	2.21	CO	1
dodecanophenone	2.27±0.1	1.000	3.89	CO	1
1-nitronaphthalene	1.91±0.05	0.999	2.16	NO_2	1
carbazole	2.28±0.09	0.997	2.93	NH	1
indole	2.01±0.07	0.998	2.41	NH	1
cinnamyl alcohol	2.4±0.2	0.991	2.09	OH	1
2-naphthol	2.50	1.000	1.94	OH	1
phenol	1.85±0.09	0.995	1.43	OH	1
8-methylquinoline	1.5±0.1	0.991	1.99	N	1
1-aminonaphthalene	2.1±0.2	0.989	1.99	NH_2	1
anisole	0.91±0.06	0.992	1.60	OCH_3	1
aniline	1.6±0.2	0.976	1.48	NH_2	1
2-nitroaniline	2.3±0.1	0.994	1.66	NH_2, NO_2	2
3-nitroaniline	2.6±0.2	0.993	1.66	NH_2, NO_2	2
4-nitroaniline	3.32±0.04	0.999	1.66	NH_2, NO_2	2
2-iodoaniline	1.6±0.1	0.998	1.66	I, NH_2	2
4-iodoaniline	1.9±0.2	0.987	1.66	I, NH_2	2
2-nitroanisole	2.26±0.05	0.999	1.78	OCH_3, NO_2	2
4-nitroacetophenone	2.4±0.1	0.995	1.78	CO, NO_2	2
1,2-dinitrobenzene	2.6±0.1	0.995	1.83	NO_2, NO_2	2

DNAP column using the conventional DCM mobile phase. The influence of an aromatic ring is larger than on polar bonded phases (**Table 4-4**). This greater dependence on DNAP could be due to retention through the pi-pi interactions with makes the solutes' aromatic rings an active contributor to the retention behavior [5, 15, 16].

As stated in **Section 4.4.1** for classical NPLC bonded phases, the number of aromatic double bonds or A_S better correlate with *n*-slope than the number of aromatic rings. Similarly, for DNAP with DCM mobile phase, the number of aromatic bonds and A_S both correlate well with the *n*-slope. Regressing the *n*-slope *vs*. N_{double} for the PAHs from **Table 5-1** (**Figure 5-2b**) yields a contribution of 0.26 per double bond. Regressing the *n*-slope *vs*. N_{double} (R^2=0.99) has slightly better correlation than *vs*. A_S (R^2 =0.97, **Figure 5-2c**). Thus, the number of double bonds is preferred when predicting *n*-slope because of its accuracy and simplicity.

Recently azaarenes (polycyclic aromatic nitrogen hydrocarbons) were separated on DNAP using IPA in our group [17]. **Figure 5-3** shows the retention behavior observed for PAHs using isopropyl alcohol (IPA) as the strong solvent. Interestingly, the *n*-slope for PAHs on DNAP is near zero when IPA is used. This means IPA does not interrupt the interactions between the PAHs and DNAP stationary phase. This explains why IPA has not been commonly used with DNAP. This behavior is consistent with the literature [18] where increasing MTBE mobile phase composition had no effect on PAH retention on the charge transfer pentabromobenzyl (PBB) column.

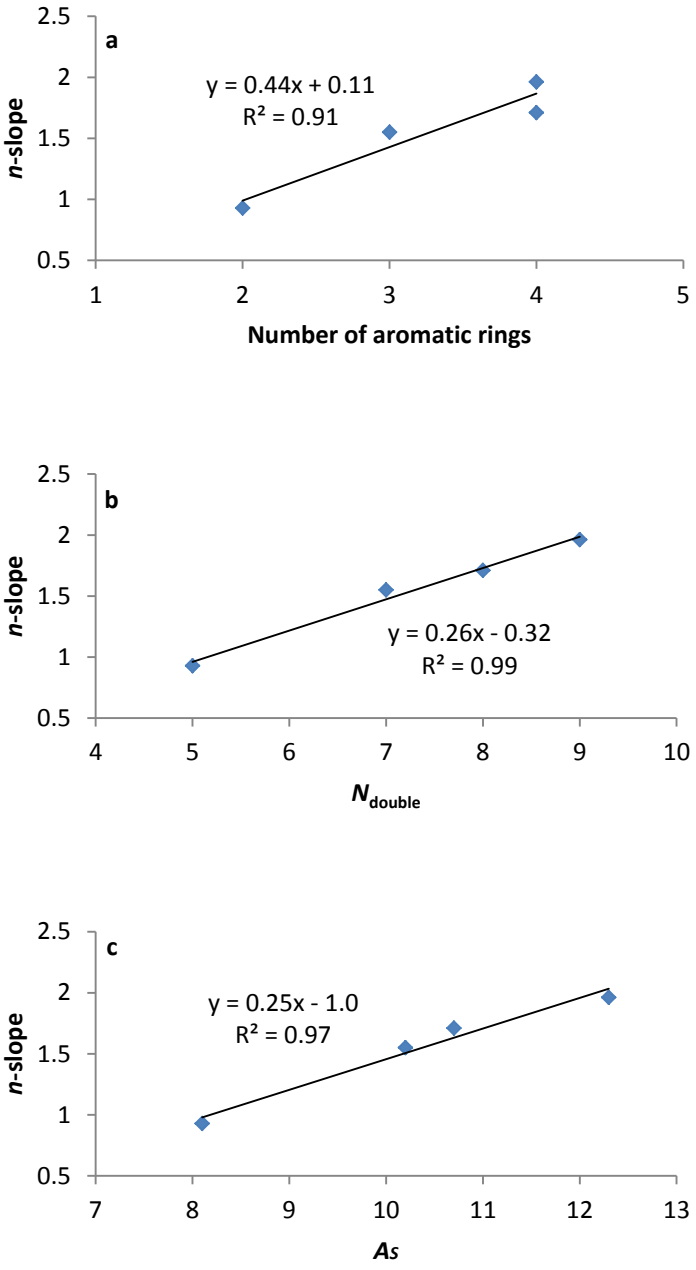

Figure 5-2 Effect of aromaticity descriptors to the *n*-slope on DNAP column with DCM/hexane mobile phase.

Table 5-2 Contribution of aromaticity to *n*-slope of PAHs on DNAP using hexane/DCM mobile phases.

	Nitrobenzene 1-nitronaphthalene	Aniline 1-aminonaphthalene	PAHs	Average
Ring contribution	0.33±0.07	0.5±0.3	0.4±0.1	0.4
Double bond contribution	0.16±0.03	0.25±0.2	0.26±0.02	0.2

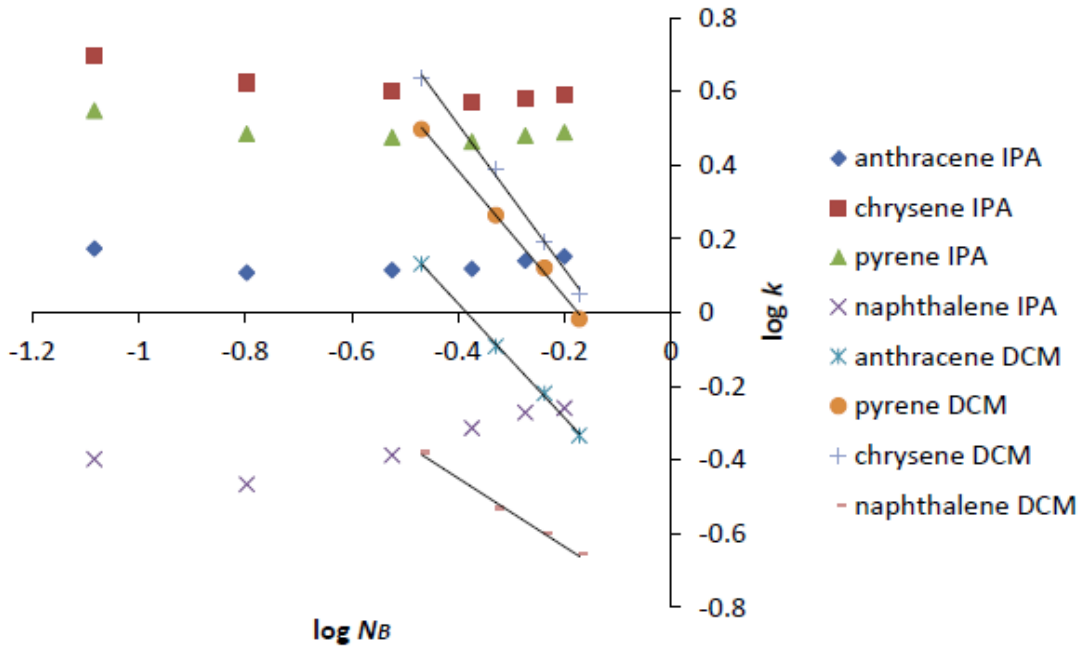

Figure 5-3 log *k*-log N_B plot for PAH on DNAP column with IPA/hexane and DCM/hexane mobile phases. Conditions: flow rate, 1.0 mL/min; injection volume, 1 μL; column temperature, 35 ˚C; detector wavelength, 254 nm.

5.3.1.2 Effect of Molecular Area

Comparing the predicted *n*-slope based on the A_S/A_B as defined in the Snyder model (**Eq. 4-4**) versus the observed *n*-slope resulted in a mean difference of +0.1 with a standard deviation of 0.6. The Soczewiñski model consistently under-estimated the *n*-slope on DNAP, with a mean difference of -0.8 and standard deviation of 0.6. Thus, like on the bonded silica phases (**Section 4.4.2**), the Soczewiñski model yields poorer predictions of the *n*-slope than the Snyder model, but both models have comparable uncertainty in the predicted *n*-slope for a given compound. This under-estimation bias of the Soczewiñski model is because it does not consider the contribution of the double bond to the *n*-slope, which was demonstrated to be important for the DNAP column in **Section 5.3.1**. For the data in **Table 5-1**, the *n*-slope was fit to the equation:

$$n = N_{Polar} + (\text{contribution per aromatic double bond}) \times N_{\text{double}} \quad (5\text{-}1)$$

where N_{Polar} is the number of polar group. The contribution of one double bond based on fitting **Eq. 5-1** to the *n*-slope in **Table 5-1** is 0.19. This contribution of one double bond to the *n*-slope is in good agreement with the contributions determined using PAHs and compound pairs (**Table 5-2**). Using the modified Soczewiñski model prediction of the *n*-slope:

$$n = N_{Polar} + 0.19 N_{\text{double}} \quad (5\text{-}2)$$

Comparing the modified Soczewiñski model (**Eq. 5-2**) prediction of *n*-slope versus the observed *n*-slopes on DNAP in **Table 5-1** has mean difference of 0 and a standard deviation of 0.4, which is better than the original Soczewiñski model and simpler than the Snyder model.

5.3.1.3 Contribution of polar group to slope

The *n*-slopes for substituted monoaromatics in **Table 5-1** are larger than those for comparable compounds on the classic NPLC phases (**Table 4-1**). On DNAP with DCM, the contributions of polar groups to the *n*-slope increase in the order:

$$\text{-OCH}_3 < \text{-NO}_2 = \text{-CO}_2\text{-R} < \text{-NH}_2 \leq \text{-CO-R} = \text{-NH-} < \text{-OH} \quad (5\text{-}3)$$

The contribution of -OCH_3 is slightly smaller than 1, while the contribution of the rest of the polar groups are all larger than 1. This order generally agrees with adsorption energy (**Table 4-8**).

The contributions of two polar groups are smaller than N_{Polar} due to delocalization of the second polar group. The relative position of the two polar groups affects the *n*-slope the same way as on polar bonded silica phases (**Section 4.4.3**). In **Table 5-1** on DNAP, the para substituents contribute more to the *n*-slope than do meta substituents, than do ortho substituents. This trend is mainly due to decreasing steric hindrance from a para substituent relative to its ortho isomer. For 2-nitroaniline, there may also be intra-molecular hydrogen bonding.

5.3.2 Hypercrosslinked polystyrene phases

Table 5-3 summarizes the *n*-slope values for PAHs on HC-Tol columns (data from **Chapter 2**). **Table 5-4** summarizes the correlation between the *n*-slope and these parameters for a wide range of stationary and mobile phases. For HC-Tol column, the *n*-slope increases with all three PAH descriptors: the number of rings, number of double bonds, and A_S. The correlation is the same for all three PAH descriptors. Overall, the number of double bonds N_{double} is more descriptive than number of rings and much easier to calculate than A_S, and so N_{double} is the preferred descriptor when estimating the relative *n*-slope of PAHs.

Table 5-3 Experimental *n*-slope values on HC-Tol.

Stationary Phase	Mobile phase	Naphthalene	Anthracene	Pyrene	Chrysene	Picene
N_{double}		5	7	8	9	11
$\boldsymbol{A_S}$		8.1	10.2	10.7	12.3	14.4
HC-Tol	THF	0.21	0.27	0.28	0.34	0.44
	DCM	0.68	1.00	1.16	1.33	1.60

Table 5-4 Dependence of *n*-slope on PAH size on HC-Tol.

Stationary phase	Mobile phase	R^2 for No. of rings	R^2 for N_{double}	R^2 for A_S
HC-Tol	THF	0.998	0.998	0.998
	DCM	0.9999	0.9999	0.9999

5.4 Conclusions

On the charge transfer DNAP column with a DCM mobile phase, the aromatic ring has a much larger contribute to the *n*-slope than on classic NPLC bonded phases. The number of aromatic double bonds correlates best with the *n*-slope. The composition of the localizing IPA mobile phase has no effect on PAHs retention. So IPA does not interrupt the interactions between the PAHs and DNAP stationary phase. The *n*-slope is best predicted using a modified Soczewiñski model in which 0.19 per aromatic double bond is added to the number of polar groups. The contributions of the polar groups to the *n*-slope also agree with adsorption energy.

5.5 References

[1] D. Cagniant, Complexation chromatography, Marcel Dekker, New York, 1992.

[2] N.E. Oro, C.A. Lucy, High performance liquid chromatographic separations of gas oil samples and their hydrotreated products using commercial normal phases, J. Chromatogr. A 1218 (2011) 7788-7795.

[3] D.A.P. Small, T. Atkinson, C.R. Lowe, High-performance liquid charge-transfer chromatography, J. Chromatogr. 248 (1982) 271-279.

[4] P.A.D. Edwardson, C.R. Lowe, T. Atkinson, Purification of homo-oligonucleotide and hetero-oligonucleotide using high-performance charge-transfer chromatography, J. Chromatogr. 368 (1986) 363-369.

[5] L. Nondek, J. Malek, Liquid-chromatography of aromatic-hydrocarbons on a chemically bonded stationary phase of charge-transfer type, J. Chromatogr. 155 (1978) 187-190.

[6] L.C. Sander, R.M. Parris, S.A. Wise, P. Garrigues, Shape-discrimination in

liquid-chromatography using charge-transfer phases, Anal. Chem. 63 (1991) 2589-2597.

[7] J.M. Roussel, A.M. Siouffi, M. Julliard, M. Chanon, Liquid-chromatography with charge-transfer complexation, Chromatographia 29 (1990) 419-428.

[8] W. Holstein, H. Hemetsberger, Donor-acceptor complex chromatography (DACC) 1. Introduction and nomenclature, Chromatographia 15 (1982) 186-190.

[9] W. Holstein, H. Hemetsberger, Donor-acceptor complex chromatography (DACC) 2. Review of papers, Chromatographia 15 (1982) 251-258.

[10] C.H. Lochmuller, C.W. Amoss, 3-(2,4,5,7-Tetranitrofluorenimino) -propyldiethoxysiloxane - highly selective, bonded pi-complexing phase for high-pressure liquid-chromatography, J. Chromatogr. 108 (1975) 85-93.

[11] P.L. Grizzle, J.S. Thomson, Liquid-chromatographic separation of aromatic-hydrocarbons with chemically bonded (2,4-dinitroanilinopropyl)silica, Anal. Chem. 54 (1982) 1071-1078.

[12] J.S. Thomson, J.W. Reynolds, Separation of aromatic-hydrocarbons using bonded-phase charge-transfer liquid-chromatography, Anal. Chem. 56 (1984) 2434-2441.

[13] L. Carbognani, Group-type separation of middle petroleum distillates by adsorption and charge-transfer liquid-chromatography with dielectric-constant detection, J. Chromatogr. A 663 (1994) 11-26.

[14] D.M. Jewell, Preparative trinitrofluorenone charge-transfer chromatography of petroleum aromatics, Anal. Chem. 47 (1975) 2048-2050.

[15] L.R. Snyder, J.J. Kirkland, J.W. Dolan, Introduction to modern liquid chromatography, 3rd ed., Wiley, Hoboken, N.J., 2010.

[16] W.K. Robbins, Quantitative measurement of mass and aromaticity distributions for heavy distillates 1. Capabilities of the HPLC-2 system, J. Chromatogr. Sci. 36 (1998) 457-466.

[17] P. Jiang, Separation and characterization of polycyclic aromatic hydrocarbons and azaarenes using normal phase liquid chromatography and electrospray ionization mass

spectrometry, Ph.D thesis, University of Alberta, May 9th, 2016.

[18] P. Olsson, I. Sadiktsis, J. Holmback, R. Westerholm, Class separation of lipids and polycyclic aromatic hydrocarbons in normal phase high performance liquid chromatography - A prospect for analysis of aromatics in edible vegetable oils and biodiesel exhaust particulates, J. Chromatogr. A 1360 (2014) 39-46.

Chapter Six. Linear solvation energy relationships in normal phase chromatography based on gradient separations

6.1 Introduction

The column is the key component of an HPLC method. Columns differ in their retention and selectivity properties. Initially isocratic separations under a range of mobile phase conditions were used to find the optimum separation conditions for each column in different situations. Later, gradient scouting separations were recognized to be a much more powerful and quicker means to optimize a separation. Dolan [1] suggested three reasons to use scouting gradients to begin method development. First of all, all peaks will be eluted either during the gradient or a few minutes after the gradient. Second, prior knowledge of the sample is not mandatory to design a good gradient separation method. It is possible to get a useful chromatogram even with the first injection. Third, gradient scouting runs let the analyst know whether an isocratic method is possible.

More fundamentally, the retention properties of HPLC can be modeled using methods such as linear solvation energy relationships (LSERs) [2-4]. Isocratic separations are typically used to build the LSER models that characterize the retention properties of HPLC columns [2, 5, 6]. However, for any given isocratic condition, some compounds have too low of retention to be accurately measured, while other compounds are too retained to elute within a reasonable time. Thus, many isocratic trials are typically required to find conditions that provide reasonable retention of the probe compounds. Even then, only a very limited number of compounds of limited properties can be studied within the narrow retention time window possible under isocratic conditions.

Thus, just as in method development, gradient elution is a more powerful means of collecting retention data for building LSERs of multicomponent samples possessing a wide range of polarities. With gradient runs, fewer trial and error experiments would be

needed to find the appropriate conditions for data collection. As a consequence, a gradient separation based retention model will be convenient means of characterizing chromatographic columns.

Gradient elution has been used to develop LSER for reversed phase LC [7-9]. However, there are no reports of gradient methods to develop LSERs in normal phase. In this chapter, a gradient method is developed to build a LSER for normal phase chromatography. Column behavior can be predicted simply, with as few as one gradient separation.

6.2 Theory

For linear gradient separations, the mobile phase composition follows the relationship:

$$\phi = \phi_0 + \frac{\phi_G - \phi_0}{t_G} t \tag{6-1}$$

where ϕ is the volume fraction of the strong solvent B at time t, ϕ_0 is the initial B%, and ϕ_G is the final %B at gradient time t_G.

Snyder [10, 11] and Soczewiñski [12] derived similar models for isocratic retention in normal phase LC using binary solvent systems. The Snyder–Soczewiñski model can be expressed as:

$$k = k_1 {N_B}^{-n} \tag{6-2}$$

where k is retention factor observed under a given mobile phase, k_1 is the retention factor in pure strong solvent, N_B is the mole fraction of the strong solvent, and n is the stoichiometric coefficient. **Eq. 6-2** is a different form of **Eq. 3-4.** The stoichiometric coefficient n is the n-slope discussed in **Chapter 4** and **5**. N_B can usually be approximated by the volume fraction of the strong solvent. So **Eq. 6-2** becomes:

$$k = k_1 \phi^{-n} \tag{6-3}$$

Based on **Eq. 6-3**, the gradient retention volume V_R in normal phase LC can be predicted by the Jandera two-parameter model [13-15]:

$$V_R = \frac{t_G F}{\Delta\phi}\left[\frac{(n+1)\Delta\phi}{t_G F} k_1 V_0 + {\phi_0}^{(n+1)}\right]^{\frac{1}{n+1}} - \frac{\phi_0 t_G F}{\Delta\phi} + V_0 \quad (6\text{-}4)$$

where $\Delta\phi$ is change of volume fraction of strong solvent during the gradient separation, V_0 is the dead volume.

The gradient retention time t_R has a similar form:

$$t_R = [\frac{(n+1){t_G}^n k_1 t_0}{\Delta\phi^n} + \left(\frac{t_G\phi_0}{\Delta\phi}\right)^{n+1}]^{\frac{1}{n+1}} - \frac{\phi_0 t_G}{\Delta\phi} + t_0 \quad (6\text{-}5)$$

where t_0 is the dead time. To calculate the retention factor under pure strong solvent (k_1), **Eq. 6-5** can be derived from **Eq. 6-4**:

$$k_1 = \frac{\Delta\phi^n}{(n+1)t_G^n t_0}[\left(t_R + \frac{t_G\phi_0}{\Delta\phi} - t_0\right)^{n+1} - \left(\frac{t_G\phi_0}{\Delta\phi}\right)^{n+1}] \quad (6\text{-}6)$$

In this chapter, retention factors calculated based on initial gradient separations will be used to build linear solvation energy relationships (LSERs) to better understand NPLC retention [2]. LSERs can be written as:

$$\log k = c + eE + sS + aA + bB + vV \quad (6\text{-}7)$$

where k is retention factor, c is intercept, and E, S, A, B and V are the solutes' excess polarizability, dipolarity/polarizability, hydrogen bond acidity, hydrogen bond basicity and molecular volume, respectively. The coefficients e, s, a, b, and v are the differences between the stationary and mobile phases' excess polarizability, polarizability/dipolarity, hydrogen bond accepting ability, hydrogen bond donating ability, and cavity formation ability. Building a robust LSER requires that the model solutes cover a wide range of each of these parameters [2]. Gradient separation can elute these solutes within a reasonable overall run time.

6.3 Experimental

6.3.1 Apparatus

All experiments were performed on an Agilent 1260 Infinity LC (Agilent, Santa Clara, CA, USA) consisting of a quaternary pump, an on-line degasser, an auto-sampler performing a 1 μL partial loop injection, a column heater at 35°C, and a variable

wavelength detector set at 254 nm with a response time of 1 s. Data acquisition at 10 Hz was controlled using Agilent Chemstation Rev. B.04.03 software. All tubing and fittings were stainless steel of 0.17 mm ID. The length of all connecting tubing was minimized. The dwell volume of the system was determined to be 1.15 mL using the procedure in Ref. [16]. To avoid the delay of mobile phase composition caused by dwell volume, sample was injected 1.15 min after the gradient start. The dinitroanilinopropyl (DNAP) column (5 × 0.46 cm) was from ES Industries (West Berlin, NJ, USA) and packed with 5 μm particles of 60 Å pore size. The silica column (5 × 0.46 cm) was home-packed using Zorbax RX-Sil Type B silica (5 μm, 180 m^2/g, 80 Å pore size, Agilent Technologies Inc., Wilmington, DE, USA). A 3 g SiO_2/17 mL isopropanol slurry was packed using a N_2 driven Haskel pump (DSF-122-87153, Burbank, CA, USA) at 6000 psi in the downward direction for 25 min with isopropanol as the driving solvent.

6.3.2 Chemicals

All solutes were >90% purity. Optima grade hexane, and dichloromethane (DCM) were from Thermo Fisher Scientific Inc. (Fairlawn, NJ, USA). Chrysene and picene were from K & K Laboratories (Carlsbad, CA, USA). All other solutes were from Sigma–Aldrich (St. Louis, MO, USA). Solute solutions were 0.05 to 5 mg/mL, and filtered through 0.20 μm Millex syringe filters (EMD Millipore Corporation, Billerica, MA, USA) prior to injection.

6.3.3 Method

For isocratic separations, retention times of samples were measured for mobile phases containing 20, 30, 40 and 50% of DCM in hexane. Retention factors were calculated using the dead time t_0 based on the first peak caused by injection of pure hexane [17]. Gradient conditions are listed in **Table 6-1**. The initial eluent contains ≥20% strong solvent to avoid artifacts caused by the preferential adsorption of the polar solvent on the stationary phase [14, 18]. Gradients 1, 2 and 4 have the same initial condition (20% DCM) but different gradient steepness to test the influence of gradient steepness. The

Solver tool in Excel 2010 was used to solve for coefficients n and k_1 values from gradient separations based on **Eq. 6-5**. The solute descriptors were from ACD/ADME suite (Advanced Chemistry Development, Inc., Toronto, ON, Canada). If available within the software, the literature solute descriptors for the compound were used, as indicated in **Table 6-2**. Otherwise, values estimated by the software were used.

6.4 Results and Discussion

When building LSER models, solutes are chosen to cover a wide range of LSER parameters and retention factors [2]. **Table 6-2** shows the 19 probe compounds used to develop the LSER herein. The solvation parameters for these compounds (**Table 6-2**) had the ranges: 0.69 to 2.6 for excess polarizability; 0.75 to 2.0 for dipolarity/polarizability; 0 to 0.6 for hydrogen bond acidity; 0.08 to 0.6 for hydrogen bond basicity; and 0.89 to 2.4 for molecular volume. These wide ranging parameters result in highly disparate retention. For instance, retention factors under pure DCM range from 0.1 to 5.77.

Table 6-1 Gradient conditions used.

Gradient	DCM composition change (%)	Gradient time (min)
G1	20-100	10
G2	20-100	20
G3	60-80	10
G4	20-100	30

Table 6-2 Probe solutes and solute descriptors.

	A	***B***	***S***	***E***	***V***
2-nitroanisole	0	0.45	1.34	0.968	1.0902
2-naphthol	0.61	0.4	1.08	1.52	1.1441
anisole	0	0.29	0.75	0.708	0.916
anthracene	0	0.28	1.34	2.29	1.4544
benzyl alcohol	0.39	0.56	0.87	0.803	0.916
dibenzofuran	0	0.17	1.02	1.407	1.2743
ethyl benzoate	0	0.46	0.85	0.689	1.2135
nitrobenzene	0	0.28	1.11	0.871	0.8906
phenol	0.6	0.3	0.89	0.805	0.7751
pyrene	0	0.25	1.52	2.6	1.5846
1-acetonaphethone	0	0.54	1.41	1.517	1.3829
dodecanophenone[a]	0	0.45	1.17	0.77	2.4229
1-nitronaphthalene	0	0.29	1.51	1.6	1.2596
naphthelene	0	0.2	0.92	1.34	1.0854
carbazole	0.18	0.08	2.01	1.787	1.3154
indole	0.44	0.22	1.12	1.2	0.9464
4-nitroacetophenone[a]	0	0.59	1.54	1.08	1.1881
dibenzothiophene	0	0.2	1.31	1.959	1.3791
cinnamyl alcohol	0.38	0.6	1.04	1.09	1.1548

a. No Exact Match in the ACD/ADME suite database. Therefore, the calculated parameters are used

6.4.1 Weakness of isocratic LSERs

Under isocratic conditions, only a limited range of retention can be measured. For example, when 70% DCM was used with the DNAP column, most of the probe compounds had retention factors less than 1. Such low *k* possess large relative errors and are not reliable for building LSER models [2]. Conversely, 30% DCM as mobile phase failed to elute the strongly retained 2-naphthol, and with 10% DCM as mobile phase benzyl alcohol, phenol, carbazole, cinnamyl alcohol and 2-naphthol did not elute.

LSER will be compromised if retention data is available for only a limited number and range of compounds. To illustrate this impact, **Table 6-3** shows LSER constructed for a series of data sets where highly retained compounds were successively excluded. Initially only benzene is excluded from the model due to its low retention and thus its large relative error in retention. Using 19 test solutes (top row in **Table 6-3**), the LSER model has a correlation coefficient value (*R*) of 0.98, standard error (*SE*) of 0.12, which are comparable to other normal phase LSERs [2, 19, 20]. The regression F value indicates significance of all the independent variables. The hydrogen bond affinity (*b*) and hydrogen bond basicity (*a*) are the predominant interactions exhibited by the DNAP column. If the strongly retained 2-naphtol could not be eluted isocratically, and so was not included in the LSER training set (middle row in **Table 6-3**), the values of *a* and *b* are under-estimated, but not to a statistically significant extent. This indicates that the model is robust. However, if the isocratic conditions cannot elute the 4 most retained compounds (*i.e*., resulting in them being excluded from the LSER training set, bottom row in **Table 6-3**), the under-estimation of *a* and *b* becomes statistically significant and the uncertainty in these terms increases. This bias is due to the strong retained solutes all having large *A* and relatively large *B* values (**Table 6-2**). The significance of all the independent variables was also impaired, as indicated by the smaller F. Thus, as shown in **Table 6-3** the solutes and mobile phase need to be selected and adjusted carefully with isocratic separations, otherwise the resultant LSER

Table 6-3 LSERs coefficients determined based on separations with and without the strong retained compounds on a DNAP column with 40% DCM mobile phase.

Data set	*c*	*a*	*b*	*S*	*e*	*v*	R	SE[c]	F[d]
19 solutes[a]	-1.39 ±0.18	2.35 ±0.15	1.21 ±0.22	0.85 ±0.12	0.13 ±0.08	-0.32 ±0.10	0.98	0.12	80
Without 2-napthol	-1.34 ±0.17	2.22 ±0.16	1.18 ±0.21	0.88 ±0.12	0.10 ±0.07	-0.34 ±0.09	0.98	0.12	66
Without 4 compounds[b]	-1.30 ±0.16	1.60 ±0.26	0.88 ±0.35	0.97 ±0.20	0.05 ±0.09	-0.33 ±0.08	0.97	0.10	29

a. Benzene was excluded due to low retention.

b. Without benzyl alcohol, phenol, carbazole, and cinnamyl alcohol

c. Standard error

d. Regression F-value. When F is larger than the F distribution value then there is a significant linear regression relationship between the retention factors and solute descriptors. All F statistic values in the table are large enough to show the significance of all the independent variables (F_{table} = 3 for 95% confidence interval).

coefficients can be inadvertently biased.

6.4.2 Comparing n and k_1 based on isocratic and gradient separations

To find the best isocratic condition to build LSERs, trial and error experiments are required. In this work gradient separations were explored to create LSER in a more convenient fashion. Our procedure determines the coefficients *n* and k_1 by fitting **Eq. 6-5** to gradient retention times using Solver. Given there are two unknowns in **Eq. 6-5** (*n* and k_1), a minimum of two runs under different gradient conditions are needed. Thesecoefficients can then be used to predict retention factors under isocratic conditions according to **Eq. 6-3**. The predicted isocratic retention factors for the probe compounds are then used to build LSERs for the isocratic conditions.

Firstly, however the *n* and k_1 values determined using gradient conditions must be validated. **Table 6-4** compares the *n* and k_1 values determined using either two or three gradient conditions versus the *n* and k_1 values determined using isocratic separations. The isocratic *n* and k_1 values were calculated by linearly regressing log *k* versus log ϕ, which is a commonly accepted procedure for normal phase LC [10, 11, 21]. At least 2 mobile phase compositions are required to determine *n* and k_1 values isocratically, and more than 3 mobile phase compositions are preferred. Twenty %, 30%, 40% and 50% DCM were used as the eluent. Twenty % was the weakest eluent that could elute all solutes (except 2-naphthol,) while higher %DCM resulted in too weak retention. The log *k* versus log ϕ plots are shown in **Figure 6-1** with R^2 typically better than 0.99. The isocratic *n* and k_1 values are shown in the second and third columns of **Table 6-4.** The *n* values range from 0.69-1.79, with higher values being associated with analytes with two polar groups. This correlation of *n* with the number of polar groups is consistent with literature behavior on other normal phase columns [22, 23] and **Chapter 4**.

The *n* and k_1 calculated based on two (G_1 and G_2), three (G_1, G_2, G_3) and four (G_1, G_2, G_3, G_4) gradient runs are shown in **Table 6-4**. The *n* and k_1 values based on two gradient runs ("2 grad" column in **Table 6-4**) are different from the values based on three

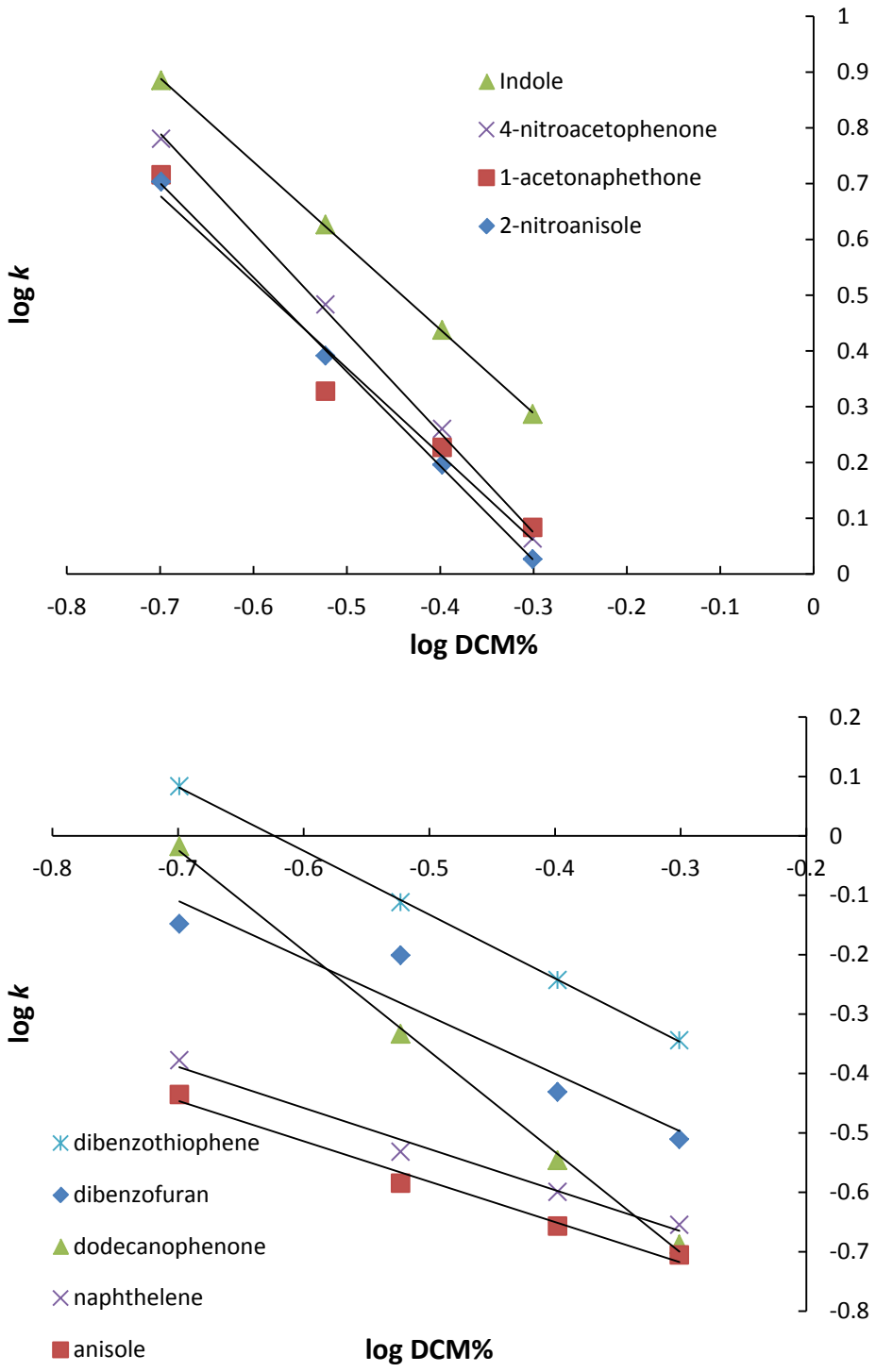

Figure 6-1a log *k*-log DCM% plot on the DNAP column with DCM/hexane mobile phase.

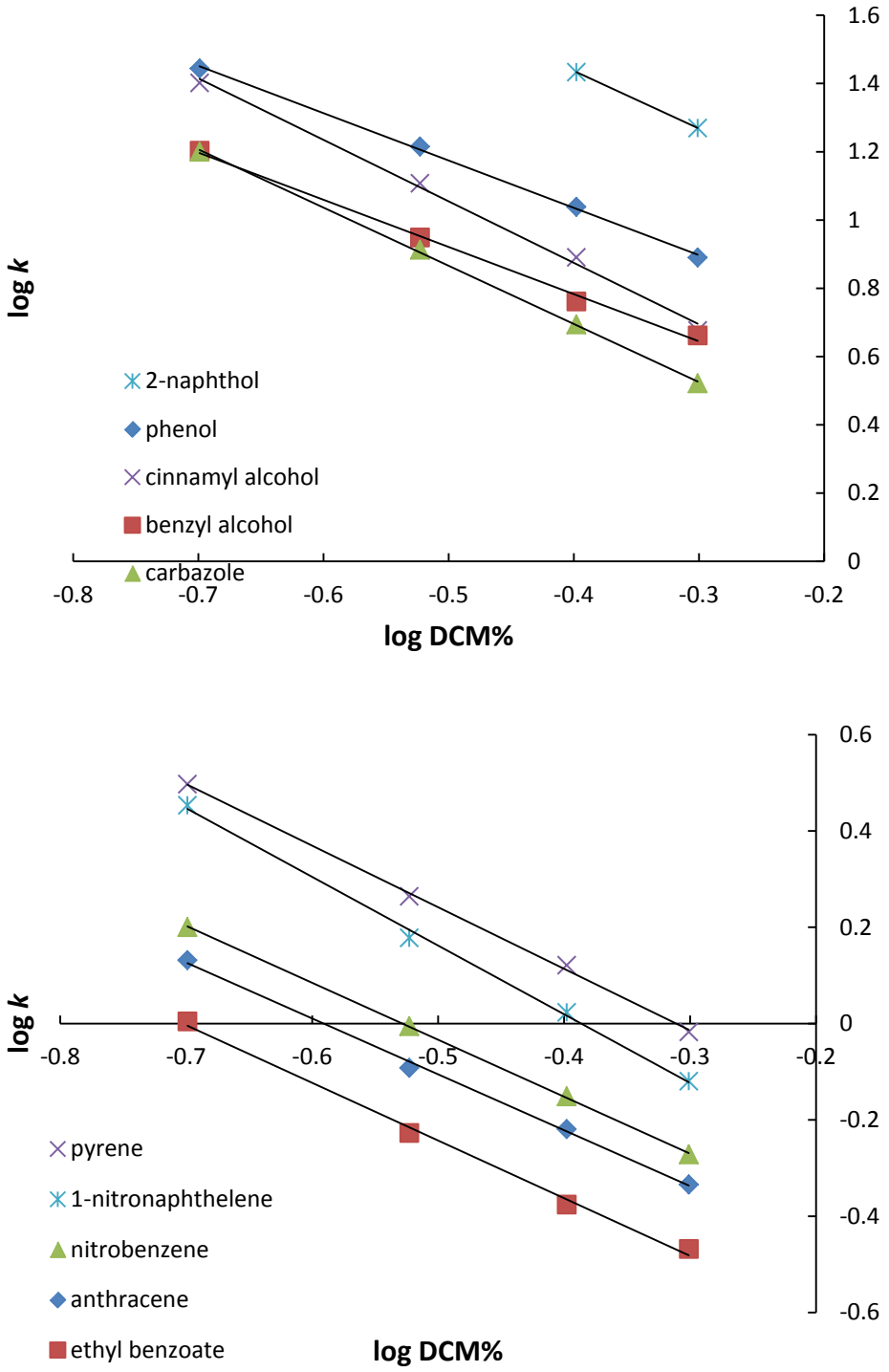

Figure 6-1b log *k*-log DCM% plot on the DNAP column with DCM/hexane mobile phase.

Table 6-4 Validation of n and k_1 determined using gradient separations on the DNAP column.

Compounds	Iso[a]		2 grad[b]		3 grad[c]		4 grad		Abs. Dev. in n [d]
	n	k_1	n	k_1	n	k_1	n	k_1	
2-nitroanisole	1.69 ±0.03	0.33 ±0.01	1.83	0.25	1.02	0.74	1.10	0.68	40
anisole	0.68 ±0.06	0.12 ±0.03	0.47	0.18	0.91	0.09	0.88	0.09	33
anthracene	1.16 ±0.04	0.21 ±0.01	0.78	0.36	0.87	0.32	0.87	0.32	25
benzyl alcohol	1.38 ±0.06	1.70 ±0.03	1.82	0.97	0.81	2.92	0.79	2.96	41
dibenzofuran	0.97 ±0.22	0.16 ±0.11	0	0.71	0.87	0.19	0.84	0.19	5
ethyl benzoate	1.20 ±0.05	0.14 ±0.03	1.59	0.08	0.95	0.21	0.95	0.21	20
nitrobenzene	1.18 ±0.01	0.24 ±0.01	1.50	0.14	0.84	0.38	0.85	0.37	29
phenol	1.39 ±0.04	3.03 ±0.02	1.57	2.21	0.74	4.88	0.82	4.63	47
pyrene	1.28 ±0.03	0.40 ±0.02	1.54	0.26	0.81	0.72	0.87	0.69	37
1-acetonaphethone	1.55 ±0.21	0.39 ±0.11	2.48	0.11	1.03	0.80	1.06	0.78	34

Table 6-4 Validation of n and k_1 determined using gradient separations on the DNAP column. (continued)

Compounds	Iso[a]		2 grad[b]		3 grad[c]		4 grad		Abs. Dev. in n [d]
	n	k_1	n	k_1	n	k_1	n	k_1	
dodecanophenone	1.69 ±0.05	0.06 ±0.02	2.18	0.03	1.34	0.11	1.32	0.11	21
1-nitronaphthalene	1.43 ±0.05	0.28 ±0.02	1.76	0.16	0.93	0.53	0.98	0.51	35
naphthalene	0.69 ±0.06	0.13 ±0.03	0.51	0.20	0.86	0.11	0.85	0.11	25
carbazole	1.70 ±0.03	1.03 ±0.01	2.06	0.60	0.95	2.11	1.12	1.85	44
indole	1.50 ±0.01	0.69 ±0.01	2.14	0.29	0.94	1.29	1.01	1.22	37
4-nitroacetophenone	1.79 ±0.05	0.34 ±0.01	2.54	0.12	1.11	0.80	1.14	0.78	38
dibenzothiophene	1.07 ±0.01	0.21 ±0.01	1.69	0.082	0.81	0.31	0.82	0.31	25
cinnamyl alcohol	1.70 ±0.02	1.43 ±0.03	2.80	0.53	0.97	3.20	0.99	3.16	46
2-naphthol	1.69	5.77	1.90	3.97	0.92	7.97	1.12	7.21	46

a. Values determined based on isocratic separations using 20%, 30%, 40% and 50% DCM. Many compounds are too strongly retained with < 20% DCM.

b. Values calculated based on two gradient separations (G1 and G2)

c. Values calculated based on three gradient separations (G1, G2 and G3)

d. Absolute Deviation =|n calculated by three gradients-isocratic n|/isocratic n×100%

("3 grad" column in **Table 6-4**) and four gradient runs ("4 grad" column in **Table 6-4**). So two gradient runs are not sufficient to give stable n and k_1 values. The n and k_1 values based on three and four gradient runs agree, which shows the gradient conditions have no impact on n and k_1 values. A minimum of three gradient runs are suggested to be used to calculate the n and k_1 values. Though gradient n and k_1 values agree amongst the different gradient runs, they are still different from the isocratic n and k_1 values (second and third columns in **Table 6-4**). The n and k_1 calculated by gradient separations are different from the isocratic values by as much as 46%, with an average difference of 33%. The gradient n values are all close to 1.

The differences between the isocratic and gradient values may be caused by experiment errors, such as inaccurate dead time. To check the influence of any error in dead time, dead time was changed manually before fitting. It was found that small changes in the dead time do not change the n-values significantly. Other aspects including the dwell time and the retention time accuracy were also checked, but did not significantly affect the results. We concluded that the differences between the isocratic and predicted n-values may be due to simplification inherent in **Eq. 6-5** and Jandera two-parameter model [13-15] (*e.g.* only two parameters are used instead of three or more paramteres).

However, gradient calculated n and k_1 values are sufficient to build LSER models, because gradient predicted and measured retentions are linearly related, as shown in **Figure 6-2**. Plotting log k predicted using three gradient runs versus log k measured isocratically yields R^2 of 0.999 (20% DCM) and 0.99 (40% DCM), with slopes 0.86 (20% DCM) and 0.94 (40% DCM). Though the slopes are close to 1, they are statistically different than 1. So the predicted log k values are close to the measured ones but not the same. **Table 6-5** compares the LSER equations for retention on DNAP with a 40% DCM isocratic mobile phase versus retention predicted for 40% DCM based on three gradient runs. Both LSER have comparable fits to the data (R = 0.98 and comparable SE and F)

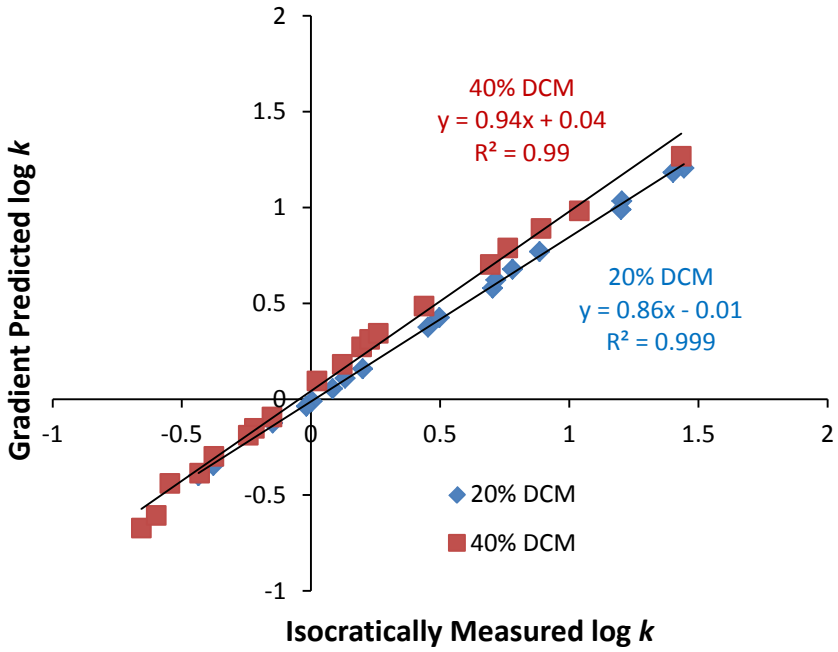

Figure 6-2 Comparison of log *k* predicted based on 3 gradient runs versus the log *k* determined isocratically with 20% and 40% DCM.

Table 6-5 LSER coefficients for the DNAP column with 40% DCM based on isocratic separation and multiple gradients.

40% DCM	***c***	***A***	***b***	***s***	***e***	***v***	**R**	**SE**	**F**
Isocratic observation	-1.39 ±0.18	2.35 ±0.15	1.21 ±0.22	0.85 ±0.12	0.13 ±0.08	-0.32 ±0.10	0.98	0.12	80
3 Gradient prediction	-1.41 ±0.16	2.16 ±0.13	1.29 ±0.20	0.90 ±0.11	0.10 ±0.07	-0.30 ±0.09	0.98	0.11	90

Also, the LSER coefficients obtained by the gradient method agrees with the coefficients obtained using the isocratic separation. This agreement is despite the poor agreement between the n and k_1 values obtained using the isocratic and gradient methods (**Table 6-4**). This suggests there is correlation between the two factors within the fit.

6.4.3 Using theoretical prediction for the stoichiometric coefficient n

The gradient calculated n and k_1 values were shown above to be capable of building LSER models. However, at least three gradient runs were required to obtain the n and k_1 values for each solute. This method loses the convenience advantage of gradient separations. To simplify the method, we will test using the modified Soczewiñski model developed in **Chapter 5** to predict the n. Specifically, **Eq. 5-1** ($n = N_{Polar}$ + (contribution per aromatic double bond)$\times N_{\text{double}}$) was used to calculate n. The n-slope values obtained using **Eq. 6-2** (which uses mole fraction) are slightly different from n-slope obtained using **Eq. 6-3** (which used volume fraction). Because this chapter used volume fraction rather than mole fraction (**Chapter 5**) to calculate n, the exact contribution per aromatic double bond is different from **Chapter 5.** Based on volume fraction and using the same procedure as in **Chapter 5**, the contribution per aromatic double bond was determined to be 0.09,.

$$n = N_{Polar} + 0.09 \times N_{\text{double}} \tag{6-8}$$

Once n is calculated using **Eq. 6-8**, k_1 can be calculated easily from as few as one gradient run. **Table 6-6** shows the agreement between the predicted n-values (**Eq. 6-8**) and the isocratically determined n-values, based on four isocratic separations. The average absolute deviation between the predicted and observed n was 24%, which based on **Chapters 4** and **5** is considered good agreement.

Table 6-6 Comparison of the *n*-slope calculated by different methods.

	Isocratic *n*	**Predicted *n* [a]**	**Abs. Dev. in *n* [b]**
2-nitroanisole	1.69±0.03	2.27	35
anisole	0.68±0.06	1.27	87
anthracene	1.16±0.04	0.64	45
benzyl alcohol	1.38±0.06	1.27	8
dibenzofuran	0.97±0.22	1.55	31
ethyl benzoate	1.20±0.05	1.27	6
nitrobenzene	1.18±0.01	1.27	8
phenol	1.39±0.04	1.27	8
pyrene	1.28±0.03	0.73	43
1-acetonaphthone	1.55±0.21	1.46	6
dodecanophenone	1.69±0.05	1.27	25
1-nitronaphthalene	1.43±0.05	1.46	2
naphthalene	0.69±0.06	0.46	34
carbazole	1.70±0.03	1.55	9
indole	1.50±0.01	1.36	9
4-nitroacetophenone	1.79±0.05	2.27	27
dibenzothiophene	1.07±0.01	1.55	45
cinnamyl alcohol	1.70±0.02	1.36	20
2-naphthol	1.69	1.46	14

a. *n* predicted using **Eq. 6-8**.

b. Absolute Deviation=| Predicted *n* -isocratic *n*|/(isocratic *n*)×100%

6.4.4 LSERs model based on one gradient run coupled with an estimated n-slope

Once n was calculated using **Eq. 6-8** and the retention time of one gradient separation was collected, k_1 was calculated using **Eq. 6-6**. With the k_1 values in place, the retention factors under any isocratic mobile phase composition can be calculated using **Eq. 6-3**. **Figure 6-3** compares the predicted log k and measured log k are linearly related as shown in LSERs can be built based on the calculated retention factors.

To evaluate the method, LSER coefficients for the DNAP column were determined using various gradient conditions and **Eq. 6-7**. The resultant LSER coefficients are listed in **Table 6-7**. The LSER coefficients obtained by the gradient method with predicted n generally agree with the LSER coefficients obtained from the isocratic separation at 40% DCM, also in **Table 6-7**. This agreement means that one gradient separation coupled with n-values predicted with **Eq. 6-8** can be used to generate robust LSERs.

To determine the impact of gradient conditions on the LSER generated, a variety of gradients (G1, G2, G3 and G4, **Table 6-1**) were tested. The results of these studies are in **Table 6-7**. G1, G2 and G4 started with the same initial mobile phase (20% DCM), but each had a different gradient steepness (*i.e.*, different change in %DCM per unit time). The coefficients under 40% DCM in **Table 6-7** calculated by G1, G2 and G4 are statistically equal. This indicates that the gradient steepness does not affect the LSERs. G3 has different initial concentration and steepness than the other three gradient methods. The coefficients obtained for 40% DCM based on G3 are similar with the other methods. **Table 6-8** shows similar comparisons of the LSER coefficients determined by the isocratic method at 20% and 50% DCM with the predictions based on a single gradient coupled with the calculated n-slope (**Eq. 6-8**). G3 has a slightly larger uncertainty when predicting coefficients at 20% DCM. This greater uncertainty may be because G3 starts from 60 DCM% (>20% DCM). However, the agreement between the isocratic and gradient-based LSER is still good. Thus the gradient conditions do not affect calculation of the LSER coefficients.

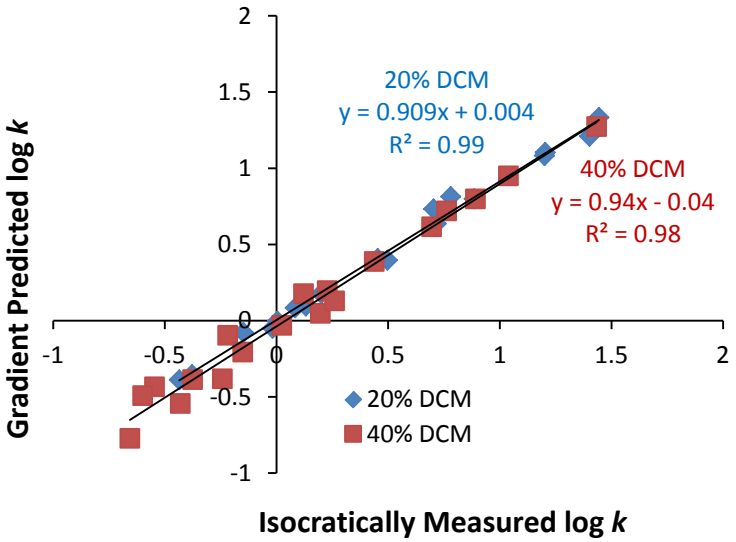

Figure 6-3 Comparison of log *k* predicted based on 1 gradient run with *n*-values calculated with **Eq. 6-8** vs. the log *k* determined isocratically with 20% and 40% DCM.

Table 6-7 LSER coefficients of DNAP column with 40% DCM.[a]

DCM %	*c*	*a*	*b*	*s*	*e*	*v*	R	SE	F
G1 40%	-1.49 ±0.17	2.30 ±0.14	1.17 ±0.21	0.73 ±0.12	0.17 ±0.07	-0.19 ±0.09	0.98	0.12	76
G2 40%	-1.52 ±0.17	2.26 ±0.14	1.19 ±0.22	0.69 ±0.12	0.19 ±0.07	-0.16 ±0.10	0.98	0.12	71
G3 40%	-1.40 ±0.20	2.23 ±0.17	1.43 ±0.25	1.10 ±0.14	0.04 ±0.09	-0.40 ±0.11	0.98	0.14	63
G4 40%	-1.6 ±0.18	2.38 ±0.15	1.28 ±0.22	0.77 ±0.12	0.18 ±0.08	-0.19 ±0.10	0.98	0.12	76
Isocratic 40%	-1.39 ±0.18	2.35 ±0.15	1.21 ±0.22	0.85 ±0.12	0.13 ±0.08	-0.32 ±0.10	0.98	0.12	80

a. Gradient conditions are detailed in **Table 6-1**.

Table 6-8 LSERs coefficients of DNAP column obtained by **Eq. 6-8** and isocratic separation.[a]

DCM %	*c*	*a*	*b*	*s*	*e*	*v*	R	SE	F
G1 20%	-1.25 ±0.17	2.28 ±0.15	1.39 ±0.22	1.07 ±0.12	0.01 ±0.08	-0.27 ±0.10	0.98	0.12	81
G2 20%	-1.28 ±0.15	2.24 ±0.12	1.41 ±0.19	1.03 ±0.10	0.03 ±0.06	-0.25 ±0.08	0.99	0.10	108
G3 20%	-1.16 ±0.31	2.22 ±0.26	1.65 ±0.39	1.44 ±0.22	-0.12 ±0.13	-0.48 ±0.17	0.96	0.22	31
G4 20%	-1.33 ±0.17	2.36 ±0.14	1.50 ±0.21	1.11 ±0.12	0.02 ±0.07	-0.28 ±0.09	0.99	0.12	92
Isocratic 20%	-1.50 ±0.16	2.35 ±0.18	1.77 ±0.31	1.09 ±0.21	0.07 ±0.11	-0.26 ±0.11	0.98	0.15	72
G1 50%	-1.57 ±0.19	2.30 ±0.16	1.10 ±0.24	0.62 ±0.14	0.22 ±0.08	-0.16 ±0.11	0.98	0.14	57
G2 50%	-1.60 ±0.20	2.26 ±0.17	1.11 ±0.26	0.58 ±0.14	0.25 ±0.09	-0.14 ±0.11	0.97	0.14	49
G3 50%	-1.48 ±0.18	2.24 ±0.15	1.36 ±0.22	0.99 0.12±	0.09 ±0.08	-0.37 ±0.10	0.98	0.13	76
G4 50%	-1.65 ±0.20	2.38 ±0.17	1.21 0.25±	0.66 ±0.14	0.23 ±0.09	-0.16 ±0.11	0.98	0.14	56
Isocratic 50%	-1.50 ±0.12	2.14 ±0.14	1.57 ±0.22	0.79 ±0.12	0.23 ±0.07	-0.41 ±0.09	0.99	0.12	105

a. Gradient conditions are detailed in **Table 6-1**.

6.4.5 LSER determination on silica using gradient methods

As a test of our gradient procedure, we also applied the method to determining LSER for separations on silica. Snyder expressed *n*-slope in **Eq. 6-2** as the ratio of the molecular area of the solute (A_S) required when adsorbed on stationary phase *vs*. the molecular area of the strong solvent (A_B) on the adsorbent surface [21, 24, 25]. Soczewiñski considered *n* as the number of polar groups in the solute molecule [22, 25, 26]. These two ways to predict *n*-slope have been compared on silica, and were both found to provide predicted values of *n* reasonably close to experimental values [24].

In this work, N_{polar} was used to predict the *n*-slope for polar compounds. To also account for the weak retention of nonpolar compounds on silica, A_S/A_B was used as *n*-slope for nonpolar PAHs on silica column. This predicted *n*-slope was then used to predict k_1 with **Eq. 6-6**. Here *n*-slope in **Eq. 6-2** (which uses mole fraction) was used as an approximation to *n*-slope in **Eq. 6-3** (which uses volume fraction).

Table 6-9 compares the LSER determined using a single gradient run (G1) coupled with the predicted *n*. The gradient LSER coefficients agree with isocratic LSER coefficients pretty well. The coefficients and uncertainties for the gradient LSER and isocratic LSER are comparable. The goodness of fit for the gradient LSER is even slightly better than that for the isocratic separation, as indicated by the larger R. The F value is also better for gradient than isocratic which means that the gradient LSER has more significant independent variables. The LSER coefficients we obtained and literature coefficients [20, 27] in **Table 6-9** both agree that silica column is quite polar and a stronger hydrogen bonding acid than base.

For the isocratic LSER，the probe compounds and mobile phase condition were carefully selected to make all compounds elute within reasonable amount of time. For comparison, the gradient LSER used the same probe compounds as the isocratic LSER. However, more strongly or weakly retained compounds could have been potentially used as probe solutes in the gradient LSER, which would make the gradient model more

robust and general.

The results in **Table 6-9** indicate that the gradient LSER method is also valid for classical NPLC phases such as silica. So LSER model can be built base on single gradient separation without needing to optimize the mobile phase conditions to achieve reasonable retention of all compounds, or having to leave out weakly or strongly retained compounds model.

6.5 Conclusions

A gradient LSERs was developed in this chapter. LSER coefficients built with gradient separations agree with LSER coefficients obtained by isocratic separations. LSERs based on a single gradient run coupled with the calculated *n*-slope are equivalent as LSERs based on three gradient runs. Gradient conditions have no effect on LSERs.

Table 6-9 Comparison of LSER coefficients for normal phase chromatography on a silica column based a single gradient run with isocratically collected parameters.

DCM %	*c*	*a*	*b*	*s*	*e*	*v*	R	SE	F
Gradient 20%	-1.77 ±0.32	2.20 ±0.27	3.29 ±0.40	1.53 ±0.22	-1.02 ±0.10	-0.10 ±0.18	0.98	0.23	65
Isocratic 20%	-1.72 ±0.37	1.71 ±0.31	3.16 ±0.46	1.23 ±0.26	-0.65 ±0.16	-0.11 ±0.20	0.96	0.26	31
1% IPA [27]	-0.62 ±0.25	1.52 ±0.21	2.69 ±0.35	0.54 ±0.22	0.51 ±0.17	-1.69 ±0.31	0.869	0.36	31
2% IPA [27]	-0.80 ±0.22	1.08 ±0.17	2.54 ±0.3	0.74 ±0.22	0.64 ±0.16	-1.91 ±0.27	0.898	0.29	37
1% methanol [20]	-1.14 ±0.09	2.23 ±0.10	1.56 ±0.13	1.06 ±0.10	-	-0.83 ±0.09	0.990	0.11	356

6.6 References

[1] J.W. Dolan, Starting out right, part VI - The scouting gradient alternative, LCGC North Am. 18 (2000) 478-487.

[2] M. Vitha, P.W. Carr, The chemical interpretation and practice of linear solvation energy relationships in chromatography, J. Chromatogr. A 1126 (2006) 143-194.

[3] M.H. Abraham, D.S. Ballantine, B.K. Callihan, Revised linear solvation energy relationship coefficients for the 77-phase McReynolds data set based on an updated set of solute descriptors, J. Chromatogr. A 878 (2000) 115-124.

[4] P.C. Sadek, P.W. Carr, R.M. Doherty, M.J. Kamlet, R.W. Taft, M.H. Abraham, Study of retention processes in reversed-phase high-performance liquid-chromatography by the use of the solvatochromic comparison method, Anal. Chem. 57 (1985) 2971-2978.

[5] L.R. Snyder, J.W. Dolan, P.W. Carr, The hydrophobic-subtraction model of reversed-phase column selectivity, J. Chromatogr. A 1060 (2004) 77-116.

[6] L.R. Snyder, J.W. Dolan, P.W. Carr, A new look at the selectivity of RPC columns. The hydrophobic subtraction model evaluates the selectivity of HPLC reversed-phased columns so that researchers can choose a suitable substitute or a sufficiently orthogonal second column, Anal. Chem. 79 (2007) 3254-3262.

[7] J. Li, B. Cai, Evaluation of the retention dependence on the physicochemical properties of solutes in reversed-phase liquid chromatographic linear gradient elution based on linear solvation energy relationships, J. Chromatogr. A 905 (2001) 35-46.

[8] K. Valko, S. Espinosa, C.M. Du, E. Bosch, M. Roses, C. Bevan, M.H. Abraham, Unique selectivity of perfluorinated stationary phases with 2,2,2-trifluoroethanol as organic mobile phase modifier, J. Chromatogr. A 933 (2001) 73-81.

[9] C.M. Du, K. Valko, C. Bevan, D. Reynolds, M.H. Abraham, Characterizing the selectivity of stationary phases and organic modifiers in reversed-phase high-performance liquid chromatographic systems by a general solvation equation using gradient elution, J. Chromatogr. Sci. 38 (2000) 503-511.

[10] L.R. Snyder, Linear elution adsorption chromatography: V. Silica as adsorbent. Adsorbent standardization, J. Chromatogr. 11 (1963) 195-227.

[11] L.R. Snyder, Linear elution adsorption chromatography: IV. Group localization in the adsorbate. Extension of the role of solute structure in separations over alumina, J. Chromatogr. 8 (1962) 319-342.

[12] E. Soczewiñski, Solvent composition effects in thin-layer chromatography systems of type silica gel-electron donor solvent, Anal. Chem. 41 (1969) 179-182.

[13] P. Jandera, Gradient elution in liquid column chromatography-prediction of retention and optimization of separation, Adv. Chromatogr. 43 (2005) 1-108.

[14] P. Jandera, Gradient elution in normal-phase high-performance liquid chromatographic systems, J. Chromatogr. A 965 (2002) 239-261.

[15] P. Jandera, M. Kucerova, J. Holikova, Description and prediction of retention in normal-phase high-performance liquid chromatography with binary and ternary mobile phase, J. Chromatogr. A 762 (1997) 15-26.

[16] J.W. Dolan, Gradient elution, part IV: dwell-volume problems, LCGC North Am. 31 (2013) 456-+.

[17] P. Jiang, D. Wu, C.A. Lucy, Determination of void volume in normal phase liquid chromatography, J. Chromatogr. A 1324 (2014) 63-70.

[18] P. Jandera, M. Kucerova, Prediction of retention in gradient-elution normal-phase high-performance liquid chromatography with binary solvent gradients, J. Chromatogr. A 759 (1997) 13-25.

[19] J.W. Li, T. Robison, Application of linear solvation energy relationships to guide selection of polar modifiers in normal-phase liquid chromatographic separations, Anal. Chim. Acta 395 (1999) 85-99.

[20] J.H. Park, M.H. Yoon, Y.K. Ryu, B.E. Kim, J.W. Ryu, M.D. Jang, Characterization of some normal-phase liquid chromatographic stationary phases based on linear solvation energy relationships, J. Chromatogr. A 796 (1998) 249-258.

[21] L.R. Snyder, Principles of adsorption chromatography; the separation of nonionic organic compounds, Marcel Dekker, New York, 1968.

[22] E. Soczewiñski, W. Golkiewicz, T. Dzido, A simple molecular model of adsorption chromatography. 10. Solvent composition effects in TLC of aromatic nitro-compounds using magnesium-silicate as adsorbent, Chromatographia 10 (1977) 221-225.

[23] M. Waksmundzka-Hajnos, A. Petruczynik, E. Soczewiñski, A. Hawryl, Retention mechanism of model compounds on polar bonded stationary phases in normal phase systems, Chem. Anal. (Warsaw) 47 (2002) 483-505.

[24] L.R. Snyder, Role of solvent in liquid-solid chromatography - review, Anal. Chem. 46 (1974) 1384-1393.

[25] E. Soczewiñski, T. Dzido, W. Golkiewicz, A simple molecular model of adsorption chromatography. 11. Adsorption of aromatic nitro-compounds with various polar groups on magnesium-silicate, Chromatographia 10 (1977) 298-302.

[26] L.R. Snyder, Solvent selectivity in normal-phase TLC, J. Planar Chromatogr. 21 (2008) 315-323.

[27] F.Z. Oumada, M. Roses, E. Bosch, M.H. Abraham, Solute-solvent interactions in normal-phase liquid chromatography: a linear free-energy relationships study, Anal. Chim. Acta 382 (1999) 301-308.

Chapter Seven. Conclusions and future work

7.1 Conclusions

This thesis explores the use of the fundamental Snyder–Soczewiñski model and linear solvation energy relationships (LSERs) in normal phase high performance liquid chromatography (HPLC), especially to elucidate the retention mechanism of hypercrosslinked polystyrene phases such as HC-Tol and charge transfer phases such as DNAP.

In **Chapter 2**, the normal phase retention on the HC-Tol column is investigated using the Snyder–Soczewiñski model. The solvent strength of binary hexane-solvent mobile phases can be predicted based on the solvent strength of pure dichloromethane, tetrahydrofuran, and benzene. Hypercrosslinked polystyrene phases have been described as quasi-normal phase, which suggests that these phases should behave as nonlocalizing stationary phases. Unlike traditional hypercrosslinked polystyrene phases, HC-Tol is a hypercrosslinked polystyrene silica hybrid phase. The HC-Tol column was proven to be a localizing adsorptive phase. Also, site-competition delocalization demonstrates that the adsorption groups on the HC-Tol stationary phase must extend above the surface.

In **Chapter 3**, the HC-Tol phase is characterized by linear solvation energy relationships (LSERs) and compared to amino and 5-HGN columns. On both the HC-Tol and amino columns, the solute acidity (*A*), basicity (*B*) and polarity (*S*) all contribute significantly to retention, while the solute excess polarizability *E* has a small but negative effect to retention. The *a*, *b* and *s* coefficients of HC-Tol column being positive and large demonstrate its polar character. The polar character of HC-Tol also supports the conclusion in **Chapter 2** that there are polar adsorption sites on the HC-Tol stationary phase. Solute volume *V* has no impact on retention on the amino column, while *V* has a slightly negative influence on retention for HC-Tol column. The difference in coefficient *v* between the amino and HC-Tol columns might explain why HC-Tol is capable of group

type separation. 5-HGN has smaller *a* and *b* values which means 5-HGN is not as basic or as acidic as HC-Tol. This suggests that the hydrogen bonding character of the HC-Tol phase arises from its silica substrate.

In **Chapters 4** and **5**, the slope of the linear relationship between retention and the mobile phase composition (Snyder-Soczewiñski model) in normal phase liquid chromatography (NPLC) was studied with bonded and charge-transfer phases. The Snyder model and the Soczewiñski model are compared on classic NPLC bonded phases using literature data, and the DNAP column using experimentally collected data. Overall, the Snyder model slightly better predicts the *n*-slope than the Soczewiñski model. However, both models give comparable uncertainty in predicting slope for a given compound. The number of aromatic double bonds was the most suitable descriptor for estimating the relative *n*-slope of PAHs, as it correlated with behavior better than the number of aromatic rings and is simpler to calculate than the solute adsorption area. On the DNAP phase, a modified Soczewiñski model was suggested to allow for the significant contribution of the aromatic rings to the *n*-slope. For classic NPLC bonded phases and DNAP columns, the contribution of polar group to *n*-slope parallels the adsorption energy of each polar group.

Finally, in **Chapter 6**, a gradient method was developed to build a LSER for normal phase chromatography. Three gradient runs were needed to build a LSER model. Using the modified Soczewiñski model developed in **Chapter 5** to predict *n*, only one gradient run was required to generate an LSER model. LSER models built based on gradient separations was as good as those based on isocratic separation, but required less trial and error experiments to find the optimum conditions.

7.2 Future work

7.2.1 *Characterize DNAP column by gradient LSERs and guidance for stationary phase selection*

A gradient method to generate LSERs for NPLC was developed in **Chapter 6**. As a consequence, LSER coefficients for DNAP column are now readily available. For DNAP column, *a* is large and positive, *b* and *s* are moderate and positive, *e* is insignificant, while *v* is small but negative. This means the solute's hydrogen bonding accepting ability, hydrogen bonding donating ability, polarity and polarizability all contribute to retention. Hydrogen bonding is the dominant intermolecular interaction governing retention. HC-Tol and DNAP columns are all very polar with both strong hydrogen bond donor and acceptor character. Thus polar compounds can be separated from PAHs on both the HC-Tol and the DNAP. But, HC-Tol columns have better hydrogen bond donor/acceptor (larger *a*, *b* values) than DNAP. The same change of solute hydrogen bond acidity *A* or hydrogen bond basicity *B* causes smaller change of retention on DNAP column, so DNAP is not as selective as the HC-Tol column for hydrogen bond characteristics. This may explain why the HC-Tol column can separate PAHs, pyridines and pyrroles, but the DNAP phase can only separate PAHs and polar compounds (pyridines and pyrroles co-elute).

The LSER coefficients of the HC-Tol, DNAP and 5-HGN columns also provide information useful for column selection. When DCM is used as the mobile phase, HC-Tol and DNAP both have negative *v*, and are capable of group-type separation. 5-HGN cannot achieve group type separation due to its near zero *v*. This indicates that stationary phase/mobile phase sets with negative *v* have a better chance to separate compounds group-wise. Solute having a larger size (larger *V*) usually have larger *S* and *E*, because their polarizability increases with the solute size and *S*/*E* both relate to polarizability. Normal phase chromatography systems usually have a positive *S*. So if the *v* is negative, the negative impact of *vV* to retention may cancel the positive impact of *sS*, making the solute size irrelevant to retention. In this case, the negative impact of the unfavorable cavity formation to retention cancels the positive impact of favorable dispersion and induction interactions to retention. To separate different polar compounds, the stationary

phases with good hydrogen bond accepting and donating ability (large *a*, *b*) would be preferred. Very basic stationary phase (large *a*) may be able to separate pyridines from pyrroles because pyrroles all have large *A*, while pyridines have an *A* value of zero.

7.2.2 Global LSERs

LSERS have been used to characterize LC columns both in reverse phase and normal phase. However, the LSER model established at one mobile phase composition cannot be applied to another mobile phase composition, even on the same column. Every mobile phase composition requires its own LSER equation. To solve this problem, a global LSER [1] was developed to express retention as a function of solute solvation parameters and mobile phase composition. A single global LSER equation can be used to model retention at any mobile phase composition. Past global LSER have been developed for reversed phase liquid chromatography [1]. Here I propose that a global LSERs can be developed to model retention under any mobile phase composition in normal phase.

In normal phase chromatography, retention is described by:

$$\log k = \log k_1 - n\log\phi \tag{7-1}$$

where k_1 is the retention factor under pure strong solvent, ϕ is the volume fraction of strong solvent, and n is a constant for a specific solute, **Eq. 7-1** is the same as **Eq. 6-3**. When ϕ=0.1, log ϕ= -1, **Eq. 7-1** becomes:

$$\log k_{0.1} = \log k_1 + n \tag{7-2}$$

where $k_{0.1}$ is the retention factor with 10% strong solvent as mobile phase. Rearranging **Eq. 7.2** yields:

$$n = \log k_{0.1} - \log k_1 \tag{7-3}$$

We also have (the same as **Eq. 1-3**):

$$\log k = \log \beta + \log K \tag{7-4}$$

where β is the phase ratio of the column, which is the volume of stationary phase over the volume of mobile phase; and K is the adsorption constant in normal phase chromatography. So, log k_1 is related to the solute adsorption free energy as follows:

$$\Delta G_1 = -RT\ln K = -2.303RT\log \frac{k_1}{\beta} \quad (7\text{-}5)$$

where ΔG_1 is the free energy of solute transfer from pure strong solvent to the stationary phase, T is temperature and R is the gas constant. We can relate n to the free energy as follows:

$$\begin{aligned}\Delta G_m &= -RT\ln K_{0.1} - (-RT\ln K_1) \\ &= -2.303RT\log \frac{k_{0.1}}{\beta} - \left(-2.303RT\log \frac{k_1}{\beta}\right) \\ &= -2.303RT(\log\ k_{0.1} - \log k_1) \\ &= -2.303\ RTn \end{aligned} \quad (7\text{-}6)$$

where ΔG_m is the free energy required for the solute to transfer from 10% strong solvent to pure strong solvent. LSERs can be written as [2]:

$$\text{SP} = c + eE + sS + aA + bB + vV \quad (7\text{-}7)$$

where SP is any free energy related property, c is intercept, and E, S, A, B and V are the solute excess polarizability, dipolarity/polarizability, hydrogen bond acidity, hydrogen bond basicity and molecular volume, respectively. The coefficients e, s, a, b, v, and c are complementary solute's properties. The coefficients reflect differences between the stationary and mobile phase. Building of LSERs require model solutes to cover a wide range of different parameters [2]. As demonstrated in **Chapter 6**, gradient separations can elute these solutes within reasonable retention time.

Both n and log k_1 are free energy parameters, and free energy parameter can be expressed by **Eq. 7-7**. When SP in **Eq. 7-7** is log k_1, we have:

$$\log k_1 = c_1 + a_1A + b_1B + s_1S + e_1E + v_1V \quad (7\text{-}8)$$

When SP in **Eq. 7-7** is n, we have:

$$n = c_n + a_nA + b_nB + s_nS + e_nE + v_nV \quad (7\text{-}9)$$

Now that log k_1 and n are expressed by LSER equations, we can substitute **Eq. 7-8** and **Eq. 7-9** into **Eq. 7-1** to express log k by a global LSER.

$$\log k = \log k_1 - n\log \phi$$

$$= c_1 + a_1A + b_1B + s_1S + e_1E + v_1V - (c_n + a_nA + b_nB + s_nS + e_nE + v_nV) \log \phi$$

$$= (c_1 - c_n \log \phi) + (a_1 - a_n \log \phi)A + (b_1 - b_n \log \phi)B + (s_1 - s_n \log \phi)S$$

$$+ (e_1 - e_n \log \phi)E + (v_1 - v_n \log \phi)V \quad (7\text{-}10)$$

In **Eq. 7-10**, retention is modeled as a function of solute solvation parameters (*A*, *B*, *S*, *E*, and *V*) and mobile phase composition (ϕ) simultaneously. Based on **Eq. 7-10**, 12 parameters are needed to describe retention with any mobile phase composition. Compared to the 6 parameter local model (**Eq. 7-7**) which is not valid over the entire range in mobile phase, the 12 parameter global LSERs can be used to simultaneously model retention as a function of both solute LSER descriptors and mobile phase composition. Without a global model, modeling each mobile phase composition would require a local LSER equation (6 parameters). To express the retention at three mobile phase compositions, we would need 3 LSER equations (18 parameters). This global model will need to be validated on different stationary phases under normal phase conditions.

7.2.3 Improved LSERs for normal phase chromatography by including a solute area parameter

The LSER uses molecular volume term *vV* to account for the cavity formation process. However，molecular area has been suggested to be a better parameter in modeling partitioning between water and another phase or partitioning between gas and non-polar gas chromatography phases than molecular volume [3-5]. This might be the case for normal phase. In normal phase, the retention mechanism is adsorption rather than partition. Thus, on the surface of an NPLC adsorbent, the adsorbed solvent molecules must leave the surface to make room for the solute molecules. The space required by the retained molecule is associated with the area of interaction between solute and stationary phase rather than its volume. Molecular area might be a better choice than volume, and should be tested as a parameter to build LSERs in normal phase.

The understanding of different columns we gained from this thesis can be used to

optimize petroleum separations. The character of HC-Tol can guide us to either select a suitable commercial column or synthesis better stationary phase for petroleum separations. The negative *v* coefficient of HC-Tol is the reason for its group type separation ability. A commercial column with negative *v* coefficient would be a prospective candidate column for group type separation. The negative *v* coefficient would compensate the positive effect of *s* associated with increasing analyte size. 5-HGN which has an insignificant *v* is not capable of group type separation. An HC polystyrene phase with a higher degree of crosslinking than 5-HGN would be a candidate column for group type separations. Once polar compounds are separated in petroleum samples, further compositional studies such as mass spectrometry can be performed. The compositional knowledge can help more effective production of petroleum.

7.3 References

[1] A.S. Wang, L.C. Tan, P.W. Carr, Global linear solvation energy relationships for retention prediction in reversed-phase liquid chromatography, J. Chromatogr. A 848 (1999) 21-37.

[2] M. Vitha, P.W. Carr, The chemical interpretation and practice of linear solvation energy relationships in chromatography, J. Chromatogr. A 1126 (2006) 143-194.

[3] R.B. Hermann, Theory of hydrophobic bonding. 2. Correlation of hydrocarbon solubility in water with solvent cavity surface-area, J. Phys. Chem. 76 (1972) 2754-2759.

[4] M.J. Harris, T. Higuchi, J.H. Rytting, Thermodynamic group contributions from ion pair extraction equilibria for use in prediction of partition coefficients. Correlation of surface area with group contributions, J. Phys. Chem. 77 (1973) 2694-2703.

[5] T. Kortvelyesi, M. Gorgenyi, L. Seres, Correlation of retention indexes with van der Waals' volumes and surface areas: Alkanes and azo compounds, Chromatographia 41 (1995) 282-286.

Appendix A. Extrapolation figures

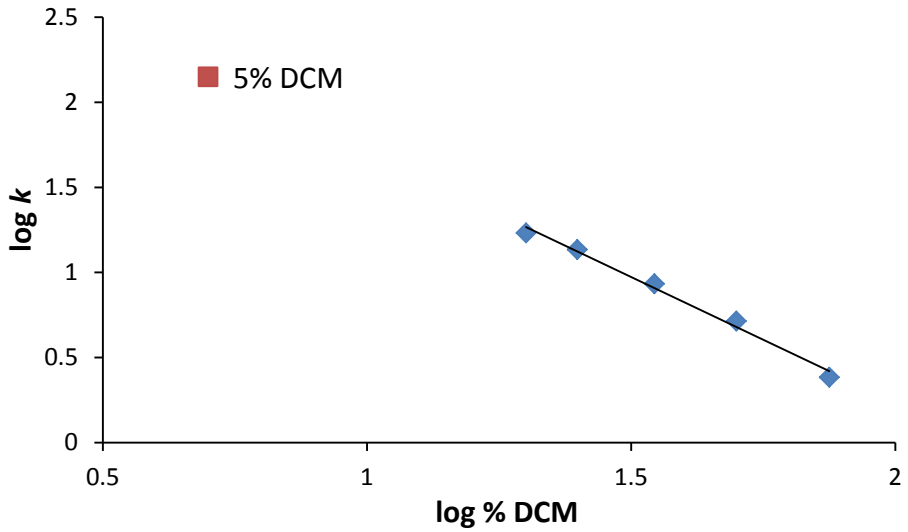

Figure A1 Extrapolation of benzyl alcohol's retention factor on the amino column. Conditions: column, Spherisorb amino; flow rate, 1.0 mL/min; mobile phase, 20%-75% DCM in hexane; injection volume, 1 μL; column temperature, 35 ˚C; detector wavelength, 254 nm.

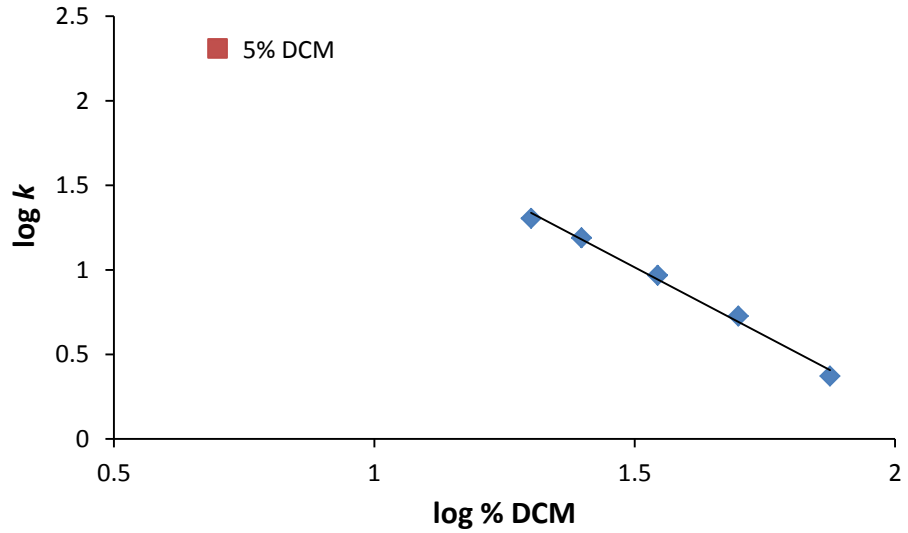

Figure A2 Extrapolation of cinnamyl alcohol's retention factor on the amino column, experimental condition as in **Figure A1**.

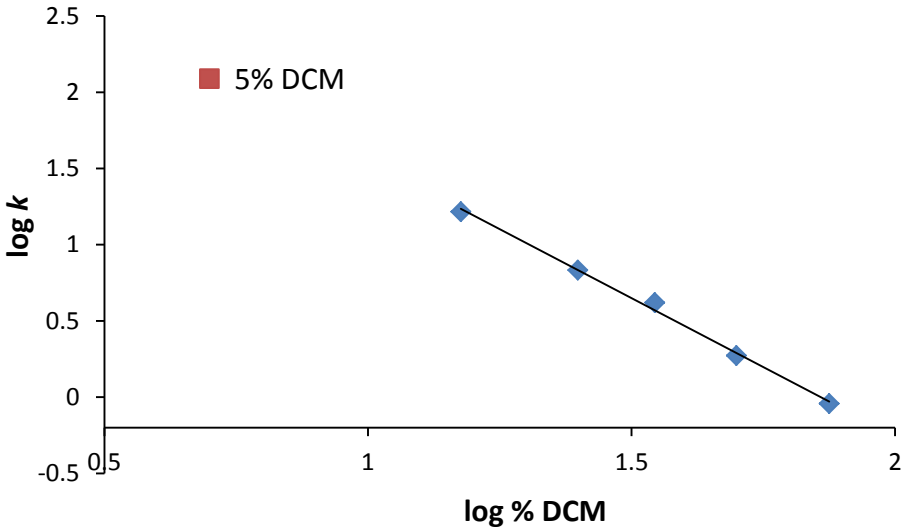

Figure A3 Extrapolation of 2-naphthol's retention factor on the HC-Tol column, experimental conditions as in **Figure A1** except: column, HC-Tol.

Bibliography

[1] M.H. Abraham, D.S. Ballantine, B.K. Callihan, Revised linear solvation energy relationship coefficients for the 77-phase McReynolds data set based on an updated set of solute descriptors, J. Chromatogr. A 878 (2000) 115-124.

[2] M.H. Abraham, J.R.M. Gola, J. Gil-Lostes, W.E. Acree, Jr., J.E. Cometto-Muniz, Determination of solvation descriptors for terpene hydrocarbons from chromatographic measurements, J. Chromatogr. A 1293 (2013) 133-141.

[3] M.H. Abraham, A. Ibrahim, A.M. Zissimos, Determination of sets of solute descriptors from chromatographic measurements, J. Chromatogr. A 1037 (2004) 29-47.

[4] M.H. Abraham, J.C. Mcgowan, The use of characteristic volumes to measure cavity terms in reversed phase liquid-chromatography, Chromatographia 23 (1987) 243-246.

[5] M.H. Abraham, Y.H. Zhao, Determination of solvation descriptors for ionic species: Hydrogen bond acidity and basicity, J. Org. Chem. 69 (2004) 4677-4685.

[6] M.P. Baya, P.A. Siskos, V.A. Davankov, Evaluation of a hypercrosslinked polystyrene, MN-200, as a sorbent for the preconcentration of volatile organic compounds in air, J. AOAC Int. 83 (2000) 579-583.

[7] D. Cagniant, Complexation chromatography, Marcel Dekker, New York, 1992.

[8] L. Carbognani, Group-type separation of middle petroleum distillates by adsorption and charge-transfer liquid-chromatography with dielectric-constant detection, J. Chromatogr. A 663 (1994) 11-26.

[9] G.V.S.M. Carrera, C.A.M. Afonso, L.C. Branco, Interfacial properties, densities, and contact angles of task specific ionic liquids, J. Chem. Eng. Data 55 (2010) 609-615.

[10] J. Cazes, Encyclopedia of chromatography, Marcel Dekker, New York, 2001.

[11] D.E. Clark, What has polar surface area ever done for drug discovery?, Future Med. Chem. 3 (2011) 469-484.

[12] A.A. D'Archivio, A. Giannitto, M.A. Maggi, F. Ruggieri, Cross-column retention prediction in reversed-phase high-performance liquid chromatography by artificial neural network modelling, Anal. Chim. Acta 717 (2012) 52-60.

[13] V. Davankov, C.S. Sychov, M.M. Ilyin, K.O. Sochilina, Hypercrosslinked

polystyrene as a novel type of high-performance liquid chromatography column packing material - Mechanisms of retention, J. Chromatogr. A 987 (2003) 67-75.
[14] V. Davankov, M. Tsyurupa, Preparative frontal size-exclusion chromatography of mineral ions on neutral hypercrosslinked polystyrene, J. Chromatogr. A 1087 (2005) 3-12.
[15] V.A. Davankov, M.P. Tsyurupa, Structure and properties of hypercrosslinked polystyrene - the 1st representative of a new class of polymer networks, React. Polym. 13 (1990) 27-42.
[16] V.A. Davankov, M.P. Tsyurupa, Hypercrosslinked polymeric networks and adsorbing materials : synthesis, properties, structure, and applications, 1st ed., Elsevier, Amsterdam ; Boston, 2011.
[17] V.A. Davankov, M.P. Tsyurupa, N.N. Alexienko, Selectivity in preparative separations of inorganic electrolytes by size-exclusion chromatography on hypercrosslinked polystyrene and microporous carbons, J. Chromatogr. A 1100 (2005) 32-39.
[18] J.W. Dolan, Starting out right, part VI - The scouting gradient alternative, LCGC North Am. 18 (2000) 478-487.
[19] J.W. Dolan, Gradient elution, part IV: dwell-volume problems, LCGC North Am. 31 (2013) 456-+.
[20] M. Dominguez-Perez, E. Rilo, L. Segade, C. Franjo, O. Cabeza, Surface tension deviations and excess molar volumes on the ternary system propyl propanoate plus hexane plus p-xylene at 298.15 K, J. Chem. Eng. Data 55 (2010) 1317-1321.
[21] C.M. Du, K. Valko, C. Bevan, D. Reynolds, M.H. Abraham, Characterizing the selectivity of stationary phases and organic modifiers in reversed-phase high-performance liquid chromatographic systems by a general solvation equation using gradient elution, J. Chromatogr. Sci. 38 (2000) 503-511.
[22] P.A.D. Edwardson, C.R. Lowe, T. Atkinson, Purification of homo-oligonucleotide and hetero-oligonucleotide using high-performance charge-transfer chromatography, J. Chromatogr. 368 (1986) 363-369.
[23] P. Ertl, B. Rohde, P. Selzer, Fast calculation of molecular polar surface area as a sum of fragment-based contributions and its application to the prediction of drug transport

properties, J. Med. Chem. 43 (2000) 3714-3717.
[24] L.S. Ettre, Jim Waters: The development of GPC and the first commercial HPLC instruments, LCGC North Am. 23 (2005) 752-761.
[25] N. Fontanals, J. Cortes, M. Galia, R.M. Marce, P.A.G. Cormack, F. Borrull, D.C. Sherrington, Synthesis of Davankov-type hypercrosslinked resins using different isomer compositions of vinylbenzyl chloride monomer, and application in the solid-phase extraction of polar compounds, J. Polym. Sci. A Polym. Chem. 43 (2005) 1718-1728.
[26] N. Fontanals, M. Galia, P.A.G. Cormack, R.M. Marce, D.C. Sherrington, F. Borrull, Evaluation of a new hypercrosslinked polymer as a sorbent for solid-phase extraction of polar compounds, J. Chromatogr. A 1075 (2005) 51-56.
[27] M. Galia, F. Svec, J.M.J. Frechet, Monodisperse polymer beads as packing material for high-performance liquid-chromatography - effect of divinylbenzene content on the porous and chromatographic properties of poly-n-styrene-co-divinylbenzene) beads prepared in presence of linear polystyrene as a porogen, J. Polym. Sci. A Polym. Chem. 32 (1994) 2169-2175.
[28] P. Geladi, B.R. Kowalski, Partial least-squares regression - a tutorial, Anal. Chim. Acta 185 (1986) 1-17.
[29] J.L. Glajch, J.J. Kirkland, J. Kohler, Effect of column degradation on the reversed-phase high-performance liquid chromatographic separation of peptides and proteins, J. Chromatogr. 384 (1987) 81-90.
[30] J.L. Glajch, L.R. Snyder, Solvent strength of multicomponent mobile phases in liquid-solid chromatography: Mixtures of three or more solvents, J. Chromatogr. 214 (1981) 21-34.
[31] W. Gołkiewicz, A simple molecular model for adsorption chromatography. IX. Comparison of adsorption mechanisms in thin-layer chromatography and high-speed liquid chromatography, Chromatographia 9 (1976) 113-118.
[32] W. Gołkiewicz, E. Soczewiński, A simple molecular model of adsorption chromatography. VI. RM-composition relationships of solutes with two functional groups, Chromatographia 5 (1972) 594-601.
[33] P.L. Grizzle, J.S. Thomson, Liquid-chromatographic separation of aromatic-hydrocarbons with chemically bonded (2,4-dinitroanilinopropyl)silica, Anal.

Chem. 54 (1982) 1071-1078.
[34] D.C. Harris, Quantitative chemical analysis, 7th ed., W. H. Freeman, New York, 2006.
[35] M.J. Harris, T. Higuchi, J.H. Rytting, Thermodynamic group contributions from ion pair extraction equilibria for use in prediction of partition coefficients. Correlation of surface area with group contributions, J. Phys. Chem. 77 (1973) 2694-2703.
[36] R.B. Hermann, Theory of hydrophobic bonding. 2. Correlation of hydrocarbon solubility in water with solvent cavity surface-area, J. Phys. Chem. 76 (1972) 2754-2759.
[37] W. Holstein, H. Hemetsberger, Donor-acceptor complex chromatography (DACC) 1. Introduction and nomenclature, Chromatographia 15 (1982) 186-190.
[38] W. Holstein, H. Hemetsberger, Donor-acceptor complex chromatography (DACC) 2. Review of papers, Chromatographia 15 (1982) 251-258.
[39] C.G. Horvath, S.R. Lipsky, Use of liquid ion exchange chromatography for separation of organic compounds, Nature 211 (1966) 748-749.
[40] G.A. Howard, A.J.P. Martin, The separation of the C12-C18 fatty acids by reversed-phase partition chromatograhy, Biochem. J 46 (1950) 532-538.
[41] P. Jandera, Gradient elution in normal-phase high-performance liquid chromatographic systems, J. Chromatogr. A 965 (2002) 239-261.
[42] P. Jandera, Gradient elution in liquid column chromatography-prediction of retention and optimization of separation, Adv. Chromatogr. 43 (2005) 1-108.
[43] P. Jandera, M. Kucerova, Prediction of retention in gradient-elution normal-phase high-performance liquid chromatography with binary solvent gradients, J. Chromatogr. A 759 (1997) 13-25.
[44] P. Jandera, M. Kucerova, J. Holikova, Description and prediction of retention in normal-phase high-performance liquid chromatography with binary and ternary mobile phase, J. Chromatogr. A 762 (1997) 15-26.
[45] M. Jaroniec, J.A. Jaroniec, Simple-model of liquid-solid chromatography involving solute-solvent and solvent-solvent interactions, J. Chromatogr. 210 (1981) 130-132.
[46] M. Jaroniec, A. Patrykiejew, Theory of adsorption from multicomponent liquid-mixtures on solid-surfaces and its application to liquid adsorption chromatography, J. Chem. Soc. Faraday Trans. 1 76 (1980) 2486-2495.

[47] D.M. Jewell, Preparative trinitrofluorenone charge-transfer chromatography of petroleum aromatics, Anal. Chem. 47 (1975) 2048-2050.
[48] P. Jiang, Separation and characterization of polycyclic aromatic hydrocarbons and azaarenes using normal phase liquid chromatography and electrospray ionization mass spectrometry, Ph.D thesis, University of Alberta, May 9th, 2016.
[49] P. Jiang, D. Wu, C.A. Lucy, Determination of void volume in normal phase liquid chromatography, J. Chromatogr. A 1324 (2014) 63-70.
[50] M.J. Kamlet, J.L. Abboud, R.W. Taft, Solvatochromic comparison method. 6. Pi-star scale of solvent polarities, J. Am. Chem. Soc. 99 (1977) 6027-6038.
[51] M.J. Kamlet, M.H. Abraham, P.W. Carr, R.M. Doherty, R.W. Taft, Solute solvent interactions in chemistry and biology. 7. An analysis of mobile phase effects on high-pressure liquid-chromatography capacity factors and relationships of the latter with octanol water partition-coefficients, Journal of the Chemical Society-Perkin Transactions 2 (1988) 2087-2092.
[52] M.J. Kamlet, R.W. Taft, The solvatochromic comparison method. I. The .beta.-scale of solvent hydrogen-bond acceptor (HBA) basicities, J. Am. Chem. Soc. 98 (1976) 377-383.
[53] T. Kortvelyesi, M. Gorgenyi, L. Seres, Correlation of retention indexes with van der Waals' volumes and surface areas: Alkanes and azo compounds, Chromatographia 41 (1995) 282-286.
[54] J. Li, B. Cai, Evaluation of the retention dependence on the physicochemical properties of solutes in reversed-phase liquid chromatographic linear gradient elution based on linear solvation energy relationships, J. Chromatogr. A 905 (2001) 35-46.
[55] J.W. Li, Prediction of internal standards in reversed-phase liquid chromatography: III. Evaluation of an alternative solvation parameter model to correlate and predict the retention of ionizable compounds, J. Chromatogr. A 982 (2002) 209-223.
[56] J.W. Li, T. Robison, Application of linear solvation energy relationships to guide selection of polar modifiers in normal-phase liquid chromatographic separations, Anal. Chim. Acta 395 (1999) 85-99.
[57] J.W. Li, D.A. Whitman, Characterization and selectivity optimization on diol, amino, and cyano normal phase columns based on linear solvation energy relationships, Anal.

Chim. Acta 368 (1998) 141-154.
[58] L.Y. Lin, W.T. Cooper, Isocratic high-performance liquid chromatographic separation and multiple-wavelength ultraviolet detection of aldicarb and its soil degradation products. Optimization of stationary phase selectivity, J. Chromatogr. A 390 (1987) 285-295.
[59] C.H. Lochmuller, C.W. Amoss, 3-(2,4,5,7-Tetranitrofluorenimino) –propyldiethoxy -siloxane - highly selective, bonded pi-complexing phase for high-pressure liquid-chromatography, J. Chromatogr. 108 (1975) 85-93.
[60] H. Luo, L. Ma, Y. Zhang, P.W. Carr, Synthesis and characterization of silica-based hyper-crosslinked sulfonate-modified reversed stationary phases, J. Chromatogr. A 1182 (2008) 41-55.
[61] L.J. Ma, H. Luo, J. Dai, P.W. Carr, Development of acid stable, hyper-crosslinked, silica-based reversed-phase liquid chromatography supports for the separation of organic bases, J. Chromatogr. A 1114 (2006) 21-28.
[62] A.J. Martin, R.L. Synge, A new form of chromatogram employing two liquid phases: A theory of chromatography. 2. Application to the micro-determination of the higher monoamino-acids in proteins, Biochem. J. 35 (1941) 1358-1368.
[63] V.L. McGuffin, Chapter 1 Theory of chromatography, in: E. Heftmann (Ed.) Chromatography : fundamentals and applications of chromatography and related differential migration methods, Elsevier, Amsterdam; Boston, 2004, pp. 1-88.
[64] Molinspiration, calculation of molecular properties and bioactivity score. http://www.molinspiration.com/cgi-bin/properties,2016 (accessed 30.03.16)
[65] J.C. Moore, Gel permeation chromatography. I. New method for molecular weight distribution of high polymers, J. Polym. Sci. Part A 2 (1964) 835-843.
[66] S. Moore, D.H. Spackman, W.H. Stein, Chromatography of amino acids on sulfonated polystyrene resins - an improved system, Anal. Chem. 30 (1958) 1185-1190.
[67] L. Nondek, J. Malek, Liquid-chromatography of aromatic-hydrocarbons on a chemically bonded stationary phase of charge-transfer type, J. Chromatogr. 155 (1978) 187-190.
[68] D. Nurok, R.M. Kleyle, K.B. Lipkowitz, S.S. Myers, M.L. Kearns, Dependence of retention and separation quality in planar chromatography on properties of the

mobile-phase, Anal. Chem. 65 (1993) 3701-3707.
[69] D. Nurok, R.R. Sorrell, C.L. McCain, M.C. Frost, P. Hajdu, T.C. Powell, T. Lahr, R.M. Kleyle, Prediction of retention using polar and nonpolar surface areas of single-solvent mobile phases, J. Planar Chromatogr. 12 (1999) 42-45.
[70] P. Olsson, I. Sadiktsis, J. Holmback, R. Westerholm, Class separation of lipids and polycyclic aromatic hydrocarbons in normal phase high performance liquid chromatography - A prospect for analysis of aromatics in edible vegetable oils and biodiesel exhaust particulates, J. Chromatogr. A 1360 (2014) 39-46.
[71] N.E. Oro, C.A. Lucy, Comparison of hypercrosslinked polystyrene columns for the separation of nitrogen group-types in petroleum using high performance liquid chromatography, J. Chromatogr. A 1217 (2010) 6178-6185.
[72] N.E. Oro, C.A. Lucy, High performance liquid chromatographic separations of gas oil samples and their hydrotreated products using commercial normal phases, J. Chromatogr. A 1218 (2011) 7788-7795.
[73] F.Z. Oumada, M. Roses, E. Bosch, M.H. Abraham, Solute-solvent interactions in normal-phase liquid chromatography: a linear free-energy relationships study, Anal. Chim. Acta 382 (1999) 301-308.
[74] R.E. Paproski, J. Cooley, C.A. Lucy, Fast supercritical fluid chromatography hydrocarbon group-type separations of diesel fuels using packed and monolithic columns, Analyst 131 (2006) 422-428.
[75] R.E. Paproski, C. Liang, C.A. Lucy, Zirconia, titania, silica, and carbon columns for the group-type characterization of heavy gas oils using high temperature normal phase liquid chromatography, Energy Fuels 25 (2011) 4469-4478.
[76] J.H. Park, M.H. Yoon, Y.K. Ryu, B.E. Kim, J.W. Ryu, M.D. Jang, Characterization of some normal-phase liquid chromatographic stationary phases based on linear solvation energy relationships, J. Chromatogr. A 796 (1998) 249-258.
[77] S.V. Prokopov, S.V. Kurbatova, V.A. Davankov, M.A. Il'in, Chromatographic retention of adamantylamidrazones and triazoles by octadecyl silica gel and hypercrosslinked polystyrenes from water-acetonitrile solutions, Russ. J. Phys. Chem. A 86 (2012) 852-859.
[78] S.V. Prokopov, E.V. Tyrina, V.A. Davankov, M.M. Il'in, S.V. Kurbatova,

Quasi-normal phase chromatography of nitrogen-containing adamantane derivatives, Russ. J. Phys. Chem. A 87 (2013) 114-119.
[79] C. Reichardt, T. Welton, Solvents and solvent effects in organic chemistry, 4th ed., Wiley-VCH, Weinheim, Germany, 2011.
[80] W.K. Robbins, Quantitative measurement of mass and aromaticity distributions for heavy distillates 1. Capabilities of the HPLC-2 system, J. Chromatogr. Sci. 36 (1998) 457-466.
[81] J.L. Robinson, W.J. Robinson, M.A. Marshall, A.D. Barnes, K.J. Johnson, D.S. Salas, Liquid-solid chromatography on amberlite xad-2 and other styrene-divinylbenzene adsorbents .1. development of a solvent eluotropic scale, J. Chromatogr. 189 (1980) 145-167.
[82] R.P. Rodgers, T.M. Schaub, A.G. Marshall, Petroleomics: MS returns to its roots, Anal. Chem. 77 (2005) 20A-27A.
[83] J.M. Roussel, A.M. Siouffi, M. Julliard, M. Chanon, Liquid-chromatography with charge-transfer complexation, Chromatographia 29 (1990) 419-428.
[84] P.C. Sadek, P.W. Carr, R.M. Doherty, M.J. Kamlet, R.W. Taft, M.H. Abraham, Study of retention processes in reversed-phase high-performance liquid-chromatography by the use of the solvatochromic comparison method, Anal. Chem. 57 (1985) 2971-2978.
[85] A.W. Salotto, E.L. Weiser, K.P. Caffey, R.L. Carty, S.C. Racine, L.R. Snyder, Relative retention and column selectivity for the common polar bonded-phase columns: The diol-silica column in normal-phase high-performance liquid-chromatography, J. Chromatogr. 498 (1990) 55-65.
[86] L.C. Sander, R.M. Parris, S.A. Wise, P. Garrigues, Shape-discrimination in liquid-chromatography using charge-transfer phases, Anal. Chem. 63 (1991) 2589-2597.
[87] R.P.W. Scott, P. Kucera, Solute interactions with mobile and stationary phases in liquid-solid chromatography, J. Chromatogr. 112 (1975) 425-442.
[88] R.P.W. Scott, P. Kucera, Solute-solvent interactions on the surface of silica-gel. 2, J. Chromatogr. 171 (1979) 37-48.
[89] D.A.P. Small, T. Atkinson, C.R. Lowe, High-performance liquid charge-transfer chromatography, J. Chromatogr. 248 (1982) 271-279.
[90] P.L. Smith, W.T. Cooper, Retention and selectivity in amino, cyano and diol normal

bonded phase high-performance liquid-chromatographic columns, J. Chromatogr. 410 (1987) 249-265.
[91] L.R. Snyder, Linear elution adsorption chromatography: IV. Group localization in the adsorbate. Extension of the role of solute structure in separations over alumina, J. Chromatogr. 8 (1962) 319-342.
[92] L.R. Snyder, Linear elution adsorption chromatography: III. Further delineation of the eluent role in separations over alumina, J. Chromatogr. 8 (1962) 178-200.
[93] L.R. Snyder, Linear elution adsorption chromatography: V. Silica as adsorbent. Adsorbent standardization, J. Chromatogr. 11 (1963) 195-227.
[94] L.R. Snyder, Linear elution adsorption chromatography: XII. Functional group adsorption energies on metal oxide adsorbents, J. Chromatogr. 23 (1966) 388-402.
[95] L.R. Snyder, Principles of adsorption chromatography; the separation of nonionic organic compounds, Marcel Dekker, New York, 1968.
[96] L.R. Snyder, Role of solvent in liquid-solid chromatography - review, Anal. Chem. 46 (1974) 1384-1393.
[97] L.R. Snyder, Solvent selectivity in normal-phase TLC, J. Planar Chromatogr. 21 (2008) 315-323.
[98] L.R. Snyder, Localization in adsorption chromatography, J. Planar Chromatogr. 25 (2012) 184-189.
[99] L.R. Snyder, J.W. Dolan, P.W. Carr, The hydrophobic-subtraction model of reversed-phase column selectivity, J. Chromatogr. A 1060 (2004) 77-116.
[100] L.R. Snyder, J.W. Dolan, P.W. Carr, A new look at the selectivity of RPC columns. The hydrophobic subtraction model evaluates the selectivity of HPLC reversed-phased columns so that researchers can choose a suitable substitute or a sufficiently orthogonal second column, Anal. Chem. 79 (2007) 3254-3262.
[101] L.R. Snyder, J.L. Glajch, Solvent strength of multicomponent mobile phases in liquid-solid chromatography: Binary-solvent mixtures and solvent localization, J. Chromatogr. 214 (1981) 1-19.
[102] L.R. Snyder, J.L. Glajch, Solvent strength of multicomponent mobile phases in liquid-solid chromatography: Further study of different mobile phases and silica as adsorbent, J. Chromatogr. 248 (1982) 165-182.

[103] L.R. Snyder, J.L. Glajch, J.J. Kirkland, Theoretical basis for systematic optimization of mobile phase selectivity in liquid-solid chromatography - solvent-solute localization effects, J. Chromatogr. 218 (1981) 299-326.
[104] L.R. Snyder, J.J. Kirkland, J.W. Dolan, Introduction to modern liquid chromatography, 3rd ed., Wiley, Hoboken, N.J., 2010.
[105] L.R. Snyder, J.J. Kirkland, J.L. Glajch, Practical HPLC method development, 2nd ed., Wiley, New York, 1997.
[106] L.R. Snyder, H. Poppe, Mechanism of solute retention in liquid-solid chromatography and the role of the mobile phase in affecting separation - competition versus sorption, J. Chromatogr. 184 (1980) 363-413.
[107] L.R. Snyder, T.C. Schunk, Retention mechanism and the role of the mobile phase in normal-phase separation on amino-bonded-phase columns, Anal. Chem. 54 (1982) 1764-1772.
[108] E. Soczewiński, Solvent composition effects in thin-layer chromatography systems of type silica gel-electron donor solvent, Anal. Chem. 41 (1969) 179-182.
[109] E. Soczewiński, Mechanistic molecular model of liquid-solid chromatography retention-eluent composition relationships, J. Chromatogr. A 965 (2002) 109-116.
[110] E. Soczewiński, T. Dzido, Effect of the eluent composition in HPLC on the retention of bi- and trifunctional aromatic solutes, Chromatographia 22 (1986) 25-30.
[111] E. Soczewiński, T. Dzido, W. Golkiewicz, A simple molecular model of adsorption chromatography. 11. Adsorption of aromatic nitro-compounds with various polar groups on magnesium-silicate, Chromatographia 10 (1977) 298-302.
[112] E. Soczewinski, W. Golkiewicz, A simple molecular model for adsorption chromatography. VII. Relationship between the RM value and the composition for phenols in systems of the type (cyclohexane+polar solvent)/silica, Chromatographia 6 (1973) 269-273.
[113] E. Soczewiński, W. Golkiewicz, T. Dzido, A simple molecular model of adsorption chromatography. 10. Solvent composition effects in TLC of aromatic nitro-compounds using magnesium-silicate as adsorbent, Chromatographia 10 (1977) 221-225.
[114] E. Soczewiński, W. Golkiewicz, W. Markowski, A simple molecular model of adsorption chromatography. 8. Solvent composition effects in thin-layer chromatography

of aromatic nitro-compounds in (cyclohexane + polar-solvent) - silica type systems, Chromatographia 8 (1975) 13-17.
[115] D.H. Spackman, W.H. Stein, S. Moore, Automatic recording apparatus for use in the chromatography of amino acids, Anal. Chem. 30 (1958) 1190-1206.
[116] T.W. Stephens, M. Loera, M. Calderas, R. Diaz, N. Montney, W.E. Acree, M.H. Abraham, Determination of Abraham model solute descriptors for benzoin based on measured solubility ratios, Phys. Chem. Liq. 50 (2012) 254-265.
[117] C.S. Sychov, M.M. Ilyin, V.A. Davankov, K.O. Sochilina, Elucidation of retention mechanisms on hypercrosslinked polystyrene used as column packing material for high-performance liquid chromatography, J. Chromatogr. A 1030 (2004) 17-24.
[118] L. Szepesy, Effect of molecular interactions on retention and selectivity in reversed-phase liquid chromatography, J. Chromatogr. A 960 (2002) 69-83.
[119] R.W. Taft, M.J. Kamlet, Solvatochromic comparison method. 2. Alpha-scale of solvent hydrogen-bond donor (hbd) acidities, J. Am. Chem. Soc. 98 (1976) 2886-2894.
[120] L.C. Tan, P.W. Carr, M.H. Abraham, Study of retention in reversed-phase liquid chromatography using linear solvation energy relationships 1. The stationary phase, J. Chromatogr. A 752 (1996) 1-18.
[121] J.S. Thomson, J.W. Reynolds, Separation of aromatic-hydrocarbons using bonded-phase charge-transfer liquid-chromatography, Anal. Chem. 56 (1984) 2434-2441.
[122] B.C. Trammell, L. Ma, H. Luo, M.A. Hillmyer, P.W. Carr, An ultra acid stable reversed stationary phase, J. Am. Chem. Soc. 125 (2003) 10504-10505.
[123] B.C. Trammell, L. Ma, H. Luo, M.A. Hillmyer, P.W. Carr, Synthesis and characterization of hypercrosslinked, surface-confined, ultra-stable silica-based stationary phases, J. Chromatogr. A 1060 (2004) 61-76.
[124] B.C. Trammell, L. Ma, H. Luo, D. Jin, M.A. Hillmyer, P.W. Carr, Highly cross-linked self-assembled monolayer stationary phases: an approach to greatly enhancing the low pH stability of silica-based stationary phases, Anal. Chem. 74 (2002) 4634-4639.
[125] M. Tswett, Adsorptionanalyse und chromatographische methode. Anwendung auf die chemie des chlorophylls, Ber. Dtsch. Bot. Ges. 24 (1906) 384-393.
[126] M. Tswett, Physikalisch-chemische studien über das chlorophyll. Die adsorption,

Ber. Dtsch. Bot. Ges. 24 (1906) 316-326.
[127] N. Ulrich, J. Muhlenberg, H. Retzbach, G. Schuurmann, W. Brack, Linear solvation energy relationships as classifiers in non-target analysis - A gas chromatographic approach, J. Chromatogr. A 1264 (2012) 95-103.
[128] K. Valko, S. Espinosa, C.M. Du, E. Bosch, M. Roses, C. Bevan, M.H. Abraham, Unique selectivity of perfluorinated stationary phases with 2,2,2-trifluoroethanol as organic mobile phase modifier, J. Chromatogr. A 933 (2001) 73-81.
[129] B.J. VanMiddlesworth, J.G. Dorsey, Quantifying injection solvent effects in reversed-phase liquid chromatography, J. Chromatogr. A 1236 (2012) 77-89.
[130] K. Varmuza, P. Filzmoser, Introduction to multivariate statistical analysis in chemometrics, CRC Press, Boca Raton, 2009.
[131] M. Vitha, P.W. Carr, The chemical interpretation and practice of linear solvation energy relationships in chromatography, J. Chromatogr. A 1126 (2006) 143-194.
[132] M. Waksmundzka-Hajnos, A. Petruczynik, A. Hawryl, Comparison of chromatographic properties of cyanopropyl-, diol- and aminopropyl- polar-bonded stationary phases by the retention of model compounds in normal-phase liquid chromatography systems, J. Chromatogr. A 919 (2001) 39-50.
[133] M. Waksmundzka-Hajnos, A. Petruczynik, E. Soczewiński, A. Hawryl, Retention mechanism of model compounds on polar bonded stationary phases in normal phase systems, Chem. Anal. (Warsaw) 47 (2002) 483-505.
[134] A.S. Wang, L.C. Tan, P.W. Carr, Global linear solvation energy relationships for retention prediction in reversed-phase liquid chromatography, J. Chromatogr. A 848 (1999) 21-37.
[135] E.L. Weiser, A.W. Salotto, S.M. Flach, L.R. Snyder, Basis of retention in normal-phase high-performance liquid-chromatography with cyano-propyl columns, J. Chromatogr. 303 (1984) 1-12.
[136] R. West, R.H. Baney, Hydrogen bonding studies. II. The acidity and basicity of silanols compared to alcohols, J. Am. Chem. Soc. 81 (1959) 6145-6148.
[137] S.A. Wise, S.N. Chesler, H.S. Hertz, L.R. Hilpert, W.E. May, Chemically-bonded aminosilane stationary phase for high-performance liquid-chromatographic separation of polynuclear aromatic-compounds, Anal. Chem. 49 (1977) 2306-2310.

[138] S. Wold, A. Ruhe, H. Wold, W.J. Dunn, The collinearity problem in linear-regression - the partial least-squares (Pls) approach to generalized inverses, SIAM J. Sci. Comput. 5 (1984) 735-743.
[139] D. Wu, G.K. Nedev, C.A. Lucy, Retention mechanism of hypercrosslinked polystyrene silica hybrid phase in normal phase chromatography, J. Chromatogr. A 1370 (2014) 50-55.
[140] J. Zhang, S.L. Wu, J. Kim, B.L. Karger, Ultratrace liquid chromatography/mass spectrometry analysis of large peptides with post-translational modifications using narrow-bore poly(styrene-divinylbenzene) monolithic columns and extended range proteomic analysis, J. Chromatogr. A 1154 (2007) 295-307.
[141] Y. Zhang, P.W. Carr, Novel ultra stable silica-based stationary phases for reversed phase liquid chromatography--study of a hydrophobically assisted weak acid cation exchange phase, J. Chromatogr. A 1218 (2011) 763-777.
[142] Y. Zhang, Y. Huang, P.W. Carr, Optimization of the synthesis of a hyper-crosslinked stationary phases: a new generation of highly efficient, acid-stable hyper-crosslinked materials for HPLC, J. Sep. Sci. 34 (2011) 1407-1422.
[143] Y. Zhang, H. Luo, P.W. Carr, Silica-based, hyper-crosslinked acid stable stationary phases for high performance liquid chromatography, J. Chromatogr. A 1228 (2012) 110-124.